Biological Hydrogen Production using *Citrobacter amalonaticus Y19* to Catalyze the Water-Gas Shift Reaction

by

Sandra Robaire

B.Eng., McGill University, 2006

A THESIS SUBMITTED IN PARTIAL FULFILLMENT OF
THE REQUIREMENTS FOR THE DEGREE OF

MASTER OF APPLIED SCIENCE

in

The Faculty of Graduate Studies

(Chemical and Biological Engineering)

THE UNIVERSITY OF BRITISH COLUMBIA
(Vancouver)

December 2008

Abstract

This research reports on investigating *Citrobacter amalonaticus Y19*, a chemoheterotrophic facultative bacterium, as a catalyst to produce hydrogen from a low-grade synthesis gas stream. Several production strategies were considered, with a two-stage batch reaction shown to be most effective. This strategy begins with aerobic growth of the organism, where the biomass is generated, followed by hydrogen production in an anaerobic environment, where production and activation of carbon monoxide dehydrogenase and the CO-induced hydrogenase enzymes is required to catalyze biological H_2 production. The anaerobic environment was created by purging the reactors with a gas mixture of 40% CO in helium (v/v). The rates of hydrogen production were analyzed by measuring the concentrations of H_2, CO, and CO_2 during the anaerobic stage by collecting gas samples from the headspace. Samples were also collected from the fermentation medium to monitor the concentration of *Ci amalonaticus Y19*, organic acids, and pH.

Design of experiments was used to investigate the dependence of hydrogen productivity on various process parameters, including reactor pressure and various media components, such as the presence of CO during the growth phase, the presence of glucose, tryptone, and trace metals such as nickel and iron. The effect of re-suspension was also investigated since decoupling the two stages allows for a larger amount of freedom in selecting process conditions. The results indicate that increasing pressure has a negligible effect on hydrogen productivity, likely due to substrate inhibition compensating increased substrate availability. The results also show that altering certain media components can increase hydrogen productivity. Nickel, in particular, increased the H_2 productivity from 0.47 to 0.87 mmol H_2/ (L x h) when its concentration was increased from 0 to 125mg/L. Re-suspension between stages decreased the inhibition of enzyme production and activation by eliminating the inhibitory metabolites produced during the growth stage. This was manifested in the form of a reduced lag phase from approximately 18 hours to 5 hours with re-suspension, as well as an increased H_2 production rate. The maximum H_2 productivity attained was 1.5 mmol H_2/ (L x h) in buffered media when the cells were re-suspended between stages.

Table of contents

List of tables

List of figures

Acknowledgements

1.0 Introduction

1.1 Background

Today's world energy requirements are strongly dependant on fossil fuels. Fossil fuels are limited resources and the strong dependence on them is leading to a fast depletion of these resources. In 2005, the world's use of liquid fuels and other petroleum products was equivalent to approximately 83.6 million barrels oil per day, and this number is growing rapidly and is expected to exceed 112 million barrels per day by 2030 (1 barrel oil equals 42 US gallons or 159 liters) (Doman et al. 2008). In addition to this depletion, the combustion of fossil fuels emits large amounts of pollutants like CO_x, NO_x, SO_x, C_xH_x, soot, ash, and other organic compounds, which contribute to global climate changes. In order to limit the amount of emitted pollutants, while still satisfying the energy requirements of the world, a large amount of research has been done in the areas of alternative energy sources, chemical feedstocks and efficient processes to maintain sustainable economic growth and reduce dependence on petroleum (Amos 2004).

While the production of lignocellulosic ethanol and other liquid biofuels is prominent in the market today, hydrogen is sometimes viewed as the next phase in the evolution of renewable fuels because of its clean-burning properties. One kilogram of hydrogen is approximately equivalent to one US gallon of gasoline on an energy basis (Turner et al. 2008). Hydrogen is not a primary energy source, as hydrogen must be produced from other substances, but serves as a medium through which primary energy sources can be stored, transmitted and utilized to fulfill energy needs (Das, Veziroglu 2001). Fuel cells can use hydrogen and oxygen to make electricity with only water as a by-product (Figure 1).
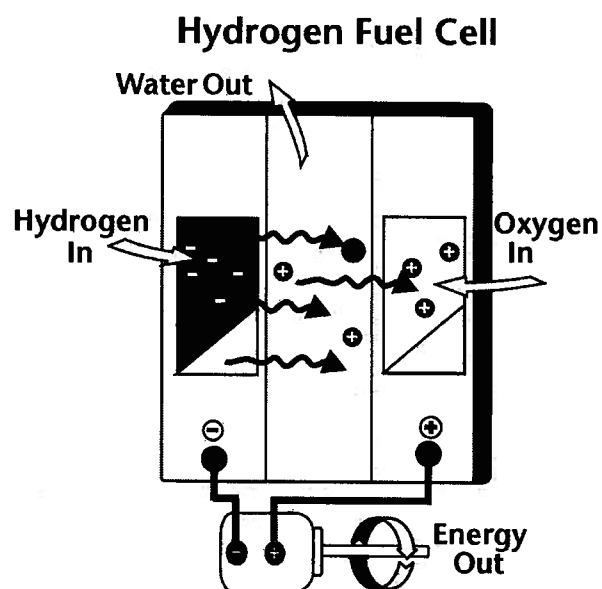
Hydrogen Fuel Cell

Figure 1- How fuel cells work (Energy information administration 2007)

Steam methane reforming is the most common method used commercially to produce hydrogen. It uses natural gas as a feedstock, predominantly composed of methane, in an energy intensive and highly endothermic process to produce a mixture of hydrogen (H_2) and carbon monoxide (CO) called synthesis gas. In order to produce additional H_2, the synthesis gas undergoes high and low temperature conventional water gas shift reactions with metal catalysts. Pressure swing adsorption is then applied to improve the purity of the H_2. The reforming process requires high temperatures (>850°C) and pressure (2.5×10^6 Pa). While H_2 production from natural gas using steam methane reforming is the most common method, many other methods exist to produce hydrogen from coal, water, and biomass. When biomass is the feedstock, gasification or pyrolysis is the process of choice. For water, electrolysis is the most common method.

Biological production of hydrogen is emerging as a viable alternative technology to the energy intensive methods. Not only is biological hydrogen production mostly operated at ambient temperatures, but it can also utilize biomass including waste materials such as starch and cellulose containing agricultural or food industry wastes, or carbohydrate rich industrial wastewaters. Biological H_2 production pathways include bio-photolysis from water, photo-fermentation, dark fermentation, and the water gas shift reaction. Bio-photolysis uses the photosynthetic pathway in green algae and

2

cyanobacteria to split water molecules into hydrogen ions and oxygen. Some of these microalgae contain hydrogenase enzymes allowing the hydrogen ions to be converted into hydrogen gas. Many anaerobic bacteria have also been found to produce hydrogen using carbohydrate-rich substrates. In the presence of light, photo-heterotrophic bacteria convert organic acids such as acetic, lactic, propionic, and butyric acid into a mixed biogas composed of H_2 and carbon dioxide (CO_2). Dark fermentations, on the other hand, do not require light, and produce H_2 and CO_2 from carbon sources such as glucose, sucrose, and more complex starch and cellulosic wastes. Stoichiometric balances suggest that the maximum H_2 production in dark fermentation is 2 or 4 moles H_2 per mole glucose depending on the end product formed during the reaction.

While many poorly degradable biomass sources and wastes cannot be converted directly to hydrogen by microorganisms, gasification of these feedstocks produces synthesis gas, mainly composed of carbon monoxide (CO). This synthesis gas, along with other CO containing gas streams (e.g. low-grade syngas used for heating in the developing world), is not an attractive feed stream for efficient technologies such as conventional WGS reactions. The energy in the waste gas streams can however be recovered by producing hydrogen through a biological water-gas shift reaction (bio-WGS). The bio-WGS is similar to the conventional WGS but bacteria are used rather than metallic catalysts. When exposed to CO, CO dehydrogenase and hydrogenase enzymes are induced in several photo-heterotrophic bacteria. The combined activity of these two enzymes catalyzes the bio-WGS:

$$CO + H_2O \longrightarrow H_2 + CO_2 \qquad \Delta G° = \text{-20 kJ mol}^{-1} \qquad (1)$$

Bacterial strains that can undergo the water gas shift include *Rhodospirillum rubrum*, *Rubrivax gelatinosa CBS*, *Rhodopseudomonas gelatinosa*, *Rhodopseudomonas palustris P4*, *Citrobacter amalonaticus Y19*, and *Carboxydothermus hydrogenoformans*. Desirable qualities of a bacterial strain include their ability to grow and produce hydrogen with no light, their ability to operate at a low temperature, and high H_2 productivity. A pure strain is preferable over an undefined mixture for ease of characterization. After an extensive review of the literature available, it was found that *Ci amalonaticus Y19* is a good candidate because it operates at low temperatures, does not require light for cell growth or hydrogen production, has high hydrogen production rates

according to the limited publications on this organism to date (Jung et al. 2002), and has the ability to grow aerobically, thus faster than organisms that grow anaerobically.

This research has thus focused on investigating *Citrobacter amalonaticus Y19*, a chemoheterotrophic facultative bacterium, as a catalyst to produce hydrogen from a carbon monoxide containing gas stream. Two stage batch processes were used to develop a better understanding of the physiological and biochemical properties of this organism. The effect of various process parameters, including pressure and media composition, on hydrogen productivity was investigated over the course of this research.

1.2 Thesis layout

An overview of the current state of the field of hydrogen production with an emphasis on biological hydrogen production and the water gas shift pathway is presented in the extensive literature review in Chapter 2. In this chapter, hydrogen and its potential for conversion into energy using fuel cells is introduced in more detail, followed by a description of conventional hydrogen production methods and a review of biological hydrogen methods. The strain selection process for the water gas shift reaction is then explained, along with a more detailed analysis of the current state of research on the organism selected.

The specific scope and objectives of the thesis project are presented in Chapter 3. Chapter 4 details the materials and methods used throughout the experimentation to quantify the results. Starting with the origin of the bacterial species used, Chapter 4 then describes the media used for growth and its composition. This is followed by the procedure for *Ci amalonaticus Y19* growth and H_2 production, and ends with a description of the analytical and measurement techniques used throughout the research project.

Chapter 5 outlines the results obtained using *Ci amalonaticus Y19* to produce hydrogen, as well as discussing the process parameters investigated and their effects on productivity. First, the growth phase of *Ci amalonaticus Y19* is examined with the parameter of CO presence. Then, the H_2 production phase is discussed in depth. Parameters investigated in this phase include the effect of substrate concentration and the effect of media components such as glucose, tryptone, buffer, and trace metals like iron

and nickel on H_2 productivity and enzyme activity. Re-suspension of the cells between the growth and hydrogen production stages is considered as a possible strategy for minimizing inhibition. The effect of mass transfer on H_2 productivity is assessed and the prospects and limitations of the H_2 productivity obtained are discussed.

Finally, Chapter 6 summarizes the results from this work which serve as a basis for quantifying the future potential of this organism as a H_2 producer, and Chapter 7 gives recommendations on how to progress and elaborate on the research already done in order to further develop this process.

2.0 Literature survey

This chapter provides an overview of the current state of the field of hydrogen production with an emphasis on biological hydrogen production and the water gas shift pathway. First, an overview of why hydrogen is of interest and how it can be used for energy purposes is discussed, followed by a description of conventional hydrogen production methods. Biological hydrogen production methods are then highlighted, along with their respective microbial species. More details are then given for the biological water gas shift reaction including the enzymatic pathway and the process of bacterial strain selection used for this project. The current state of research on the organism selected, *Citrobacter amalonaticus Y19*, is then detailed.

2.1 Hydrogen and fuel cells

According to a report on the International energy outlook in 2008, world marketed energy consumption is projected to grow by 50 percent over the 2005 to 2030 period. Total world energy will rise from 462 quadrillion British thermal units (Btu) in 2005 to 563 quadrillion Btu in 2015, and then to 695 quadrillion Btu in 2030 (Doman et al. 2008). Since oil reserves are finite, there is a need to focus on an alternative energy carrier from a potentially renewable feedstock. Hydrogen, if produced from renewable energy sources, can be the clean and sustainable energy carrier of the future. It also has the advantage of having an approximately 3-fold higher energy content than gasoline (142 MJ/kg for hydrogen versus 44.2 MJ/kg for gasoline). Many countries worldwide are committed to the possibility of a hydrogen economy, and organizations exist that bring the efforts of these countries together such as the International Partnership for a Hydrogen Economy (IPHE) formed in 2003 with 16 participating countries. In addition to these organizations, some technologies are already in place such as hydrogen-powered buses in Spain, Iceland, and several other countries across the world, and hydrogen refueling stations, including one at the National Research Council (NRC) Institute for fuel cell innovation in Vancouver, BC. In April 2004, the Canadian government also announced funding for the Canadian Hydrogen Highway to be built between Vancouver and Whistler, British Columbia. In order to reach a point where H_2 is produced

commercially worldwide, many advances need to be made in the production, storage, and uses of H_2.

Hydrogen is the most abundant element in the universe, constituting approximately 75% of the universe's elemental mass (Palmer 2005). However, most of the Earth's hydrogen is in the form of chemical compounds such as water and hydrocarbons. Elemental hydrogen in the form of diatomic gas, H_2, must therefore be produced from these other chemical compounds in order to be used as an energy carrier.

The energy from hydrogen can be released in one of two methods, internal combustion or the electro-chemical reaction that occurs in fuel cells. Although the combustion process is well known as it is similar to the one used in vehicles today, it does not significantly decrease the production of nitrous oxides that pollute the atmosphere and contribute to climate change. The nitrous oxides are created due to the high temperatures generated within the combustion chamber, which cause some of the nitrogen in the air to combine with the oxygen in the air. Combustion also releases a lot of energy in the form of heat, which decreases the efficiency of the process. Fuel cells are thus the most promising energy conversion devices for hydrogen and can achieve efficiencies that are two to three times greater than the internal combustion engine (The national hydrogen association a).

A fuel cell is a device that converts chemical energy supplied as input fuels to the device into electric energy. Fuel cells are composed of two electrodes, an anode and a cathode, and an intermediate electrolyte layer capable of transferring positive ions in either direction, while a corresponding flow of electrons in an external circuit provides the desired power (Figure 2)(Sorensen 2005).

In a proton exchange membrane fuel cell (PEMFC), the intermediate electrolyte layer is a proton-conducting polymer membrane. Hydrogen is fed to the anode catalyst (negative electrode) where it dissociates into protons and electrons. The protons are then conducted through the electrolyte membrane to the cathode (positive electrode), but since the membrane is electrically insulated, the electrons travel through in an external circuit supplying power. At the cathode catalyst, oxygen reacts with the protons and the electrons to form water, which is the only by-product of the PEMFC.
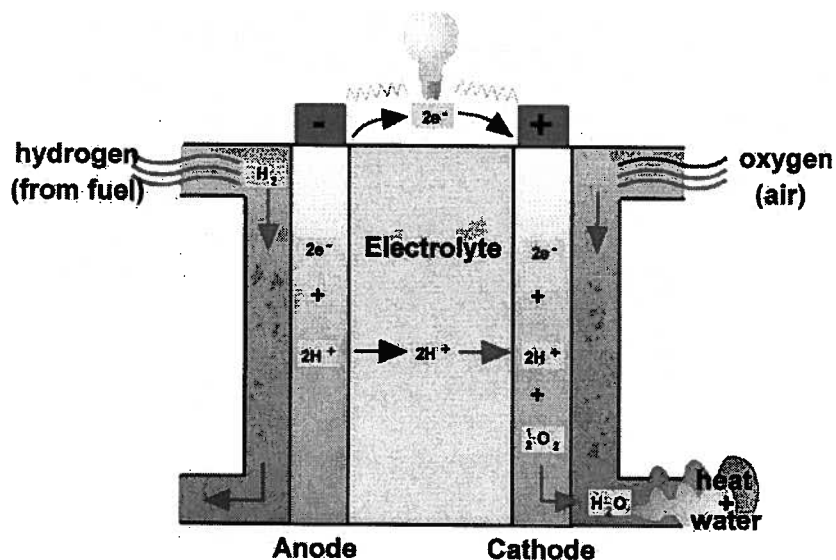
Figure 2 – Fuel cell schematic (Wells et al. 2005)

Not only are fuel cells pollution free, but they are also quiet and scalable. The scalability of fuel cells makes them ideal for a wide variety of applications from laptops (50-100 Watts) to central power generation (1-200 MWatts) (The national hydrogen association a). Today, fuel cells are still relatively expensive to build compared to internal combustion engines; therefore, they will need further development to increase their durability and bring down their cost in order to compete economically.

One recurring concern that arises from the idea of using hydrogen as an energy carrier is that most of the hydrogen currently being produced is from natural gas using steam methane reforming, so although PEMFC's only have water as a by-product, the methane usually comes from a non-renewable source, and steam methane reforming produces greenhouse gases, which thus does not alleviate global warming concerns. One answer to this is that the fossil fuels that are gasified to make hydrogen would be more centralized in a small number of generating plants where the emissions could be scrubbed, rather than having air pollution coming from millions of tail pipes. Another answer is that while in the near to mid-term, hydrogen will most likely be produced by steam methane reforming since it is a well understood and time tested technology, the mid- to long-term promises that new hydrogen production technologies from renewable resources will become more cost effective.

2.2 Conventional hydrogen production methods

Hydrogen is mainly produced from fossil fuels, water, and biomass. Using fossil fuels, hydrogen can be produced by steam reforming of natural gas, thermal cracking of natural gas, partial oxidation of heavy hydrocarbons, and gasification of coal. However, all of these methods are energy intensive processes that require high temperatures (> 850°C) (Kapdan, Kargi 2006). Other methods of producing hydrogen include electrolysis or photolysis from water, and pyrolysis or gasification from biomass. While this list is not exhaustive, it shows that there is no shortage of methods that exist for hydrogen production.

2.2.1 Steam methane reforming

Currently, the least expensive method is steam reforming of natural gas, which accounts for nearly 90% of the hydrogen produced industrially (Das, Veziroglu 2001, Crabtree, Dresselhaus & Buchanan 2004). Steam reforming starts from methane, the main constituent of natural gas, which undergoes, along with water vapour, the highly endothermic reaction,

$$CH_4 + H_2O \rightarrow CO + 3H_2 - \Delta H° \qquad \Delta G° = +151 kJ \qquad (2)$$
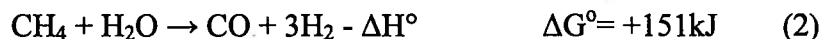
where the enthalpy change $\Delta H°$ equals 252.3 kJ mol^{-1} or 206.2 kJ mol^{-1} if the input water is already in gas form. The $\Delta H°$ and $\Delta G°$ are reported at ambient temperature and pressure, not at the significantly higher reaction temperature and pressure. This reaction requires a catalyst, typically nickel or a more complex nickel on aluminum oxide, cobalt, or alkali, and is operated at a high pressure of around 2.5 x 10^6 Pa and high temperature of around 850°C (Sorensen 2005). The reaction is controlled by several factors including the reaction temperature, the catalyst, the design of the reactor, and the input steam to methane ratio. Typical steam to methane ratios are 2 to 3 in order to avoid carbon (char) formation and prevent excess CO formation. High temperatures may also damage the catalyst and make it possible for methane cracking to occur, producing carbon which may appear as filaments on the catalyst surface blocking the steam reforming reaction.

In order to produce additional H_2, the reformate, also known as synthesis gas composed mainly of CO and H_2, undergoes high and low temperature conventional water gas shift reactions (WGS) in separate reactors. The WGS is slightly exothermic.

$$CO + H_2O \rightarrow CO_2 + H_2 - \Delta H° \qquad \Delta G° = -20kJ \qquad (3)$$
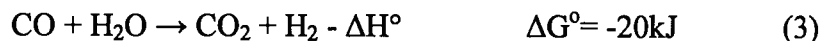
With the enthalpy change $\Delta H°$ equal to -41.1 kJ mol^{-1} when all reactants are in the gas form, and -5.0 kJ mol^{-1} if the input water is liquid. The $\Delta H°$ and $\Delta G°$ are reported at ambient temperature and pressure. Conceptually, a low temperature for the water gas shift reaction would shift the equilibrium to the right favoring the production of H_2; however, the reaction kinetics are faster at higher temperatures. The high temperature stage (HTS) can employ a Fe-Cr-based catalyst and is operated at 300-500°C to reduce CO concentrations to less than 4%. The low temperature stage can use Cu-Zn-Al operated at 200-260°C to further reduce the CO concentration to about 0.25% (Merida et al. 2004). As these temperatures are lower than the reforming temperature, some heat recovery can be done by cooling the reactants and recycling the heat to the reforming stage. If the hydrogen produced is required to be very pure, pressure swing adsorption is used to remove the CO_2 as well as the un-reacted CO and CH_4 from the product stream. The main reason for the high cost of production by steam methane reforming is the heat exchangers needed for the heat recovery between the water gas shift and the reformer.

2.2.2 Electrolysis

While steam reforming accounts for about 90% of the H_2 in the market, about 5% is attributed to electrolysis of water (Sorensen 2005). Electrolysis of water, which consists of splitting hydrogen from water using an electric current results in no emissions when the electricity is produced via renewable energy. It is a reliable and clean method that is capable of producing ultra pure H_2 (>99.999%) (Turner et al. 2008), which is necessary for some applications. Electrolysis is basically the reverse fuel cell operation where electric energy is converted into hydrogen and oxygen.

$$2H_2O - \Delta H° \rightarrow O_2 + 2H_2 \qquad (4)$$

At ambient pressure and temperature, the change in enthalpy, $\Delta H°$, is equal to -288 kJ mol^{-1} for liquid water and -242 kJ mol^{-1} for water in gas form.

More specifically, the electric current charges the water, breaks the chemical bond between H and O, and splits apart the atomic components, creating oppositely charged ions (Figure 3). The negative electrode (anode) attracts the positively charged hydrogen ions, while the positive electrode (cathode) attracts the negatively charged hydroxide ions. As the ions reach the electrodes, the hydrogen and oxygen gases rise and are collected separately.
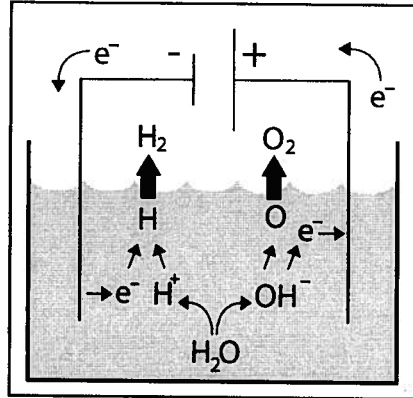
Figure 3 - Diagram showing the process of conventional electrolysis
(The national hydrogen association b)

Manufacturers currently produce two types of low temperature electrolyzers: alkaline and polymer electrolyte membrane or proton exchange membrane (both PEM). The alkaline electrolyzer typically uses an aqueous solution of water and 25-30 wt% potassium hydroxide (KOH) as an electrolyte. This liquid electrolyte enables the conduction of ions between the electrodes. Typical alkaline electrolyzers are run with current densities in the range of 100-300mA/cm^2. PEM electrolysis, on the other hand, uses a solid proton-conducting membrane that is not electrically conductive. The membrane serves as a gas separation device as well as a proton conductor. PEM electrolyzers are typically operated at higher current densities above 1600mA/cm^2. While PEM electrolyzers require a higher current density, they avoid the hazards surrounding KOH and are more easily able to maintain a significant differential pressure across the anode and cathode (Turner et al. 2008). Current research in this field includes comparing multiple electrolyzer technologies (alkaline and PEM) to gauge their efficiencies and abilities to be brought on- and off-line quickly, as well as exploring the synergies of

coproduction of electricity and hydrogen using wind power. This is particularly interesting due to the intermittent nature of wind power.

According to Kroposki et al. (2006), 39 kilowatt-hours (kWh) of electricity and 8.9 liters (L) of water are required to produce 1 kilogram (kg) of hydrogen at 25°C and 1 atmosphere pressure. Typical commercial electrolyzers system efficiencies are 56-73%, which corresponds to 70.1-53.4 kWh electricity per kg H_2 (Ivy 2004, Kroposki et al. 2006). The cost of electrolysis thus highly depends on the cost of electricity, which is a function of market fluctuations and can render this method of hydrogen production very expensive.

2.3 Biological hydrogen production methods

Biological hydrogen production processes are an alternative to the energy intensive methods currently in place. Not only is biological hydrogen production mostly operated at ambient temperatures and pressures, thus making it more environmentally friendly and inherently safer, but this method of production can also potentially utilize renewable resources and in some cases waste materials such as starch and cellulose containing agricultural or food industry wastes, or carbohydrate rich industrial wastewaters in the form of biomass. In this section, several biological pathways used for hydrogen production will be described including bio-photolysis of water, dark fermentation, light fermentation and the water gas shift reaction.

2.3.1 Bio-photolysis of water

Some microorganisms can adapt the photosynthetic process found in plants and algae for the production of hydrogen.

$$2H_2O \rightarrow 2H_2 + O_2 \qquad \Delta G^\circ = +1498kJ \qquad (5)$$

The ΔG° is reported at ambient temperature and pressure. Light energy is used in photosynthesis to split water molecules to hydrogen ions (H^+) and oxygen. In green plants, the photons produced are used only for CO_2 reduction; while in some microalgae, hydrogenase enzymes are present, allowing for the hydrogen ions to be converted into H_2 gas. Both eukaryotic green algae and prokaryotic cyanobacteria (blue-green algae) have

been shown to produce H_2 under certain conditions (Benemann 1997). Bio-photolysis of water using green algae is termed direct bio-photolysis while the use of cyanobacteria induces indirect bio-photolysis.

Bio-photolysis by green algae requires a period of anaerobic incubation in the dark in order to induce the synthesis and/or activation of the hydrogenase enzymes. Green algae that have been shown to produce hydrogen by bio-photolysis include *Chlamydomonas reindardtii* (Ghirardi et al. 2000, Melis 2002) and *Scenedesmus obliquus* (Florin, Tsokoglou & Happe 2001). A study performed by Winkler et al. (Winkler et al. 2002) compared the enzyme activity of several algae species and found that *C. reindhartii* had one of the highest activities at 200nmol/(µg chlorophyll a x h). One major obstacle with bio-photolysis of water is the O_2 generated which irreversibly inactivates the H_2 producing system. Using sulfur-deprived media for culturing *C. reindhartii* is one possible solution because it significantly decreases the rates of O_2 synthesis and CO_2 fixation (Ghirardi et al. 2000). Several studies have been done using sulfur-deprived media, and the highest reported rate of H_2 production for this system is around 7.95 mmol H_2/ L after 100 hours (Kosourov et al. 2002, Melis et al. 2000). This corresponds to 0.07 mmol H_2/ (L x h) in the standardized units used by Levin et al. to compare several biological hydrogen production methods (Levin, Pitt & Love 2004).

Bio-photolysis by cyanobacteria is termed indirect bio-photolysis because it undergoes the following set of reactions that both require light energy to proceed:

$$12H_2O + 6CO_2 \rightarrow C_6H_{12}O_6 + 6O_2 \tag{6}$$

$$C_6H_{12}O_6 + 12H_2O \rightarrow 6CO_2 + 12H_2 \qquad \Delta G^\circ = +3.2kJ \tag{7}$$
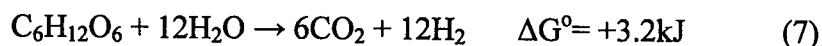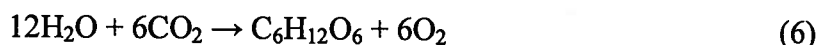
The ΔG° is reported at ambient temperature and pressure. Hydrogen production has been investigated in many cyanobacter species and strains, within at least 14 genera, and under a wide range of culture conditions (Pinto, Troshina & Lindblad 2002). These species may possess several of the enzymes involved in H_2 synthesis that include nitrogenases, which catalyze the production of H_2 as a by-product of nitrogen reduction to ammonia, uptake hydrogenases, which catalyze the oxidation of H_2 synthesized by the nitrogenase, and bi-directional hydrogenases, which have the ability to both oxidize and synthesize H_2 (Tamagnini et al. 2002). According to a review by Levin et al. (Levin, Pitt & Love 2004), rates of H_2 production by non-nitrogen fixing cyanobacteria, which range

from 0.02 to 0.4 μmol H_2/ (mg chlorophyll a x h), are very low compared with those of heterocystous cyanobacteria, which range from 0.17 to 4.2 μmol H_2/ (mg chlorophyll a x h). *Anabaena variablilis* is responsible for the high end of this H_2 production range. *Anabaena* species were shown to have the highest hydrogen evolution potential (Pinto, Troshina & Lindblad 2002) and thus have been the subject of much research. According to Levin et al., it is a mutant strain of this species, *A. variabilis PK84*, that has the highest H_2 productivity of 0.355 mmol H_2/ (L x h) in converted standardized units (Sveshnikov et al. 1997).

While the H_2 production processes using green algae and cyanobacteria can be considered sustainable as they use only water as a resource and consume CO_2 thus decreasing air pollutants, their sensitivity to O_2 along with their low hydrogen production potential make bio-photolysis unattractive as a H_2 production method.

2.3.2 Dark fermentations on carbohydrate-rich substrates

While bio-photolysis requires a light source, hydrogen can also be produced in the dark using anaerobic bacteria and carbohydrate-rich substrates. Production in the dark is advantageous because of the lower process cost, as photo-bioreactors are very expensive. These fermentations produce a mixed biogas containing mainly hydrogen and carbon dioxide. Some examples of anaerobic bacteria that produce hydrogen in this manner are species from the genus *Enterobactericeae* and species from the genus *Clostridium* (Jung et al. 2002). Dark fermentations can be operated at mesophilic (25-40°C), thermophilic (40-65°C), and extreme thermophilic (65-80°C) temperatures, depending on the microbe being used. Hydrogen production by these dark fermentations depends highly on environmental conditions such as pH, temperature, composition of the substrate, media composition, gas partial pressure, hydraulic retention time, and the type of microbial culture used (Kapdan, Kargi 2006).

Many carbohydrate-rich substrates can be used for these fermentations including simple sugars such as glucose and sucrose, or more complex wastes such as starch containing wastes, cellulose containing wastes, and food industry wastes or wastewater. Each of these substrates yields different amounts of hydrogen, depending on the fermentation pathway and end products (Kapdan, Kargi 2006). Catabolism of these

carbohydrate rich substrates first forms pyruvate, which is then metabolized in an anaerobic environment to produce acetyl CoA and either formate or reduced ferredoxin. Cellular ATP is subsequently derived from acetyl-CoA, and H_2 is derived from the formate or reduced ferrodoxin (Hallenbeck, Benemann 2002). Enteric bacteria mainly use the pyruvate-formate lyase enzyme complex to form formate from pyruvate, while strictly anaerobic bacteria use pyruvate-ferredoxin oxidoreductase enzyme system to form ferredoxin from pyruvate.

Using glucose as a model substrate, stoichiometric balances suggest that when acetic acid is the end product, the theoretical maximum yield is 4 moles H_2 per mole glucose (Equation 8); whereas, when butyric acid is the end product, the theoretical maximum yield is 2 moles H_2 per mole glucose (Equation 9).

$$C_6H_{12}O_6 + 2H_2O \rightarrow 2CH_3COOH + 2CO_2 + 4H_2 \qquad \Delta G^o = -182.4kJ \qquad (8)$$

$$C_6H_{12}O_6 \rightarrow CH_3CH_2CH_2COOH + 2CO_2 + 2H_2 \qquad \Delta G^o = -257.1kJ \qquad (9)$$

The Gibbs free energy changes are reported at ambient temperature and pressure. If only the H_2 yield is considered, thus ignoring the economic value of butyric and acetic acid, acetic acid is the more desirable end product as it results in the higher theoretical yield; however, the literature suggests that the production of hydrogen does not follow these stoichiometric ratios. Most microbes opt to produce an array of waste products such as small organic acids and alcohols at the expense of the hydrogen molar yield. Moreover, the production of acids decreases the pH of the medium further lowering the yield of hydrogen (Hallenbeck 2005). While the theoretical maximum hydrogen molar yield is 4 mol H_2/mol glucose, current research has been reporting values around 2-3 mol H_2/mol glucose by using pure cultures or mixed microbial consortiums (Turner et al. 2008). While glucose is the most easily fermentable substrate, it is also very costly. In order to realize the full potential of fermentation, less expensive and more abundant feedstocks must be explored. One such abundant and sustainable feedstock is lignocellulosic biomass, consisting of hemicellulose (mainly xylose, arabinose and galactose), cellulose, and lignin. Cellulose is more crystalline than hemicellulose, adding the difficult challenge of breaking down this polymer into its glucose monomers. In most cases, using cellulose as a substrate would require an expensive enzymatic break down step to render the substrate useful.

While dark fermentations using simple sugars have been extensively characterized and give high production rates, the use of more complex waste materials is still in its infancy. Some of the most extensively studied dark fermentation bacteria are *Clostridium* species. Some pure cultures of *Clostridium* and *Enterobacter* species can degrade insoluble and soluble starch, respectively (Taguchi et al. 1994). Other *Clostridium* species have been shown to produce hydrogen from xylose, xylan, arabinose, galactose, delignified wood fibers, and corn stover lignocellulose (Taguchi et al. 1996, Levin et al. 2006, Datar et al. 2007). The molar yield for these *Clostridium* species conversions was between 2 and 3.2. *Clostridium* species No.2 has been shown to have a very high hydrogen production rate of 21 mmol H_2/ (L x hr) using 3% xylose as substrate (Taguchi et al. 1996). Overall, the H_2 synthesis rates vary between 8.2 and 121.0 mmol H_2/ (L x h) (Levin, Pitt & Love 2004). The maximum rate of 121.0 mmol H_2/ (L x h) was found for a mesophilic undefined consortium (mostly Clostridium species) derived from domestic sewage sludge (Chang, Lee & Lin 2002).

While much progress has been made over the past decade in the field of hydrogen production using dark fermentation pathways, continued research promises to increase H_2 yields as well as production rates. Fields of particular interest include finding new bacterial species to convert cellulosic substrates directly rather than needing an initial enzymatic breakdown step, and metabolic engineering to get around the molar yield barrier by redirecting metabolic pathways to H_2 production rather than by-product pathways such as organic acid production.

2.3.3 Photo-fermentations

Some photoheterotrophic bacteria can produce hydrogen and carbon dioxide by converting organic acids such as acetic, lactic, propionic, and butyric acid, while others produce hydrogen by converting carbon monoxide through the biological water gas shift reaction. The latter will be discussed in section 2.3.4. While the photosystem of purple photoheterotrophic bacteria is not powerful enough to split water, it can use simple organic acids under anaerobic conditions using light energy. The electrons liberated from the organic carbon are transported to the electron acceptor ferredoxin. Under nitrogen-

deficient conditions, the nitrogenase enzyme present in these bacteria reduces protons into H_2 gas, with the electrons derived from the ferredoxin (Akkerman et al. 2002).

$$CH_3COOH + 2H_2O \rightarrow 2CO_2 + 4H_2 \qquad \Delta G^o = +104kJ \qquad (10)$$
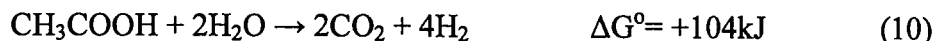
The ΔG^o is reported at ambient temperature and pressure. In the presence of N_2, the nitrogenase enzyme will catalyze N_2 fixation rather than H_2 evolution. The nitrogenase enzyme is also highly sensitive to oxygen, and inhibited by ammonium ions and high N/C ratios. Since no O_2 is produced during this process, the sensitivity to O_2 is not as critical as during bio-photolysis. Some of the major benefits of photo-fermentations are the high theoretical conversion yields, the lack of O_2-evolving activity, the ability of the purple photosynthetic bacteria to use a wide spectrum of light, and the ability to consume organic substrates derived from wastes, thus giving them a potential to be coupled with wastewater treatment. The coupling with wastewater treatment must, nonetheless, first overcome barriers such as reduced light penetration due to the colour of the wastewater (Kapdan, Kargi 2006).

Hydrogen production capabilities have been investigated for some purple photosynthetic bacteria such as *Rhodobacter spheroides*, *Rhodobacter capsulatus*, *Rhodovulum sulfidophilum W-1S*, and *Rhodospeudomonas palustris* (Kapdan, Kargi 2006). Hydrogen production rates from photo-fermentations vary according to many factors including light intensity, carbon source, and the type of microbial culture used. The highest conversion efficiency from organic acids reported in the literature was found using lactic acid as the carbon source, giving between 80 and 86% efficiency (Kapdan, Kargi 2006). The maximum volumetric H_2 production rate found was 2.5 mmol H_2/ (L x h) in converted standardized units using *R sphaeroides RV* as a catalyst (Fascetti, Todini 1995).

Research into photo-fermentations has also been done using several reactor configurations including batch processes, continuous cultures, and immobilized cell cultures in or on a solid matrix. Levin et al. reviewed these reactor configurations and found that when cells are immobilized, the rates of hydrogen production by photoheterotrophic bacteria are higher (Levin, Pitt & Love 2004).

Although the theoretical yield of photo-fermentations is quite high, the yields and H_2 production rates found so far are lower than dark fermentation yields. Dark

fermentation produces organic acid by-products that lower the hydrogen yield on substrates such as glucose. Because photo-fermentations can use small organic acids to produce hydrogen, an interesting new development and research area is the use of an integrated approach between dark and photo-fermentations. In this integrated approach, the organic acids produced by dark fermentation can be further processed by photo-fermentation to generate additional hydrogen. This could lead to higher yields and conversion efficiencies of carbohydrate carbon sources into H_2.

2.3.4 Water-gas shift reaction

The biological water-gas shift pathway is similar to the conventional water gas shift mentioned in section 2.2 (Equation 2), but rather than using a metallic catalyst, a set of enzymes is utilized. In order for this pathway to be considered, sources of CO, which is the substrate of the reaction, must be available. One source of CO is synthesis gas (syngas), which is mainly a mixture of CO, H_2, and CO_2, but may also contain minor amounts of methane, N_2, and H_2S. Current industrial H_2 production processes consist mainly of steam methane reforming which, as mentioned in section 2.2, must first produce synthesis gas (or syngas) from catalytic steam reforming at very high temperatures in order to produce hydrogen. While fossil fuels are the most common source of syngas, some solid wastes and biomass can also be gasified to produce syngas. Gasification of solid wastes and biomass is more complex because of the heterogeneity of the carbon based materials, and not all wastes can be gasified, but a few promising waste types include paper mill waste, mixed plastic waste, forest industry waste and agricultural residues (Sipma et al. 2006).

It is important to make the distinction between low and high-grade syngas. The amount of energy held in the syngas defines the grade, which for the purpose of this thesis can be quantified in terms of the composition and temperature of the syngas. A combination of a low percentage of CO and H_2, as well as a low temperature, would thus result in a lower grade syngas. For quantification purposes, and since the WGS reaction is mostly concerned with the amount of CO available, 40% CO (v/v) or higher will be considered high-grade syngas while 10-20% CO (v/v) will be low-grade syngas. The cut-off temperature for low-grade syngas will be assigned at 100°C since temperatures below

this carry less energy. Low-grade syngas, also known as town gas, is abundant in developing countries and is used for applications such as heating but inefficiently. This low-grade synthesis gas can be considered a waste stream, and is not an attractive feedstock option for energy intensive technologies such as conventional WGS. Using this low chemical energy feedstock in the biological water gas shift pathway is thus of particular interest to improve the value of this waste stream. Photo-heterotrophic bacteria can convert low-grade syngas into H_2, a useful energy carrier, through bioconversion.

The biological water gas shift reaction operates at ambient temperatures and pressures. Several photo-heterotrophic bacteria can utilize carbon monoxide (CO) as a sole carbon source in the presence or absence of light. When exposed to CO, both a carbon monoxide dehydrogenase (CODH) enzyme and a hydrogenase enzyme are induced. The combined activity of these two enzymes catalyzes the intracellular water-gas shift reaction:

$$CO + H_2O \rightarrow H_2 + CO_2 \qquad \Delta G° = -20 kJ/mol \qquad (11)$$

The $\Delta G°$ is reported at ambient temperature and pressure. Unlike the high temperatures used for conventional WGS, the ambient temperatures used for biological WGS make CO-oxidation and H_2 synthesis thermodynamically favorable, since the equilibrium of this reaction is shifted to the right. Bacterial strains that can undergo the water gas shift reaction include *Rhodospirillum rubrum, Rubrivax gelatinosa CBS, Rhodopseudomonas gelatinosa, Rhodopseudomonas palustris P4, Citrobacter amalonaticus Y19, and Carboxydothermus hydrogenoformans*. More details on these bacterial strains can be found in section 2.4.

Table 1, adapted from Levin et al., summarizes the maximum production rates using the various biological hydrogen systems discussed above (Levin, Pitt & Love 2004). The units have been converted into mmol H_2/ (L x h) in order to make a valid comparison between methods.

It is observed that while photolysis and photo-fermentations have exceedingly low H_2 production rates, the water gas shift reaction is comparable to some dark fermentation results. The highest production rate is found using dark fermentation with an undefined consortium of mesophilic bacteria, while the second highest, at 96 mmol H_2/(L x h), is attributed to CO-oxidation by *R gelatinosus*, using the water gas shift reaction. Using an

undefined mixture of bacterial strains may give the highest production rates, but scientifically, the results are hard to reproduce and even more difficult to quantify as the specific bacteria involved are unknown. The water gas shift was, therefore, the pathway studied for the remainder of this thesis because of its great potential not only to give high yields of H_2, but also to convert waste syngas to H_2.

Table 1 - Comparison of hydrogen production rates by various biohydrogen systems

BioH$_2$ System	H$_2$ synthesis rate (reported units)	H$_2$ synthesis rate (converted units)	References
Direct photolysis	4.67 mmol H$_2$/l/80h	0.07 mmol H$_2$/(l x h)	(Melis et al. 2000)
Indirect photolysis	12.6 nmol H$_2$/µg protein/h	0.355 mmol H$_2$/(l x h)	(Sveshnikov et al. 1997)
Photo-fermentation	4.0 ml H$_2$/ml/h	0.16 mmol H$_2$/(l x h)	(Tsygankov et al. 1998)
CO-oxidation	0.8 mmol H$_2$/g cdw/min	96.0 mmol H$_2$/(l x h)	(Wolfrum et al. 2002)
Dark fermentations			
Mesophilic, pure strain	21.0 mmol H$_2$/1 l/h	21.0 mmol H$_2$/(l x h)	(Taguchi et al. 1996)
Mesophilic, undefined	1,600.0 l H$_2$/m^3/h	64.5 mmol H$_2$/(l x h)	(Lay 2000)
Mesophilic, undefined	3.0 l H$_2$/l/h	121.0 mmol H$_2$/(l x h)	(Chang et al. 2002)
Thermophilic, undefined	198.0 mmol H$_2$/l/24 h	8.2 mmol H$_2$/(l x h)	(Ueno et al. 1996)
Extreme thermophilic, pure strain	8.4 mmol H$_2$/l/h	8.4 mmol H$_2$/(l x h)	(Van Niel et al. 2002)

2.4 More on the biological water gas shift reaction

2.4.1 Enzymatic pathway of the bio-WGS

Microorganisms that undergo the water gas shift reaction are called hydrogenogens. These microorganisms conserve energy by oxidation of CO to CO_2 coupled to the reduction of protons to H_2, catalyzed by CO dehydrogenase (CODH) and hydrogenase, respectively. The energy conserving mechanism used by these hydrogenogens is still unknown as it has been found that CODH and hydrogenase do not conserve energy in the same manner as the classical theories, substrate level phosphorylation (SLP) and electron transfer phosphorylation (ETP) (Sipma et al. 2006). Instead, it has been proposed that a membrane associated enzyme complex is formed by CODH and hydrogenase, which facilitates CO oxidation and proton reduction (Figure 4).
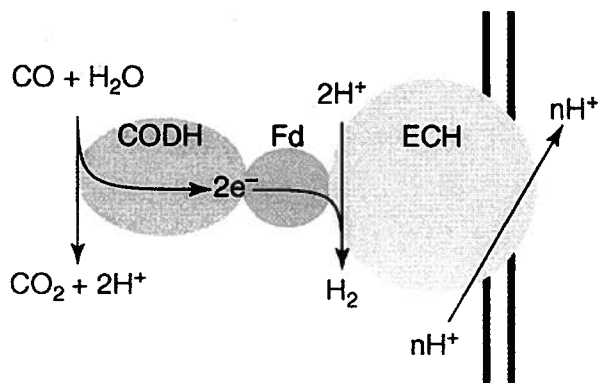
Figure 4 - Schematic representation of the WGS pathway. CODH, CO dehydrogenase; Fd, ferrodoxin; ECH, energy-conserving hydrogenase (Henstra et al. 2007)

The two key enzymes necessary for the biological water gas shift reaction to proceed are CODH and hydrogenase. CODHs are nickel containing, O_2 sensitive enzymes, and are either monofunctional or bifunctional (Lindahl 2002). While monofunctional CODHs catalyze the oxidation of CO as part of the energy metabolism, bifunctional CODHs catalyze the synthesis of acetyl-CoA or its decarbonylation beside the oxidation of CO (Equation 12).

$$CO + H_2O \leftrightarrow 2H^+ + CO_2 + 2e^- \qquad (12)$$
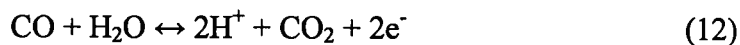
Monofunctional CODHs have been identified in several microorganisms that undergo the biological WGS including *R. rubrum* and *C. hydrogenoformans*. These enzymes are functionally associated with the iron-sulfur protein CooF, that contains 4 [4Fe-4S] clusters (Sipma et al. 2006).

Hydrogenases are the other key enzymes and they catalyze the reduction of protons to H_2:

$$2H^+ + 2e^- \leftrightarrow H_2 \qquad (13)$$
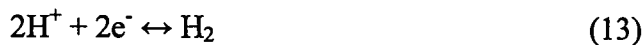
Three classes of hydrogenases exist based on phylogeny and metal content: [NiFe]-hydrogenases, [FeFe]-hydrogenase, and iron-sulfur cluster free hydrogenases. Energy converting hydrogenases (ECHs) are a subclass of [NiFe]-hydrogenases. ECHs are membrane bound enzyme complexes that play a key role in energy generation in the hydrogenogenic metabolism (Hedderich 2004).

The overall enzymatic process thus starts with the oxidation of CO by a monofunctional CO dehydrogenase. The electrons that are released by the oxidation are

then transferred to the ECH that reduces the protons to form molecular H_2. Since the ECH is membrane bound, it couples the formation of H_2 to the membrane translocation of protons or sodium ions, creating an ion gradient that can drive ATP synthesis through an ATP-synthase. Energy conservation in these types of microorganisms is thus independent of the acetyl-CoA pathway (Henstra et al. 2007).

2.4.2 Bacterial strain selection for the water gas shift reaction

The feasibility of biological H_2 production from CO largely depends on the performance of the microorganism that catalyzes this reaction, and considerable efforts to isolate appropriate strains have been conducted thus far. The partial list in the literature includes several anaerobic photosynthetic bacteria such as *Rhodospirillum rubrum*, an anaerobic bacterium, *Carboxydothermus hydrogenoformans*, and several facultative bacteria, such as *Rubrivivax gelatinosus CBS*, *Citrobacter amalonaticus Y19*, and *Rhodospeudomonas palustris P4*. The majority of bacterial strains that catalyze the WGS are purple non-sulfur photosynthetic bacteria, a non-taxonomic group. These bacteria can grow as photoheterotrophs, photoautotrophs or chemoheterotrophs, switching from one mode to another depending on the available conditions such as: degree of anaerobiosis, availability of carbon sources, and availability of a light source (Basak, Das 2007).

R rubrum, a photosynthetic purple non-sulfur bacterium, has drawn much attention due to the high specific CO uptake rate and the high conversion yield close to the theoretical value (Jung et al. 1999a). However, *R rubrum* always requires light for its growth and the growth is relatively slow. In addition, H_2 production is inhibited by moderate CO partial pressures above 0.2 atm.

Rhodopseudomonas bacteria are also purple non-sulfur phototrophic organisms, and they can be found in many types of marine environments and soils. *Rhodopseudomonas palustris P4* has a high growth rate of $0.3h^{-1}$ and a moderate rate of hydrogen production 20.7 mmol/ (g cell x h)(Jung et al. 1999a). While *Rh palustris P4* was not inhibited by high CO concentrations almost up to 1 atmosphere, the light requirement for cell growth was an important drawback.

Carboxydothermus hydrogenoformans is a gram positive, thermophilic, strict anaerobic bacterium that was isolated from hydrothermal freshwater springs in Russia.

This bacterium has the ability of using CO as the sole carbon source and has been shown to grow on CO with a doubling time of 2 hours. While thermophilic organisms can be advantageous because of higher conversion rates, higher temperatures also have a negative impact on the solubility of CO in water. The rate of H_2 production reported in the literature is 48.7 mmol H_2 /L of medium after 45 hours (Henstra, Stams 2004). It has also been shown that CO thresholds below 2ppm could be obtained if CO_2 was removed from the gas phase of batch cultures using *C hydrogenoformans*. Without CO_2 removal, 117ppm CO remained from an original gas phase of 100% CO, whereas conventional chemical water gas shift technology leaves 1000ppm of CO (Henstra et al. 2007).

Citrobacter is a genus of gram-negative bacteria in the family of the Enterobacteriaceae. It can be isolated from wastewater sludge digesters. *Ci amalonaticus Y19* is a facultative anaerobe, able to grow aerobically or anaerobically, although much faster growth was observed under aerobic conditions. Hydrogen production, however, was observed only under anaerobic conditions. Since the conditions for cell growth and hydrogen production were very different, a two-step process, which separates the growth phase from the hydrogen production phase, has been suggested for maximizing hydrogen production. The maximum hydrogen production activity found was 27.1 mmol H_2/(g cell x h) (Jung et al. 2002).

Rubrivivax gelatinosus CBS is a non-sulphur, purple photosynthetic bacteria that is also capable of performing the water-gas shift reaction under anaerobic conditions, atmospheric pressure and an ambient temperature of 25°C (Amos 2004). *Rx Gelatinosus CBS* can obtain energy in several ways including photosynthesis, aerobic heterotrophic metabolism, and anaerobic fermentation pathways. The biological water gas shift reaction can utilize dark anaerobic fermentation. This pathway produces much less energy than the aerobic or photosynthetic pathways, meaning a lower growth rate, but also produces less waste than the other pathways. In darkness, the CO oxidation pathway contains CO dehydrogenase (CODH) and hydrogenase enzymes, both of which are induced in CO, similar to that reported for *R rubrum* (Maness, Weaver 2002). *Rx gelatinosus CBS* was found to have a doubling time of approximately 7 hours in the light when CO was used as the only carbon source and the maximum specific hydrogen production rate was found to be 48 mmol H_2/ (g cell x h) (Wolfrum, Watt & Huang 2002, Maness, Weaver 2002)

Several selection criteria were used to determine which bacterial strain would be used for this thesis research project. The first criterion is the ability of the bacterial strain to grow and produce hydrogen with no light in order to decrease the cost of the process by eliminating expensive photo-bioreactors. A second criterion is their ability to operate at a low temperature in order to increase the substrate availability since lower temperatures result in higher CO solubility in water, and high H_2 productivity. A pure strain is preferable over an undefined mixture for ease of characterization and availability of the organism is crucial in order to obtain a sample of the organism for study. Table 2 summarizes many of the qualities desired for these bacteria, as well as their maximum H_2 production rates found in the literature.

Table 2 - Summary of properties of some bacterial strains used for the water gas shift reaction

	Temp (°C)	Need light for growth?	Can use CO as sole energy source?	Max H_2 production rate	Reference
Rhodospirillum rubrum	30	Yes	Not specified	11 mmol/(g cell x h)	(Klasson et al. 1992)
	30	Yes	Not specified	0.87 mmol H_2 /mmol CO	(Najafpour, Younesi & Mohamed 2004)
Rhodopseudomonas palustris P4	30	Yes	No	20.7 mmol/(g cell x h)	(Jung et al. 1999a)
Citrobacter amalonaticus Y19	30-40	No	Yes (but use C source too)	27.1 mmol/(g cell x h)	(Jung et al. 2002)
Carboxydothermus hydrogenoformans	70	No	Yes	Not known	(Soboh, Linder & Hedderich 2002)
	60-65	No	Yes (but use pyruvate too)	48.7 mmol/L medium (in approx 45 hrs)	(Henstra, Stams 2004)
Rubrivivax gelatinosus CBS	25	No (but uses it)	Yes	48 mmol/(g cell x h) (96 mmol/ L h)	(Maness, Weaver 2002)
Anaeorobic bioreactor sludges	55	No	Yes	Not known	(Sipma et al. 2004, Sipma et al. 2003)

All of these bacteria have their advantages and disadvantages, and perform differently in terms of hydrogen production rates and growth rates. *R rubrum* and *Rh Palustris P4* need light for growth, and thus will not be used for this study. Of the remaining strains, *Ci amalonaticus Y19, C hydrogenoformans*, and *Rx gelatinosus CBS* are pure strains, but although none of these require light for growth, after closer analysis,

it is suggested that *Rx gelatinosus CBS* prefers light and grows very slowly in the absence of it. Between the remaining two strains, *Ci amalonaticus Y19* operates at the lower temperature and thus may allow for the alleviation of any substrate mass transfer limitations that occur in the process. *Ci amalonaticus Y19* was the bacterial strain selected for further studies. It served as a good system for study using the low-pressure reactors available.

2.4.3   Citrobacter amalonaticus Y19

As *Ci amalonaticus Y19* was the bacterial strain used for this study, this section will provide more details on the strain characteristics and the parameters studied in the literature so far. This organism was first isolated from an anaerobic wastewater sludge digester by the researchers at the Pusan national university in Korea. This research group has studied the bacteria as a catalyst for H_2 production using both the water gas shift reaction and dark fermentation pathways. In this review, the focus will be on the use of *Ci amalonaticus Y19* to catalyze the WGS pathway, which was predominantly studied in batch serum-bottle cultivations (Jung et al. 2002, Kim et al. 2003, Jung et al. 1999b).

An important first discovery was that *Ci amalonaticus Y19* grew fast with a specific growth rate of 0.7 h^{-1} aerobically to a cell density of 2 g/L, whereas under anaerobic conditions, the cell specific growth rate and the maximum cell density were only 0.12 h^{-1} and 0.4g/L, respectively. It was also shown that no H_2 could be produced aerobically, which suggests that it would be desirable to separate the growth phase from the H_2 production phase in order to increase the rate of production. The medium used for both growth and H_2 production phases was only described as a mineral salt medium supplemented with 3g/L yeast extract and 5g/L sucrose. Through direct contact with the researchers, it was later discovered that the media used for growth was LB media supplemented with glucose and phosphate buffer. In particular, it was mentioned that glucose was used rather than sucrose because Citrobacter species are known to not use sucrose as a carbon source. Due to the contradictory nature of these statements and the lack of details in the published research papers on the composition of the media, the research in this thesis investigated the effect of several different media components on growth and H_2 productivity using *Ci amalonaticus Y19.*

Once a method for this two-phase process was established, optimal conditions for the growth phase were investigated, including pH, temperature, and O_2 and CO partial pressure. Optimal temperatures and pH for growth were found to be 30-40°C and 5-8, respectively. The experiment on the effect of O_2 partial pressure was conducted in the presence of 0.05atm CO in the headspace and varying O_2 partial pressures. H_2 productivity was shown to be affected by the P_{O2} in the gas phase and inhibited by P_{O2} above 0.4 atm. Considering both cell growth and H_2 production, the optimal P_{O2} was estimated to be 0.2-0.4atm (Jung et al. 2002). Another study more specifically on the O_2 sensitivity of hydrogen production activity of *Ci amalonaticus Y19* found that in whole cells, the deactivation of hydrogenase by O_2 was reversible. On the contrary, CO dehydrogenase activity was not recovered once deactivated by O_2, and the only way to recover the activity was to synthesize new CO dehydrogenase (Kim et al. 2003).

The effect of CO-partial pressure (P_{CO}) in the growth phase on cell growth rate and H_2 production activity was also studied in the range of 0.0 to 0.5atm P_{CO}. The maximum specific growth rate was shown to decrease linearly with increasing P_{CO}. The H_2 production activity was found to be almost negligible when P_{CO} was zero but rapidly increased when P_{CO} was raised to 0.05 atm. At higher P_{CO}, the activity decreased until P_{CO} reached 0.3 atm at which time activity levelled off. The researchers attribute the linear decrease of the maximum specific growth rate with increasing P_{CO} to an interference with the electron transport chain (Jung et al. 2002). They also conclude that the presence of CO during the growth phase was necessary for the induction of H_2 production activity, and that the activity might be developed during the cell-growth period via a CO-dependant mechanism. They further suggest that the relevant enzymes for CO-dependent H_2 production are synthesized during aerobic growth and activated during the subsequent anaerobic incubation. It seems unlikely that this conclusion is accurate because bacteria will not expend energy producing unnecessary enzymes when it is under desirable growth conditions. Furthermore, if the serum bottles are sealed in order to contain CO in the headspace, it is likely that the batch cultivations will run out of air before the bacteria reach their full growth potential.

The effect of the time at which the culture was shifted from the aerobic growth stage to the anaerobic H_2 production stage was also investigated. The best result was

obtained when the culture was transferred after 12 hours of growth, which corresponds to the start of the stationary growth phase. When the shift was performed at longer and shorter times, the hydrogen production activity obtained in the anaerobic hydrogen production stage was significantly lower (Jung et al. 2002).

The effect of temperature and pH were also examined during the hydrogen production stage. Optimal conditions were found to be between 30-40°C for temperature and between 5.5-7.5 for pH. Above pH 9 or below 5.5, the hydrogen production activity decreased rapidly and the stability of the system became very low.

As previously noted, sucrose and/or glucose was used to supplement the media for all of these experiments, thus adding another carbon source. Consequently, if there was any remaining carbon source after the growth phase, any hydrogen productivity result may not come solely from the effect of CO as a substrate. In order to differentiate the effect of the additional carbon source on the growth and H_2 productivity of *Ci amalonaticus Y19* from the effect of CO, experiments were performed in this research project using only CO as the carbon source added to LB media, as well as using CO with additional glucose in LB media.

Another observation made by the researchers was on the effect of deleting tryptone from the media. Tryptone is hydrolyzed milk protein and is thus made up of many essential amino acids that contribute to the complexity of the media. Jung et al. (1999) reported that while both cases exhibit high rates of CO consumption and H_2 production, the media with tryptone-deletion showed much higher rates than the media containing tryptone. From this result, they further concluded that the presence of a carbon source during the H_2 production stage inhibits the utilization of CO in *Ci amalonaticus Y19*. Biologically, this result is troubling because tryptone consists of an assortment of amino acids, but cannot actually be considered a carbon source. The yeast extract in LB media would be more accurately the carbon source among other things, and thus the effect of the tryptone deletion observed must be attributed to another factor. The research in this thesis addresses the confusion of this result by re-investigating the effect of deleting tryptone from LB media.

The batch shake flask reactors have also been used for kinetic studies in order to determine the kinetic parameters of *Ci amalonaticus Y19* (Jung et al. 2002). The data

follow a second order polynomial curve rather than a straight line, indicating that the cellular system undergoes substrate inhibition during the water-gas shift reaction. This observation suggests that the Andrews model with the substrate inhibition term is more accurate than the Monod model for hydrogen productivity of *Ci amalonaticus Y19* (Jung et al. 2002). Andrews model contains non-competitive substrate inhibition:

$$q = \frac{q_{max} P_{co}}{K_p' + P_{co} + \frac{P_{co}^2}{K_i'}} \tag{14}$$

where q is the specific H_2 production rate (mmol/(g cell x h)), q_{max} is the maximum H_2 production rate, P_{CO} is the partial pressure of CO, K_p' is the Monod constant when the substrate is gas (atm), and K_i' is the substrate inhibition constant (atm). Jung et al. fit their experimental data to Andrews model and obtained a q_{max} of 266.18 mmol/(g cell x h), a K_p of 3.49 atm, and a K_i of 0.18 atm.

Overall, some of the results presented in this section serve as a starting point for the research performed in this study, while others bring up interesting questions, which are further verified or challenged. These questions include: is CO necessary in the growth phase for the production of the key enzymes used during H_2 production? Can CO be used as the sole carbon source for H_2 production or is it necessary to add sucrose and/or glucose? Does the deletion of tryptone indeed increase H_2 productivity, and if so, how can this be more accurately explained?

3.0 Scope and objectives

The world's oil usage per annum is projected to increase by over 40% over the next 25 years to meet our growing need for energy, materials, and chemicals. In the near term, Canada can and most likely will address this increased demand through more aggressive harvesting of its oil sands and offshore reserves. However, these reserves are finite and non-renewable, a fact that is driving an unprecedented rise in retail prices for fuels, growing interest in national energy security, and deep concerns about the diversity, health, and sustainability of our global ecosystems. Our national energy policy must therefore foster development of a broad range of options to reduce vulnerabilities to supply disruptions while protecting the environment. We must find alternative energy and chemicals feedstocks and efficient processes to maintain sustainable economic growth and reduce our dependence on fossil fuels. One viable option is to derive fuels, materials, and chemicals from lignocellulose, a chemically complex and renewable feedstock that can be grown on low-value non-agricultural land and therefore offers the advantage of not competing with food production.

This research focuses on biological hydrogen production using the water gas shift pathway as catalyzed by *Citrobacter amalonaticus Y19*, a chemoheterotrophic mesophilic bacterium classified as gram negative and facultative. Relatively little is known about the H_2 production capabilities of *Ci amalonaticus Y19*, though its ability to produce hydrogen anaerobically using carbon monoxide as the substrate has been demonstrated in the one published study to date (Jung et al. 2002). As the intent of this research is to use this system as a model for evaluating the potential and economics of biological hydrogen production, the following objectives are defined:

1. To find and evaluate a media that allows *Citrobacter amalonaticus Y19* to grow aerobically.

2. To utilize a gas representative of low-grade syngas in a two-stage process to produce H_2 using the biological water gas shift reaction.

3. To determine the effects of media composition and growth conditions on the hydrogen productivity of the system, and relate the H_2 productivity results to enzyme activity. The media modifications include the presence of CO during the growth phase, the addition of glucose, the deletion of tryptone, and the addition of trace metals to the media during the hydrogen production phase.

4. To define a strategy for minimizing the inhibition of enzyme function.

5. To determine whether the mass transfer of CO from the gaseous to the liquid phase is a limiting factor on hydrogen productivity.

In order to accomplish these objectives, extensive experimental work was conducted including a design of experiment (DOE) factorial design on iron and nickel concentrations for objective 3. The value of the thesis is thus to add insight and elaborate on the limited literature available regarding the water gas shift pathway using *Ci amalonaticus Y19* with an emphasis on mass transfer and media alterations, as well as to assess the large scale feasibility of this technology.

4.0 Materials and methods

4.1 Materials and media composition

4.1.1 Microorganism

The microorganism used throughout this study was a pure strain of *Citrobacter amalonaticus Y19*, a chemoheterotrophic facultative bacterium isolated from an anaerobic wastewater sludge digester in Korea. *Citrobacter* is a genus of gram-negative coliform bacteria in the *Enterobacteriaceae* family. *Ci amalonaticus Y19* has been characterized by 16S rDNA analysis, Basic Local Alignment Search Tool (BLAST), and an Application Programming Interface kit (API 20E kit), which is a standardized micro-method for the identification of unknown gram-negative bacteria. The BLAST search showed that the 16S rDNA sequences of the bacteria previously known as *Citrobacter Y19* were 99% identical to those of both *Ci farmeri* and *Ci amalonaticus* in the GenBank database. The API biochemical test kit showed that the general biochemical characteristics of Y19 were exactly the same as *Ci amalonaticus*, and not *Ci farmeri* (Oh et al. 2008). The bacterium was shipped from Korea at room temperature in agar.

4.1.2 Media composition

Several media compositions were investigated throughout the project, thus a base condition is defined and the modifications to this base condition are described. It should be noted that because the process has two stages, the media sometimes differs in the H_2 production stage from in the growth stage if the culture was re-suspended in between.

The base media used was Lysogeny Broth (LB; also known as Luria Bertani) media (Table 3) supplemented with 0.5 mL/L of PTM1 trace salts (Table 4). The PTM1 trace salts were pre-made at the Michael Smith Laboratories (MSL). The trace salts were filter sterilized, stored at room temperature, and covered with foil to avoid light penetration. The LB media, along with all of the glassware and the septa used to seal the bottles, was autoclaved at 121°C for 15 minutes in a Steris-Amsco Century SV-136H Prevac Steam Sterilizer, and stored at 4°C.

Table 3 – Lennox's Luria Bertani media composition (LB)

Compound Name	Description	Amount per L H_2O	Source
Bacto-Tryptone	Pancreatic digest of casein	10g	BD
Bacto-Yeast Extract	Extract of autolysed yeast cells	5g	BD
Sodium Chloride (NaCl)	_____	5g	99.9%, Fisher

Table 4 - PTM1 trace salts composition, pre-made from MSL

Compound Name	Compound Formula	Amount per L H_2O
Cupric sulfate, pentahydrate	$CuSO_4\text{-}5H_2O$	6.0 g
Sodium iodide	NaI	0.08 g
Manganese sulfate, monohydrate	$MnSO_4\text{-}H_2O$	3.0 g
Sodium molybdate, dihydrate	$Na_2MoO_4\text{-}2H_2O$	0.2 g
Boric Acid	H_3BO_3	0.02 g
Cobalt chloride, hexahydrate	$CoCl_2\text{-}6H_2O$	0.5 g
Zinc chloride	$ZnCl_2$	20 g
Ferrous sulfate, heptahydrate	$FeSO_4\text{-}7H_2O$	65 g
Biotin (aka vitamin H or B_7)	$C_{10}H_{16}N_2O_3S$	0.2 g
Sulfuric acid	H_2SO_4	5.0 mL

Modifications made to the base media included the deletion of tryptone from the base media, the addition of glucose (anhydrous, EMD chemicals), and the addition of buffer. In more detail, the deletion of tryptone was done during the H_2 production stage and resulted in a media containing 5g/L of yeast extract, 5g/L of NaCl, and 0.5mL/L of PTM1 salts. When glucose was added to the base media, it was added at a concentration of 5g/L. The buffer used to stabilize the pH was a 20mM potassium phosphate buffer at pH 6.5. A 1M-potassium phosphate buffer was made from 200mL of 1M-monobasic potassium phosphate (99.5%, Fisher) and 140mL of 1M-dibasic potassium phosphate

(99.5%, Fisher). In the instances when the reaction was buffered, 0.8mL of the 1M-potassium phosphate buffer was added to the 40mL LB media resulting in a 20mM buffer concentration.

4.1.3 Design of experiments (DOE)

In a DOE, a factorial design was completed to observe the effect of adding trace metals to the base media. The trace metals investigated were iron ($FeSO_4 \cdot 7H_2O$, 101.0%, Fisher) and nickel ($NiCl_2 \cdot 6H_2O$, 98.88%, Fisher) at three different concentrations for each. A full factorial was effectuated on this 2-factor, 3-level experimental design. The base amount of iron contained in the PTM1 salts was taken into account and the total concentrations are the numbers reported in Table 5. A 10g/L nickel solution and a 20g/L iron solution were prepared as stock solutions for ease of addition to the fermentation broth. The nickel and iron solutions were filter sterilized before being added to the media for the H_2 production stage.

Table 5 - Metal ion concentrations

Level Designation	Fe concentration (mg/L)	Ni concentration (mg/L)
0	32.5	0
1	125	62.5
2	250	125

4.2 Methodology

The experiments were performed as two stage batch reactions in 165mL Wheaton serum bottles made of clear borosilicate glass. A 12 hour aerobic growth stage was used to increase the cell density above 2 g/L, at which time the culture was switched to an anaerobic environment by purging the crimp-sealed bottles with a gas mixture of 40% CO in helium.

4.2.1 Citrobacter amalonaticus Y19 growth

Cultivations were performed at 30°C in an incubator shaking at a speed of 250rpm. The liquid working volume was 40mL in serum bottles of 165mL total volume. 0.5 mL of *Ci amalonaticus Y19* glycerol stock (Appendix A) was used as inoculum in 40mL of LB media (unless modifications are specified otherwise). While growth was always done aerobically, the serum bottles were either sealed or open to air during growth. For the experiments where the bottles were sealed, a rubber crimp seal was put in place after inoculation, followed by an addition of 6.5mL of CO gas using a sterilized gas tight syringe. It should be noted that for the growth curve analyses of *Ci amalonaticus Y19* under sealed conditions, 10mL of CO were injected rather than the 6.5mL of CO used for the experiments that were carried on to the next stage. The bottles grown open to air were covered with foil to avoid contamination.

After the 12-hour growth stage, a 1mL sample was taken from the fermentation broth to measure cell density. When pH was measured after the growth stage, a 5mL sample was taken from the liquid phase. Organic acid concentrations were only measured at the end of the growth stage when the process was terminated at this point; therefore, the entire fermentation broth was further filtered as explained in section 4.3.3.

4.2.2 Hydrogen production

The anaerobic H_2 production stage was started immediately after the 12-hour growth stage. Once the cell density was measured, depending on the specific experiment, any additional media components such as nickel, iron and buffer were added to the fermentation broth. For example, in the nickel and iron factorial design experiments, 0.5mL of the filtered 10g/L nickel solution was added with a pipette directly to the liquid broth at this stage for the highest nickel concentration of 125mg/L. Bottles that were open to air during growth were then crimp sealed with sterile septa once all the additional media components were added. The headspace of each reactor was then purged with a 40% CO in He gas mixture (v/v) for two minutes in order to remove all of the air and ensure that no oxygen was present. The purging was done continuously through the septum with one needle connected directly to a gas cylinder containing pre-mixed 40%

CO in He (v/v), and another needle of the same gauge size which is not connected to anything allowing for the gas to circulate. A pressure of 6 psig is sustained in the line from the cylinder with a regulator to maintain a constant gas flowrate. The time at which the bottles are purged represents time zero for all hydrogen production graphs. The purged serum bottles were placed in a shaking incubator at 30°C and 250rpm for approximately 100 hours or until all the carbon monoxide was converted into hydrogen and carbon dioxide. Gas phase measurements of H_2, CO, and CO_2 concentrations were taken every 10-12 hours depending on the pace of CO conversion.

For the experiments where pressure was increased above 1 atmosphere, a pressure gauge (Omega engineering, 0-100psi, Connecticut) inserted through the septum with a needle was used to monitor the pressure increase in the bottle. After the 2 minutes of purging, the unconnected needle was removed allowing the pressure to build by pumping more of the 40% CO in He gas mixture (v/v) into the bottle.

4.2.3 Re-suspension procedure

In specified cases, cells were re-suspended in fresh media between the growth and hydrogen production stages. After the 12-hour growth period, the cell cultures were spun down at 5500rpm for 10 minutes using a Fisher scientific 5810R centrifuge. The supernatant was discarded and 40mL of fresh media was added to the cells. Cell density was always measured before and after re-suspension.

4.3 Analytical and measurement techniques

4.3.1 Cell density and pH

Samples were collected from the fermentation medium for monitoring the concentration of Ci amalonaticus Y19, and pH. 1mL samples were collected for cell density measurements and 5mL samples for pH. Two UV/visible spectrophotometers were used throughout the study: a Milton Roy Spectronic 20D+, and a Pharmacia Biotech Ultrospec 1000. The cell growth was measured in terms of the optical density (OD) at 600nm. The 1mL samples collected before and after the H_2 production stage of the experiment were diluted in order to keep the OD measurement below an absorbance of

0.9. In order to find the conversion from optical density to dry cell weight, *Ci amalonaticus Y19* was grown in a serum bottle open to air in 40mL LB media supplemented with 0.5mL/L PTM1 salts. Duplicate bottles were incubated at 30°C and 250 rpm for 14 hours. The OD was first measured, and then the broth was centrifuged at 14,000rpm for 5 minutes. The OD of the decanted supernatant was measured in order to ensure no cells remained in the liquid. The cells were dried in an oven at 70°C for 12 hours before measuring the dry cell weight. The dry cell weight conversion was found to be 0.48 ± 0.01 g DCW /L /unit of OD.

The pH meter used was a VWR SB20 sympHony. pH was measured after the completion of the H_2 production phase, and occasionally in between the growth and H_2 production stages.

4.3.2 Gas concentrations

Gas phase analysis involved monitoring the concentrations of H_2, CO, and CO_2 formed during the fermentation process using a gas chromatograph (GC). The GC used is a Varian model 3800 equipped with a thermal conductivity detection (TCD) system and a 6' CTR I packed column by Alltech (Calgary, Alberta). The CTR I packing is made up of concentric columns, the outer column is packed with an activated molecular sieve and the inner column is packed with a porous polymer mixture. The operational temperatures of the rear valve, injector, and detector were all 120°C. For H_2 detection, nitrogen was used as the carrier gas with a flow pressure of 5psi and a column oven temperature of 35°C held for 4.5 minutes. The retention time of H_2 under these conditions was around 2.9 minutes. For CO and CO_2 detection, helium was used as the carrier gas with a flow pressure of 5psi and a column oven temperature of 90°C held for 12 minutes. The retention times of CO and CO_2 were approximately 9.0 and 1.5 minutes, respectively.

Samples of 0.5 mL in volume were taken from the headspace of the crimp-sealed serum bottles with a gas tight syringe and manually injected into the CTR I column. The software used to communicate with the GC was Varian's Star chromatography workstation System Control version 6.41 and to acquire areas under the curves was Varian's Star chromatography workstation Interactive Graphics version 6.41.

Calibrations were performed for H_2, CO, and CO_2 using 2% H_2 in N_2 (v/v), 40% CO in He (v/v), and 2% CO_2 in He (v/v) as standards, respectively (Appendix A).

· Injecting the same sample several times tested the repeatability of the GC measurements. The results showed a very high repeatability with an average standard deviation of 2% of the total value.

4.3.3 Organic acid concentrations

A Waters High-Performance Liquid Chromatography (HPLC) system equipped with a 2487 Dual λ absorbance detector and an IC-Pak ion exclusion column was used to determine the presence and concentrations of small acids such as lactate, acetate, and formate. Samples were prepared by first centrifuging the fermentation broth at 5500rpm for 10 minutes, then filtering the supernatant with a 0.22μm syringe driven filter before manual injections of 50μL into the HPLC. The eluent used was 13mM H_2SO_4 (95-98%, Fisher). The software used to communicate with the HPLC pump and detector, and to acquire areas under the curve was Waters' Breeze version 3.20.

Organic acids were present at several retention times: 8.3, 9.0, 9.8, 11.8, 13.4, and 14.5 minutes. The elution times of 8.3, 9.0, 9.8, and 11.8 minutes corresponded to lactic acid, formic acid, acetic acid, and fumaric acid, respectively. Even though a wide range of compounds were tested, the compounds with 13.4 and 14.5-minute retention times were not identified. It is assumed that these compounds have a higher electrical affinity for the IC-Pak ion exclusion column. Calibrations were performed for some of the known acids using pure chemicals under their sodium salt form: sodium acetate ($\geq$ 99.0%, enzyme grade, Fisher), and DL-lactic acid sodium salt (98%, Sigma) (Appendix A).

5.0 Results and discussion

5.1 Two-stage process for H_2 production from CO

5.1.1 Growth stage

In order to verify the necessity of CO during the growth stage, two conditions were investigated: a completely aerobic system where the serum bottle was covered only with aluminum foil, and a crimp-sealed aerobic system that contained 8% CO (v/v) in the gas phase, with the remainder being air (Figure 5). All experiments were performed in a shaking incubator where the temperature and agitation rate were maintained constant at 30°C and 250rpm, respectively.
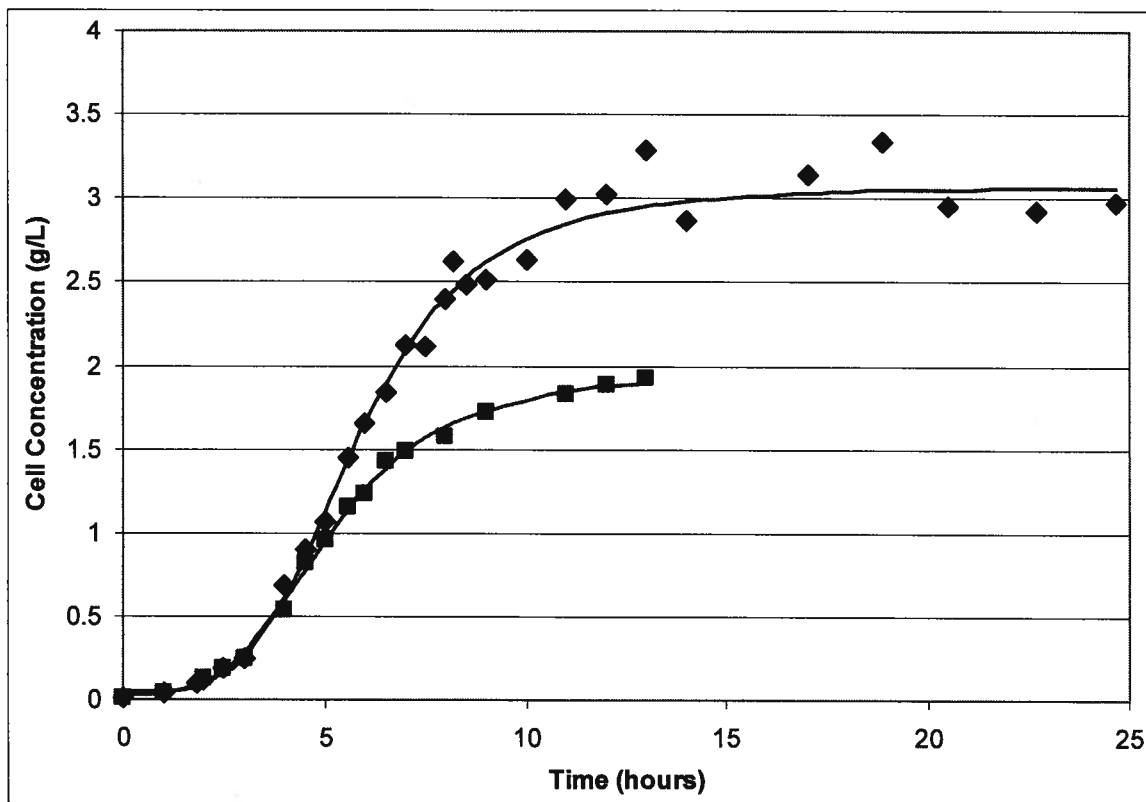
Figure 5 - *Citrobacter amalonaticus Y19* growth curve under two conditions. Symbols: -♦-, cell concentration under completely aerobic conditions; -■-, cell concentration under sealed aerobic conditions with 8% CO (v/v) present in the headspace. Symbols represent the experimental data and lines represent the best-fit model obtained using CurveExperts 1.3.

After the lag phase and during the exponential growth phase, from 2.5 to 4.5 hours, the specific growth rates for the open and sealed conditions were 0.84 and 0.74 h^{-1}, respectively (see Appendix B for logarithmic growth curve). Following the exponential growth phase, there is a linear growth phase for the time period from 4.5 to 7 hours. The growth rates during this linear growth phase are 0.54 h^{-1} for the open condition, and 0.45 h^{-1} for the sealed condition. At 7 hours, the decelerated growth stage began, followed by the stationary phase at around 12 hours. The maximum cell densities obtained for the open and sealed conditions were 3.1 and 1.9 g/L, respectively. These results indicate that while the growth patterns were almost identical prior to the 4-hour mark, the completely aerobic conditions allowed *Ci amalonaticus Y19* to grow to higher cell densities. This signifies that while the CO concentration in the sealed serum bottles is not inhibitory to cell growth, there is likely a lack of oxygen after 4 hours. When sealed, the bacteria run out of air, which prevents cell growth to its full capacity.

The concentration of organic acids was also measured before and after growth for both the open and sealed conditions. The effect of buffering the growth at a pH of 6.5 with 20mM potassium phosphate was also considered (Figure 6). While other organic acids were present due to the complex nature of the LB media, lactate and acetate were the only components that increased significantly in concentration during the growth stage. Lactate was produced during the growth stage to a final concentration of 4 g/L after 12 hours of growth whether the system was open or sealed. Under open conditions, the concentration of acetate was 2.3g/L, while sealed conditions resulted in acetate concentrations up to 3.4g/L. This increase in acetate concentration between the open and sealed conditions, in the absence of buffer, was statistically significant at a 95% confidence level. This suggests that acetate may be produced more rapidly under sealed growth conditions once the culture ran out of air and became anaerobic. When the system was buffered, the concentrations of lactic and acetic acid decreased proportionally for all conditions.

In the previous studies on this organism (section 2.4.3), *Citrobacter amalonaticus Y19* grew with a specific growth rate of 0.7 h^{-1} to a cell density of 2g/L in the presence of a CO-air (20:80, v/v) mixture, while a completely aerobic condition was not reported (Jung et al. 1999b). This culture was sealed and thus may have run out of oxygen after a

certain length of time, which would explain the lower cell density of 2g/L as compared to the cell density of 3.1 g/L obtained under completely aerobic condition (Figure 5).
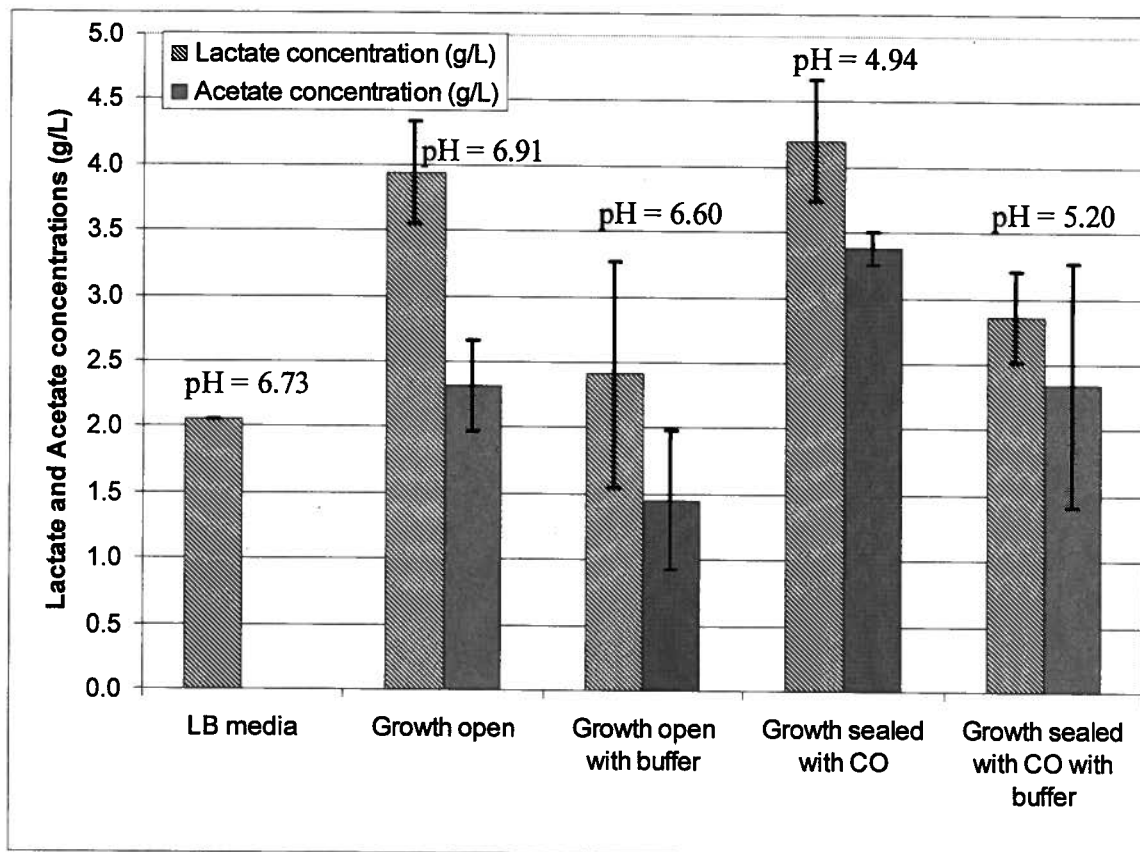
Figure 6 - Concentration of lactate and acetate, as well as pH after the growth phase. Hashed boxes, lactate; dotted boxes, acetate. Error bars represent the average of 2 measurements.

The effect of CO content in the gas phase during the growth stage was also previously studied, and the researchers (Jung et al. 2002) determined that the hydrogen production activity was almost negligible when no CO was present in the growth stage. The conclusion made based on this result was that the presence of CO during the growth stage induced the synthesis of the relevant enzymes that were later activated in the H_2 production stage (Jung et al. 2002). As explained in section 2.4.3, this result was troubling because bacteria have a tendency to only produce enzymes that are immediately necessary for their survival. Since the bacteria were under desirable growth conditions, the production of CO dehydrogenase and hydrogenase that were to be activated in a later stage seemed unlikely. Neither the previous study, nor this study created an assay for these two enzymes to confirm or deny their presence during the growth stage. One such

assay would be necessary to assess the stage at which the CO dehydrogenase and hydrogenase enzymes are produced. In this study, it has been shown that the sealed growth condition with 8% CO (v/v) present in air decreased the growth rate, and consequently, the final cell density attained. This result was most probably attributed to the fact that the serum bottles were sealed, and not to the presence of CO during growth; however, this was not verified with dissolved oxygen (DO) measurements. It should be noted that these results, along with the increased simplicity of the reactor conditions when open to the atmosphere, make the completely aerobic condition favorable over the sealed condition. The effect of these growth conditions on the H_2 productivity in the anaerobic phase will be discussed in section 5.3.

5.1.2 Hydrogen production stage

Because *Ci amalonaticus Y19* does not produce hydrogen aerobically, a two-stage process was suggested where the bacteria are first grown aerobically followed by an anaerobic hydrogen production stage. After 12 hours of growth, the serum bottles were crimp-sealed and purged for two minutes with a gas mixture of 40% CO in helium (v/v). The hydrogen production phase was carried out until the culture used all of the available CO substrate. Figure 7 shows the evolution of CO, H_2 and CO_2 for the H_2 production stage of a buffered system where growth was open to air and the cells were re-suspended in fresh media after the growth stage. Note that H_2 concentration curves for other conditions (all experimental conditions investigated) are shown in Appendix B.

The increase in H_2 and CO_2 concentration was proportional to the decrease in CO concentration as expected from the water-gas shift reaction:

$$CO + H_2O \longrightarrow H_2 + CO_2 \qquad \Delta G^\circ = \text{-20 kJ mol}^{-1} \qquad (1)$$

The ΔG° is reported at ambient temperature and pressure. The conversion of CO into H_2 and CO_2 was stoichiometrically consistent with the theory. Also, the thermodynamics of the reaction suggest that all of the CO will be converted since the reaction is shifted to the right, and indeed, the CO is depleted beyond the detection limit of the gas chromatograph. The molar yield of H_2 on CO was 70 ± 4% for most conditions that did not exhibit any inhibition characteristics. This suggests that some of the CO substrate is used to produce by-products, possibly in the form of organic acids.
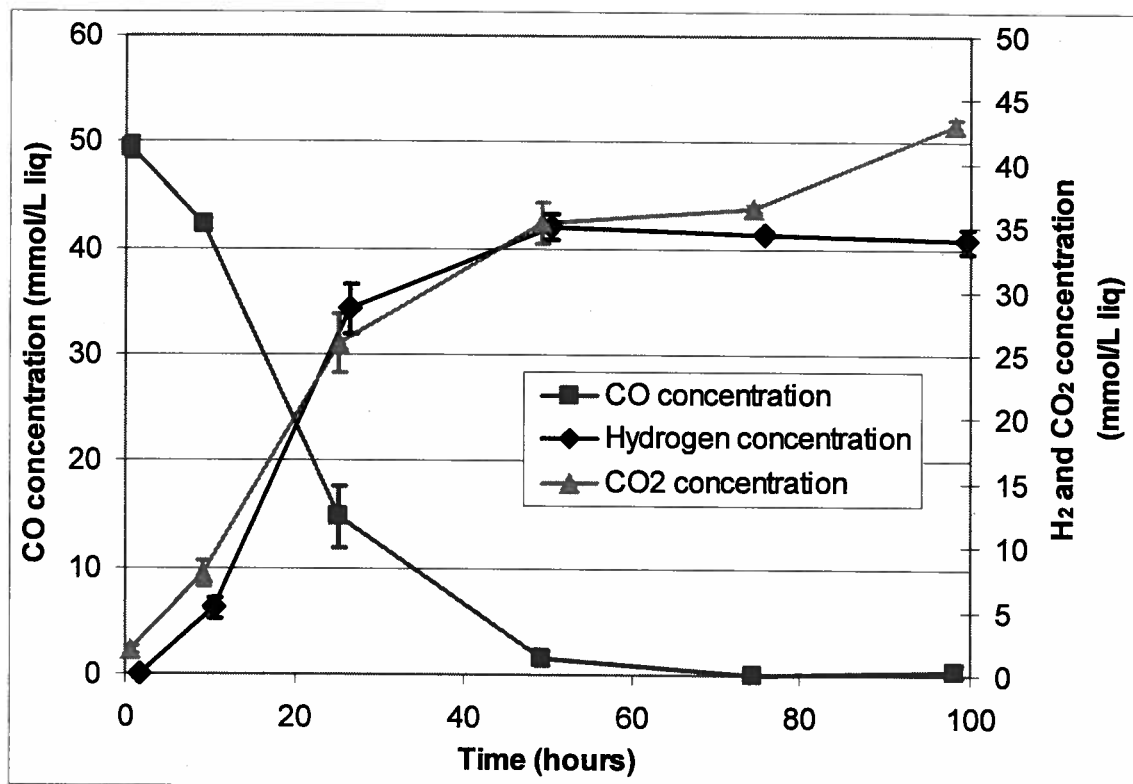
Figure 7 – CO, CO_2 and H_2 concentrations during the H_2 production phase for a buffered system where growth was open to air. Purged with 40% CO in He (v/v) at time 0. Symbols: -◆-, H_2; -■-, CO; - ▲ -, CO_2. Data points represent the average of 2 runs and the error bars represent the standard deviation.

In order to convert H_2 concentrations into H_2 productivities, the slope between each set of consecutive data points was calculated. This slope represents the H_2 productivity at the average time between these two data points (Figure 8). It is known that while batch production is very helpful for initial system characterization, it is inefficient. Continuous H_2 production would thus be necessary to ultimately commercialize this H_2 producing system. Therefore, only the maximum H_2 productivities attained are relevant since the decrease in productivity was simply due to the gaseous substrate, CO, being depleted. The time at which these maximum productivities were achieved (t_{max}) is also shown because it indicates the amount of time necessary to produce the enzymes used for H_2 production. It should be noted that if the lifetime of the enzyme activity is long, attaining a shorter t_{max} might not be an important parameter. The maximum productivity is illustrated in the form of bar graphs for the remainder of this discussion. While the slope of consecutive data points gave the time evolution of H_2 productivity, the maximum

42

productivities were more accurately determined mathematically by using CurveExperts 1.3 to find the best-fit model of H_2 concentration versus time, when sufficient data was available. The best-fit model for the lag and H_2 production phases used was a 3rd degree polynomial:

$$[H_2] = a + bt + ct^2 + dt^3 \qquad (15)$$

Setting the second derivative of this equation equal to zero, and solving for the 1st derivative of H_2 concentration provided the maximum productivity.
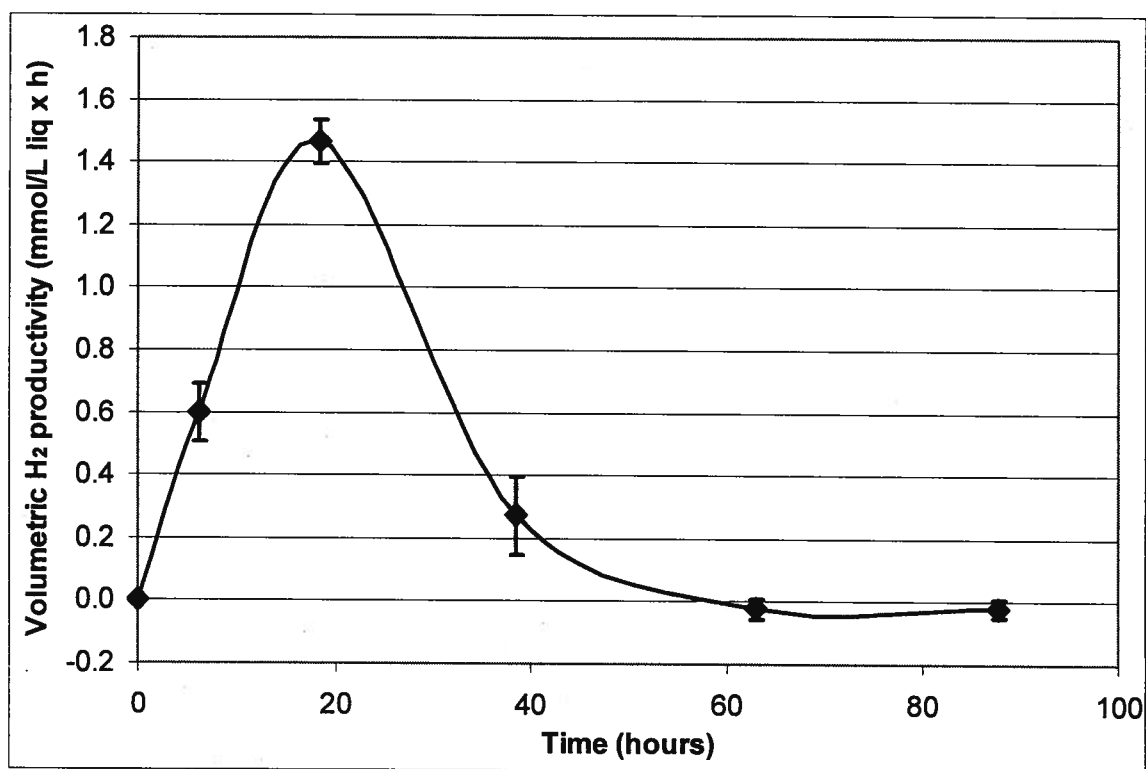
Figure 8 – Volumetric H_2 productivity for a buffered system where growth was open to air. Purged with 40% CO in He (v/v) at time 0. Data points represent the average of 2 runs and the error bars represent the standard deviation.

Organic acid concentrations were measured after the H_2 production stage for both a buffered and non-buffered system. Unlike the growth stage, there was no increase in lactic acid production during the anaerobic H_2 production stage. However, acetic acid concentration increased from 0 g/L in LB media to 3 g/L in the buffered and non-buffered systems alike. Formate was also produced in the H_2 production stage where there was none in pure LB media, and an unknown organic acid that eluted at 14.5 minutes from the HPLC also increased dramatically in concentration during this stage.

Although the composition of this organic acid that elutes at 14.5 minutes is unknown, it is assumed that it has a high electrical affinity to the IC-pak charged solid separation medium in the column, as it is the compound that is retained the longest.

The maximum H_2 productivities for all the conditions throughout this research project ranged from 0 to 1.5 mmol H_2/ (L x h) (or 0 to 0.7 mmol H_2/(g cell x h)) as will be detailed in the following sections. While this suggests that many of the conditions investigated had a significant impact on the H_2 productivity, it is also a lower productivity than what has been previously reported for this organism. The research group that has investigated using *Ci amalonaticus Y19* for the water gas shift reaction reported a maximum specific H_2 production activity of 27.1 mmol H_2/ (g cell x h) (Jung et al. 2002). Using the cell concentration range of 0.1 to 0.4mg/mL reported for the measurements of specific H_2 production activity, the maximum volumetric H_2 productivity they attained was between 2.71 and 10.84 mmol H_2/ (L x h). The discrepancy between these results of up to one order of magnitude can be explained by several reasons including the different media used due to a lack of details in the publications, and an alternate method of measuring the H_2 productivity.

The exact composition of the media was not specified in the literature publications on this organism, and the papers that were referred to regarding the media resulted in a fruitless effort to find the exact composition used. Direct contact with the authors of the publication resulted in vague descriptions of media compositions that sometimes conflicted with what was reported in the publications. The conflict mainly regarded the supplementation of the media with either glucose or sucrose. Sucrose was reported in the publication, but an email communication suggested that *Ci amalonaticus Y19* did not utilize sucrose but rather glucose. The deletion of tryptone from the media was also declared in an earlier publication but not mentioned in a later paper (Jung et al. 2002, Jung et al. 1999b). These many unknowns regarding the media composition used for the aerobic and anaerobic stages of the reaction could be one explanation for the discrepancy in H_2 productivities.

The differing methods of measuring H_2 productivity seemed to be the major cause of the discrepancy between the results reported here and the results from the Korean research group. According to the previous research papers, specific H_2 production

activity was determined as a point measurement after a 24-hour induction phase in 20% CO. The cells were harvested after 24 hours and re-suspended in a buffer solution at a concentration between 0.1 and 0.4 mg/mL. A 1mL sample of this cell suspension is charged with a CO-Argon gas mixture in the headspace and the H_2 concentration is then measured for an hour. These point measurements at 24 hours are not as insightful into the kinetics of the reaction as the continuous measurements done in this research. Re-suspending the cells at a different concentration and with fresh CO may also affect the measurement accuracy.

Overall, this discussion concludes that a comparison between the volumetric H_2 productivities obtained in this research with the specific H_2 production activities obtained in the previous publications is invalid. Rather than comparing values with previous publications, the H_2 productivities obtained are evaluated in comparison to a base case presented here, and each experimental condition was run in parallel with standards.

5.2 Effect of CO concentration during H_2 production phase

In order to select the best concentration of CO to use in the experimental runs, two factors were considered: the possibility of substrate inhibition at high levels of CO, and the typical amount of CO in low-grade synthesis gas. In order to assess whether substrate inhibition takes place, experiments were performed at several initial CO concentrations ranging from 7 to 100% CO (v/v), with the remainder of the gas phase being helium. The cultures were grown open to the atmosphere in LB media, and then sealed and purged to ensure the oxygen was completely removed, without re-suspension between the growth and H_2 production stages. Helium was used as the inert gas in the system because it had the most distinct conductivity, and thus retention time, in the gas chromatograph when considering all the gases measured (CO, CO_2 and H_2). For the range from 7-60% CO, the serum bottles were first purged with pure helium, and the headspace ratio was then adjusted by removing the appropriate amount of helium and adding CO using a gas-tight syringe to ensure the bottle was not pressurized in this process. Figure 9 illustrates the results obtained for this range of CO concentrations.

This figure illustrates that while the H_2 productivity after the lag phase of approximately 15 hours seemed relatively constant throughout this range of

concentrations, as seen from the slope of the curves, the H_2 production stage lasted longer for higher CO concentrations. This is simply because at low initial CO concentrations, the substrate was exhausted faster. Figure 9 also shows no evidence of substrate inhibition up to initial concentrations of 60% CO.
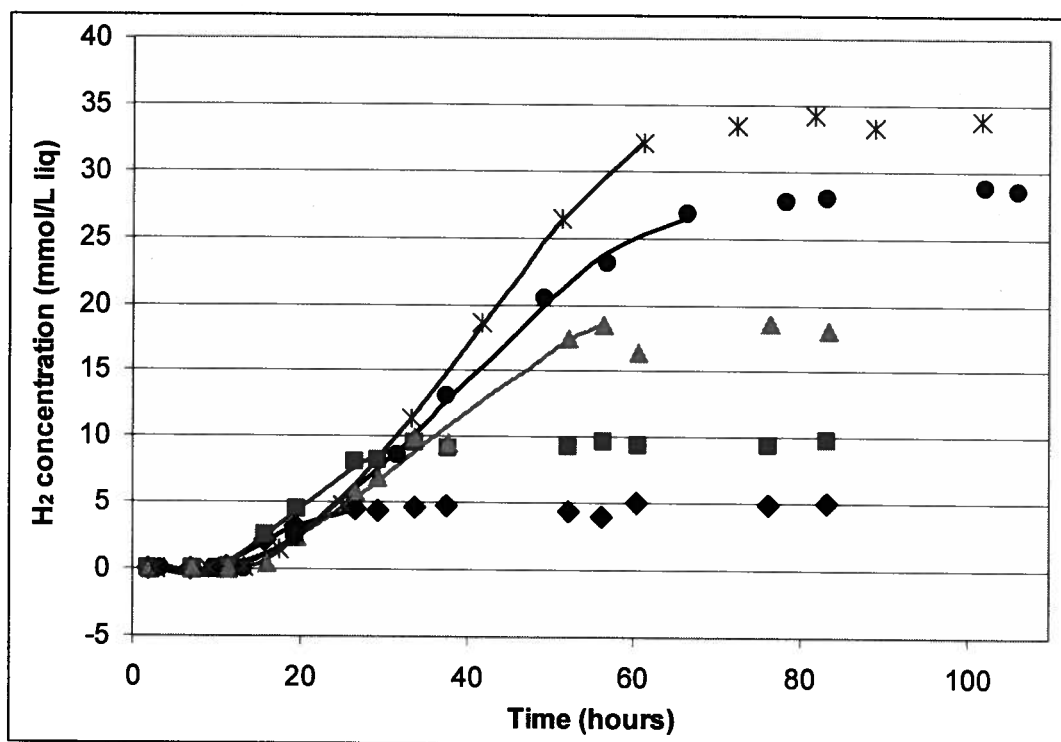
Figure 9 - Batch evolution of H_2 concentration for varying initial CO concentrations. CO concentrations vary from 7 to 60% CO in Helium (v/v). Symbols: -♦-, 7% CO; -■-, 14% CO; -▲-, 27% CO; -●-, 40% CO; -*-, 60% CO. Symbols represent the experimental data and lines represent the 3rd degree polynomial best-fit curves.

An estimate of maximum H_2 productivity was obtained by fitting the H_2 concentration versus time data to a 3rd degree polynomial equation and setting the 2nd derivative of this fitted equation to zero as described in section 5.1.2 (Figure 10). Since this screening experiment was used to determine which concentration of CO should be used for the remainder of the tests, only one serum bottle was run for each condition. First, it should be noted that since the maximal H_2 productivity at the 6.8% CO condition was reached so quickly, only 6 data points were used to fit the 3rd degree polynomial, and only three of these data points were collected during the H_2 production phase, decreasing the reliability of this model and the validity of the maximal H_2 productivity. Looking at the remaining three conditions in Figure 10, tripling the concentration from 13.6% CO to

40% CO (v/v) resulted in nearly doubling the time at which the maximum productivity occurred from 20 to 38 hours, but the maximum H_2 productivity only increased by 0.1 mmol/ L liq x h, or 25%. The total time it took to convert CO including the lag phase ranged from 26 hours for 7% CO to 66 hours for 40% CO. This shows that using higher initial CO concentrations allows for significantly longer time periods to monitor the conversion of CO to H_2, which is more informative because the kinetics can be observed for longer.
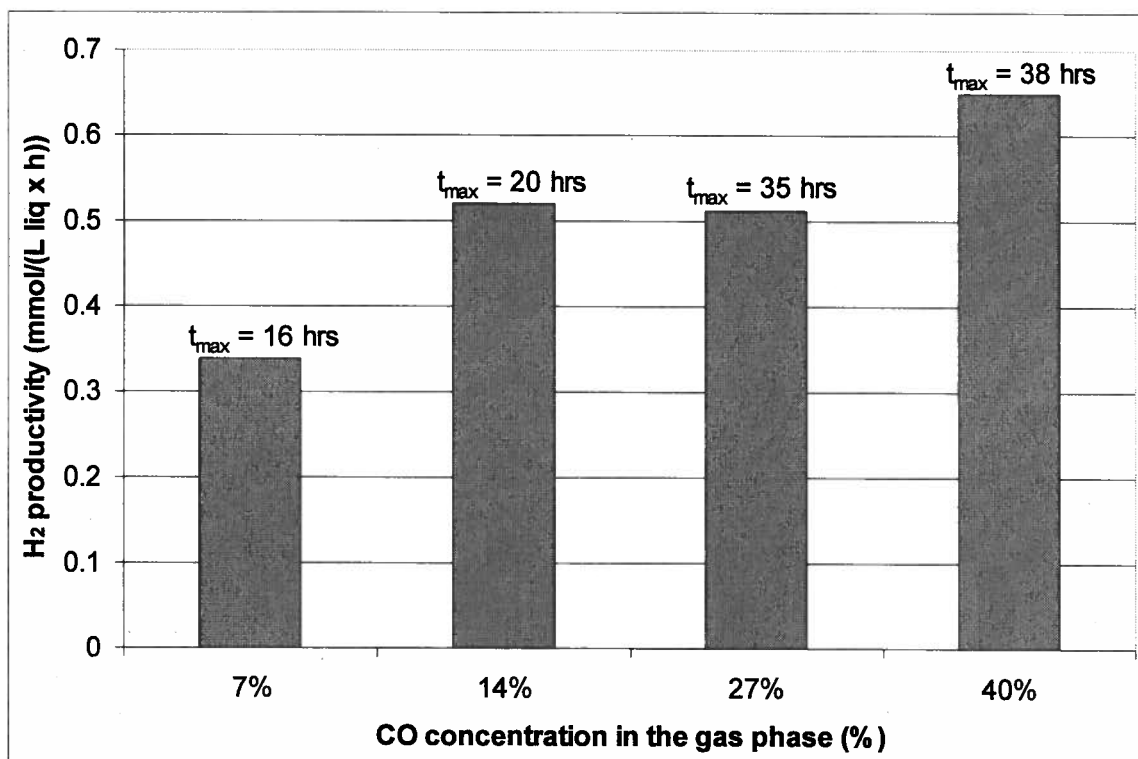
Figure 10 - Maximum H_2 productivity and the time at which the maximum productivities are reached for initial CO concentrations ranging from 7 to 40%CO in He (v/v).

For concentrations equal to or above 60%, the reverse method was performed to attain the desired concentrations. Serum bottles were first purged with 100% CO for two minutes, and the headspace ratio was then adjusted by removing CO and adding pure helium (Figure 11). This experiment showed decreased H_2 production rates for bottles that were first purged with 100% CO, suggesting that this purging process inhibits the H_2-producing enzymes. The H_2 was produced at a much slower rate and the CO was not completely exhausted after 105 hours. Perhaps purging the culture with pure CO drives

the CO, which has a very low solubility in water, into the media, resulting in an underestimation of the initial CO concentration. While this substrate inhibition at very high levels of CO is present, it is not a concern for the biological H_2 production process, as these high levels of CO are not in the targeted range of initial CO concentrations, which is under 40% CO (v/v).
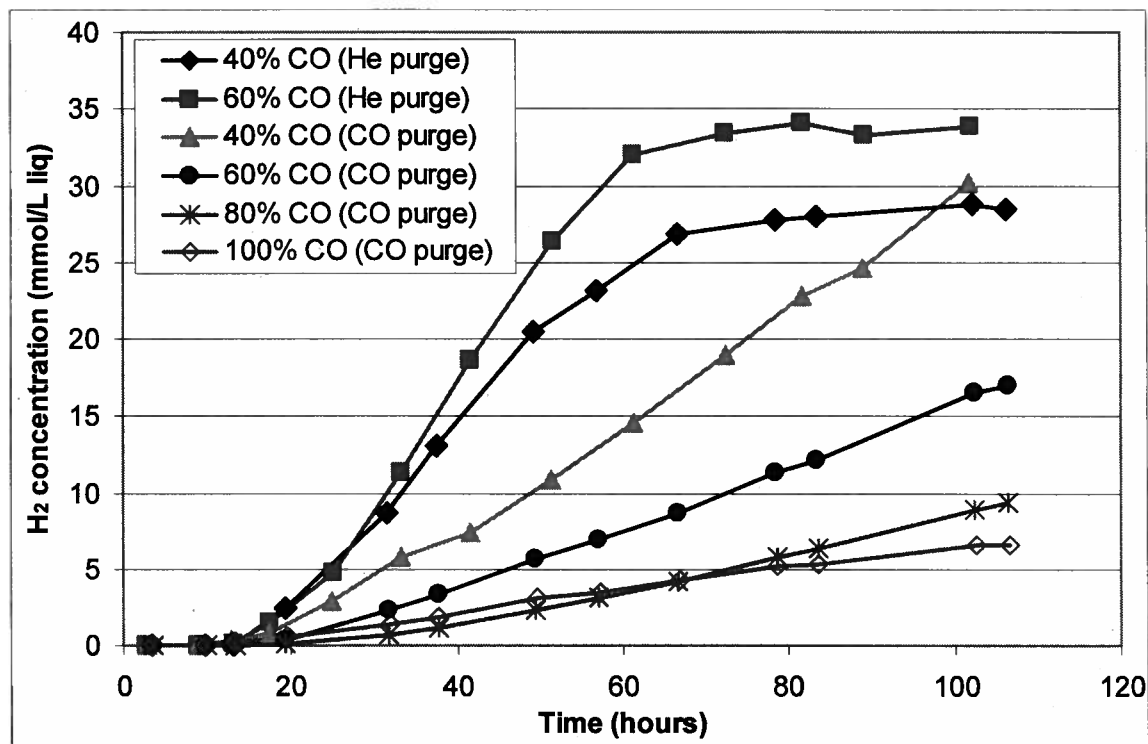
Figure 11 - Effect of the purging gas used (CO or He) on the H_2 concentration evolution. Initial CO concentration adjusted after purge from 40-100% (v/v). Symbols: -◆-, 40% CO, purged with He; - ■-, 60% CO, purged with He; -▲-, 40% CO, purged with CO; -●-, 60% CO, purged with CO; - *-, 80% CO, purged with CO; -◊-, 100% CO, purged with CO. Symbols represent data points, and lines connect the symbols for ease of visualization.

Low-grade synthesis gas is the desired substrate for this system as it is a low chemical energy feedstock that can be considered a waste stream. As previously defined, low-grade syngas has a low CO concentration, under 20% CO, and is at a low temperature, close to ambient temperatures. While lower than 20% CO is the targeted range of initial CO concentration, this screening experiment showed that increasing the initial CO concentration to 40% significantly increases the time period available to observe the conversion of CO to H_2, while not reaching the limit of substrate inhibition.

40% CO was thus considered optimal as it did not inhibit the reaction, but allowed for sufficient observation of the reaction kinetics. As for the temperature, the substrate was received and dispensed into the system at ambient temperatures and heated up to 30°C in the shaking incubator. While syngas with less than 20% CO can still be efficiently processed by a conventional WGS using a metal catalyst, it would not be economically beneficial to heat up syngas that is at ambient temperatures. In conventional WGS, LTS reactions operate between 200 and 260°C, and HTS reactions operate between 300 and 500°C. For situations where syngas is at ambient temperatures, the biological WGS can thus be very practical.

The method of purging the serum bottles with pure gasses and adjusting the concentration to the desired ratio afterwards caused several problems, including a significant effect from the purging gas used, but also compromising of the septa used to seal the serum bottles by repeated injections with needles. While the data is not shown, several data sets had to be discarded because the many holes created in the septa by repeated needle injections caused air to enter the bottles. This end to the anaerobic conditions in the serum bottle caused an abrupt halt to H_2 production. All experiments hereafter were thus purged with a pre-mixed 40% CO in He mixture (v/v) directly from a gas cylinder to minimize experimental problems such as holes in the septa, and to maximize the observation time of the reaction kinetics without reaching a level of substrate inhibition.

It should be noted that syngas generally contains not only CO, but also many other components such as CO_2, H_2, and minor amounts of other gases such as CH_4, N_2, and H_2S. There is a large variation in syngas composition depending on the source from which it was produced. The gas used as substrate for the experiments in this research contained only CO and inert gas at the start of the anaerobic phase of H_2 production. It would be interesting to investigate the impact of the other components of syngas on the biological WGS reaction. Since H_2 and CO_2 are on the right hand side of the WGS reaction, it is speculated that the presence of these gases might decrease the efficacy of the process by product inhibition. At ambient temperatures, the WGS is shifted to the right, so the magnitude of the product inhibition is unknown, but may only be quite small.

5.3 Effect of media composition

The H_2 productivities obtained thus far in the research were low, and so effort has been put into investigating various means of increasing these productivities. One possible method of increasing the H_2 productivity was to develop a media optimized for H_2 production. The initial parameters were selected based on literature data using *Ci amalonaticus Y19* (Jung et al. 2002 and 1999b). These parameters include the presence of CO in the headspace during the growth stage, the addition of a carbon source such as glucose or sucrose to the media, and the deletion of tryptone from LB media. As explained in section 2.4.3, it is speculated that these media modifications do not have as positive of an effect on H_2 productivity as is claimed in the two literature studies. The maximum H_2 productivities obtained experimentally for these modifications are expressed in Figure 12. The productivities were found using the maximum slope of consecutive data points rather than the 3rd degree polynomial best-fit approach because the small amount of data points would produce inaccurate curve fitting with insufficient degrees of freedom. The H_2 concentration curves for these conditions are in Appendix B.
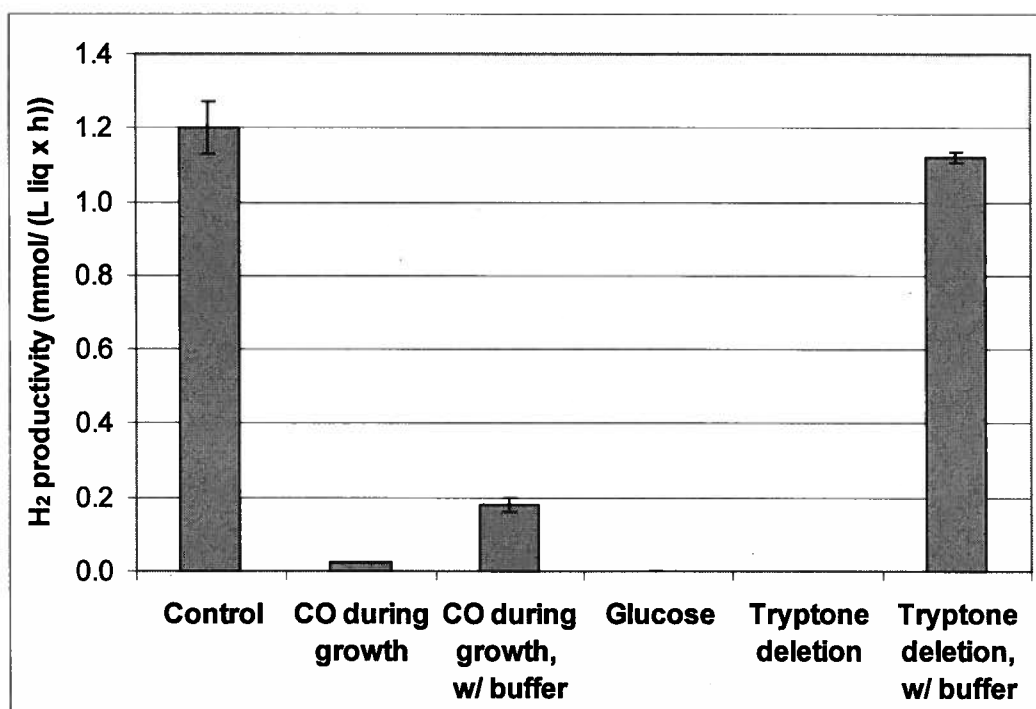

Figure 12 - Effect of addition of CO during the growth phase, addition of glucose in the H_2 production phase, and deletion of tryptone in the H_2 production stage on H_2 productivity compared to an average productivity found throughout the research experiments. Bars represent the average of 2 runs and the error bars represent the standard deviation.

The maximum H_2 productivity attained for a re-suspended system in LB media, where the growth stage was completely aerobic, was approximately 1.2 mmol H_2/ (L x h) with pH 6. This productivity serves as a control to compare with the other productivities obtained. The cell density at the beginning of the H_2 production stage was between 2.0 and 2.3 g cell/L liq for all of these conditions except for the conditions with CO present during the growth phase. As explained in section 5.1.1, the sealed growth condition with CO present resulted in a lower cell density. The cell density at the start of the H_2 production stage for both sealed conditions, with and without buffer, was approximately 1.4 g cell/L liq.

The sealed growth condition with CO present reduced H_2 productivity in the H_2 production stage by a factor of 50 to 0.023 mmol H_2/ (L x h). The pH was measured after the H_2 production stage when CO was present during sealed growth and was found to be 5, which is below the optimal range of 5.5-7.5 (Jung et al. 2002). With the addition of 20mM potassium phosphate buffer at pH 6.5, the maximum H_2 productivity increased to 0.18 mmol H_2 /(L x h), still a 7-fold decrease from the average number. The pH for this buffered solution was 5.3, still below the optimal range, thus suggesting that a higher buffer concentration should have been used. These results suggest that the sealed growth condition with CO present produced some acidic metabolites at high concentrations that decreased the pH significantly. As shown in Figure 6, the concentration of lactic acid was similar for both the opened and sealed growth conditions; therefore, acetic acid, which was produced at higher concentration in the sealed condition, may be the cause of the pH decrease.

It should be noted that the experiments discussed above with CO present in the growth phase were not re-suspended in fresh LB media between the growth and H_2 production phases. One such experiment, with re-suspension, was completed to verify that it is the acidic metabolites produced during sealed growth that decrease the H_2 productivity (Figure 13). When the media is re-suspended between phases, the sealed growth condition with CO present does not have a significant impact on H_2 productivity. This confirmed that it is the metabolites produced during the growth stage that inhibit the production of H_2 or decrease the pH to an inhibitory level.
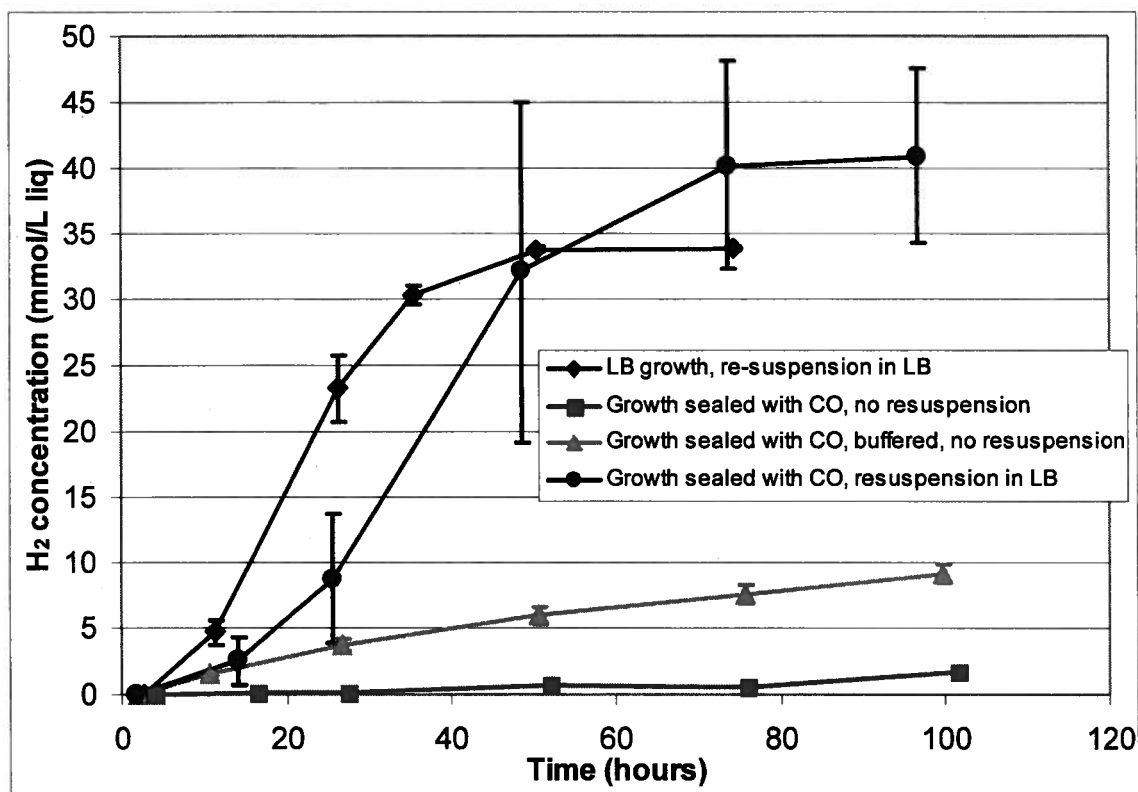
Figure 13- Effect of sealing the growth stage with 6.25mL CO in the headspace under several conditions. Symbols: -♦-, LB growth, re-suspended in LB; -■-, Sealed LB growth with CO; -▲-, Sealed LB growth with CO, buffered; -●-, Sealed LB growth with CO, re-suspended in LB. Symbols represent average of 2 experimental runs and error bars represent the standard deviation. Lines connect the symbols for ease of visualization.

These results oppose the previous study's finding, explained in section 2.4.3, where the presence of CO in the growth phase was necessary to achieve any H_2 production at all (Jung et al. 2002). The previous rationalization was that the CO dehydrogenase and hydrogenase enzymes were synthesized during aerobic growth via a CO-dependent mechanism. Bacteria have a tendency to only produce what is necessary for their survival, and under desirable growth conditions, it seems unlikely that these unessential enzymes are synthesized. The claim that CO is necessary during the growth stage for later H_2 production is thus refuted, as not only is H_2 productivity higher when the growth stage is completely aerobic, but higher cell densities can also be attained under this condition (Figure 5). These results show that the sealed growth condition with CO present not only increases the complexity of the growth stage, but also produces inhibitory metabolites that have a negative impact on H_2 productivity. These results also

provide insight into the sensitivity of *Ci amalonaticus* Y19 to pH. pH significantly decreased productivity when it dropped below 5.5, thus suggesting that the pH should be carefully controlled for this process.

The impact of adding an external carbon source on H_2 productivity was also investigated. Opposing statements between direct contact with the authors of the publication and what is printed in the publication created confusion about which carbon source was present, glucose or sucrose. While there is still confusion about the specific carbon source used in the literature study, the conclusion remains that an external carbon source was added to the growth media for all of the experiments performed in the previous study.

The results from these experiments show that when glucose was added to the LB media at a concentration of 5g/L, there was no H_2 production whatsoever. It was also observed that the CO was not utilized and remained at its initial concentration throughout the H_2 production stage. Strong catabolite repression seemed to be taking place because glucose was the preferred substrate over CO. This suggests that the *Ci amalonaticus Y19* used the glucose for continued growth, even under anaerobic conditions, which was verified with cell density measurements (Figure 14). Indeed, the cell density increased while CO concentrations remained constant in the reactor throughout the 100-hour anaerobic stage.

The discrepancy with the previous study regarding addition of carbon sources to the LB media may be a result of the time at which the glucose was added. Jung et al. (2002) suggest the carbon source is added to the media at the start of the growth stage, so it is possible that the sucrose (or glucose) is exhausted before the start of the H_2 production phase. In any case, this experiment has demonstrated that external carbon sources are unnecessary and inhibitory to H_2 production. As carbon sources such as glucose and sucrose are expensive, this finding also decreases the cost of the media.
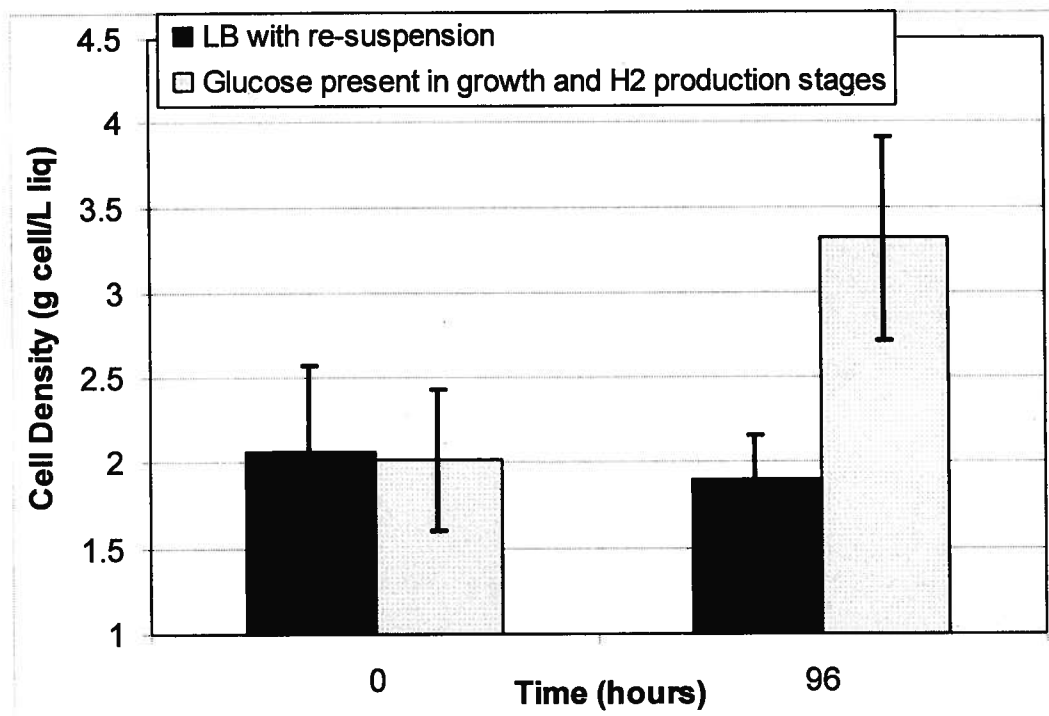
Figure 14 - Effect of glucose in cell density measured before and after the hydrogen production phase. Bars represent the average of 2 runs and the error bars represent the standard deviation.

One literature study suggested that deleting tryptone before the anaerobic stage increased H_2 productivity (Jung et al. 1999b). These researchers said that it is the presence of a carbon source during the H_2 production stage that inhibits the utilization of CO in *Ci amalonaticus Y19*. As tryptone is not a carbon source, but rather a source of amino acids because it consists of hydrolyzed casein, deleting it should not increase the H_2 productivity on CO. In the experiments conducted, tryptone deletion resulted in no H_2 production (Figure 12). This result suggests that *Ci amalonaticus Y19* could be auxotrophic for certain amino acids, which are provided by the addition of tryptone. In order to confirm this, the pH was checked and found to be 5, which is below the suggested optimal pH range (5.5-7.5). Buffer was added to see whether it was the effect of tryptone deletion or the pH that ceased the production of H_2. Adding 20mM phosphate buffer at pH 6.5 increased the pH to 6 and reversed the negative effect seen previously. While the buffered tryptone-deleted condition brought the H_2 productivity back to average levels, it did not increase H_2 productivity, thus opposing the previous literature finding. The HPLC results showed that while fresh tryptone deleted media had a similar

composition to LB media, the concentration of all the organic acids after the H_2 production stage were lower with tryptone deleted LB media, as compared to LB media. These experiments suggest that tryptone acts as a buffer, and can be converted into organic acids during the anaerobic stage. However, tryptone is not necessary to H_2 production and *Ci amalonaticus Y19* is not auxotrophic for components of tryptone.

From the effects observed in this section regarding media components, one finding stands out: pH. For the sealed growth conditions containing CO and the condition with tryptone deletion, pH dropped below 5.5, which caused a significant decrease in productivity. pH thus had a strong effect on H_2 productivity of *Ci amalonaticus Y19*, and should be controlled carefully throughout the process. For this study, pH was partially controlled with a 20mM phosphate buffer at pH 6.5, but a more precise method, particularly if a continuous is used, would be preferable.

5.4 Effect of trace metals

Design of experiment was used to see whether the addition of several trace metals would have an impact on hydrogen productivity. Nickel (Ni) and iron (Fe) were the metals investigated due to their predicted impact on the two enzymes responsible for producing hydrogen in this water gas shift reaction: carbon monoxide dehydrogenase and CO-induced hydrogenase. A full factorial design experiment with 3 levels of each metal was used to ensure an interaction effect between the metal ions was not overlooked in the analysis. The levels were based on typical concentrations of Fe, and zinc rather than nickel, in PTM1 salt solutions. Zinc was used because it has similar properties to nickel and nickel is not present in PTM1 salts. These levels were 32.5, 125 and 250 mg/L for Fe, where level 0 is not zero because of the basal level of Fe in the LB media supplemented with PTM1 salts, and 0, 62.5 and 125 mg/L for Ni. Most conditions were run in duplicate, but the four conditions that demonstrated an increased H_2 productivity after the initial data set were run in quadruplicate, making the total number of runs and data sets 26, rather than the 18 attributed to running duplicates of the full factorial design. The maximum volumetric H_2 productivities, and the time at which these productivities were obtained, are shown in Figure 15 for each condition in the factorial design.
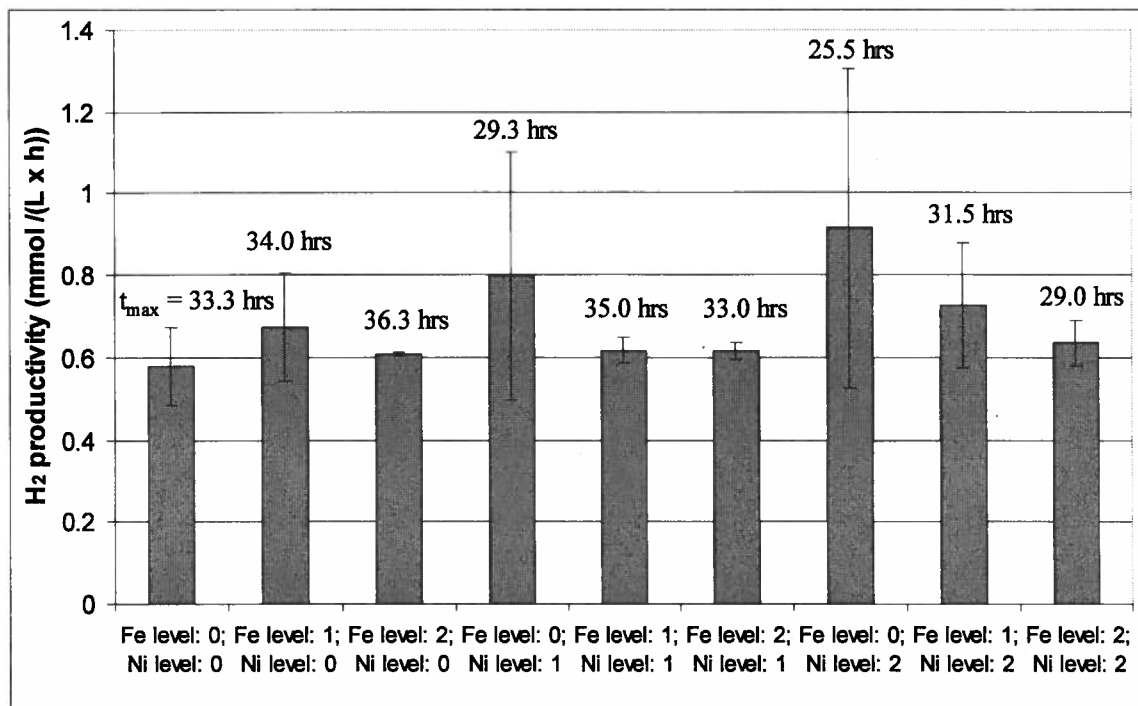
Figure 15 - Maximum H_2 productivity for all the combinations of levels in the factorial design on Fe and Ni concentrations. Data bars represent the average of 2 or 4 runs depending on the condition, and the error bars represent the standard deviation. The average time at which the maximum productivity is attained is shown above the data bars.

The trend observed in the factorial design was an increase in H_2 productivity with increased Ni concentration, but only when the Fe was at level 0 (32.5 mg/L). At increased Fe concentrations, there was no obvious effect on productivity, possibly due to an interaction effect between Ni and Fe. While Ni seemed to increase H_2 productivity, Fe at high concentrations might cause the productivity to decrease, thus making the effect unclear at mixed concentrations. Another observation is that while the time at which the maximum productivity is reached was most often in the range of 33 to 36 hours, several conditions had lower times, suggesting that the active form of the enzyme was produced more rapidly. These conditions included all the conditions at the highest Ni concentration of 125 mg/L, and the condition at the Ni concentration of 62.5 mg/L when the Fe concentration was at its lowest (32.5 mg/L).

An analysis of variance was performed for the factorial design with Minitab software setting H_2 productivity as the response and Ni concentration, Fe concentration, and the combination of Ni and Fe concentrations as the factors (Table 6). For this

analysis, the H_2 productivity was calculated as the slope of H_2 concentration versus time between 10 and 48 hours. Nickel was shown to have the strongest effect with the smallest P-value of 0.194, even though this effect was not statistically significant at a 95% confidence level. Both the effect of Fe and the interaction effect between Ni and Fe were not detected at a confidence level of 95%. Although the ANOVA did not detect any significant effects, the plot of main effects generated by the Minitab software showed a linear increase in H_2 productivity with increasing Nickel concentration, and a decrease in H_2 productivity at the highest level of Fe (Figure 16).

Table 6- Analysis of variance (ANOVA) for the effect of Fe and Ni on H_2 productivity between 10 and 48 hours.

Source	DF	Seq SS	Adj SS	Adj MS	F	P
Ni level	2	0.047795	0.030218	0.015109	1.81	0.194
Fe level	2	0.008734	0.008645	0.004323	0.52	0.605
Ni level*Fe level	4	0.018312	0.018312	0.004578	0.55	0.703
Error	17	0.141938	0.141938	0.008349		
Total	25	0.216779				
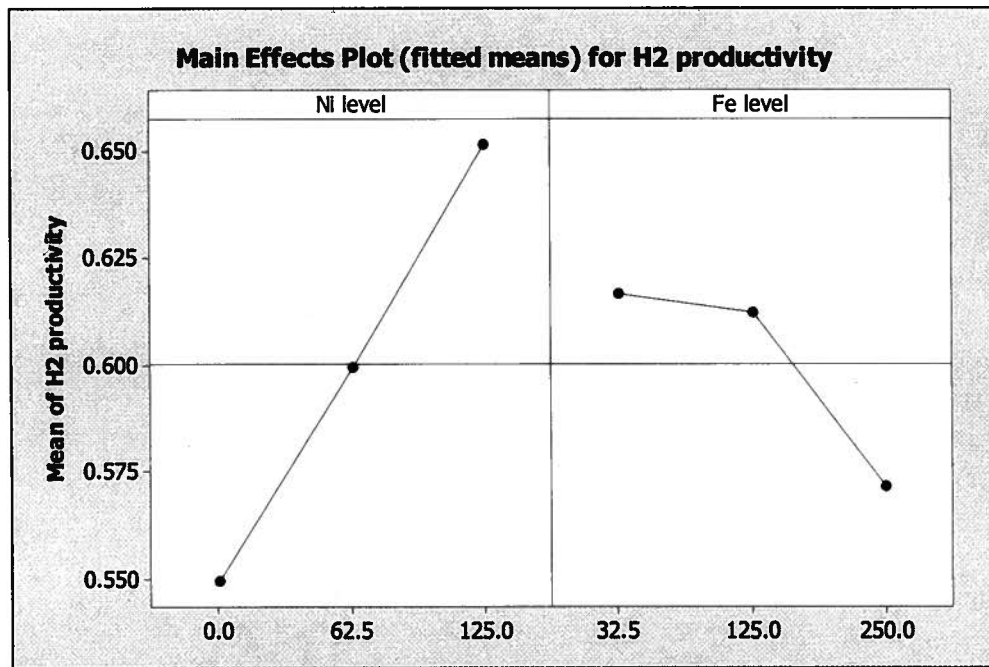
Figure 16 - Effects of nickel and iron on H_2 productivity between 10 and 48 hours. Graph generated by Minitab software during ANOVA analysis.

57

Another ANOVA analysis was performed with Minitab using H_2 productivity as the response, but this time using only Ni as a factor and ignoring any effect of Fe. While Fe was not considered as a factor, all of the data collected from the factorial design was still used for the analysis. The results show a P-value of 0.057 for the effect of Ni concentration (Table 7). This analysis suggests Ni did have a statistically significant impact on hydrogen productivity at a confidence level of 94%. In order to visualize the effect of Ni concentration on both H_2 productivity and time at which the maximum productivity was attained, H_2 productivity was plotted versus time, and a bar graph of the H_2 productivities used for the statistical analysis is also shown (Figures 17 and 18). The H_2 productivity used for the statistical analysis was the slope of H_2 concentration versus time graph between 10 and 48 hours. Note that the H_2 productivity only decreased after attaining a maximum because the experiments were performed in batch reactors, so the substrate, CO, was depleted.

Table 7 - Analysis of variance for the effect of Ni on H_2 productivity between 10 and 48 hours.

Source	DF	Seq SS	Adj SS	Adj MS	F	P
Ni level	2	0.047795	0.047795	0.023897	3.25	0.057
Error	23	0.168985	0.168985	0.007347		
Total	25	0.216779				

Figure 17 demonstrates an almost two-fold increase in H_2 productivity when the concentration of Ni was increased from 0 to 125 mg/L at a time of 20 hours, when Fe was at level 0. A hypothesis test on the mean of the overall productivity between 10 and 48 hours for both of these Ni concentrations showed a statistically significant increase of volumetric H_2 productivity at a 95% confidence level. Also, the maximum H_2 productivity was reached at a notably shorter time for increased Ni concentrations, suggesting that the active enzyme complex was present sooner (Figure 18). These results suggest that CO-dehydrogenase and hydrogenase do bind to nickel and its presence increases the efficiency of enzyme activation, as well as the H_2 productivity.
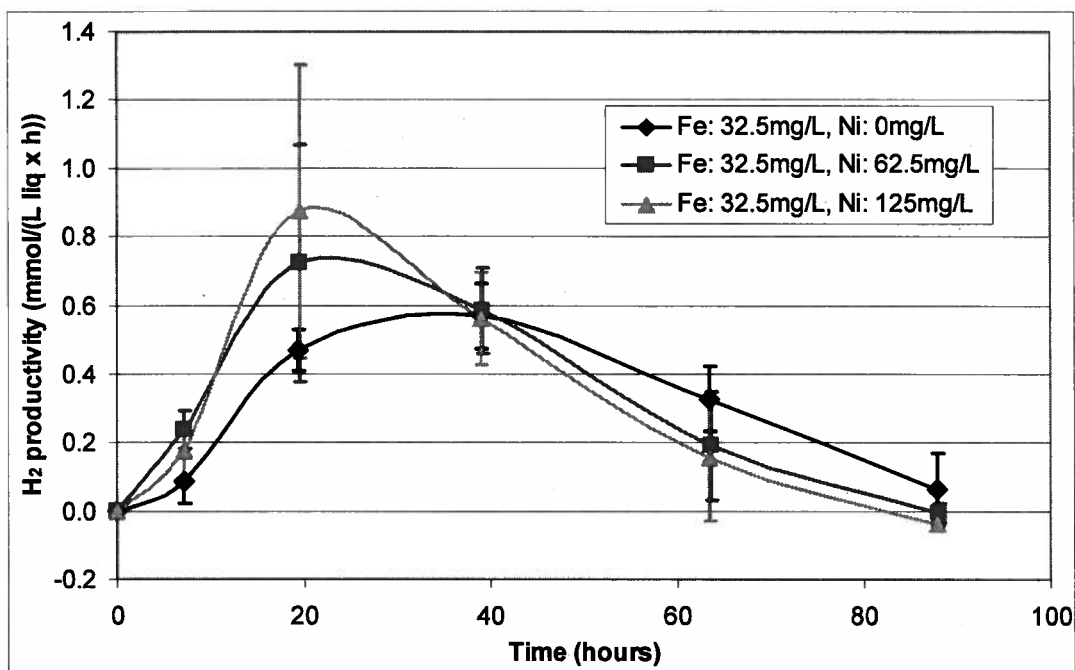
Figure 17 - The effect of nickel concentration on the evolution of H_2 productivity throughout the batch H_2 production phase when Iron concentration is kept constant at 32.5mg/L. Symbols: -◆-, 0mg/L Ni; -■-, 62.5mg/L Ni; -▲-, 125mg/L Ni. Data points represent the average of 4 runs and the error bars represent the standard deviation.

Figure 18 - Effect of nickel on the H_2 productivity between 10 and 48 hours, and the time at which the maximum productivity is reached when Fe is present at the constant level of 32.5 mg/L. Data bars represent the average of four measurements and the error bars represent the standard deviations.

The effect of iron on H_2 productivity between 10 and 48 hours when no nickel was present is shown in Figure 19. The data suggests that there was no effect on p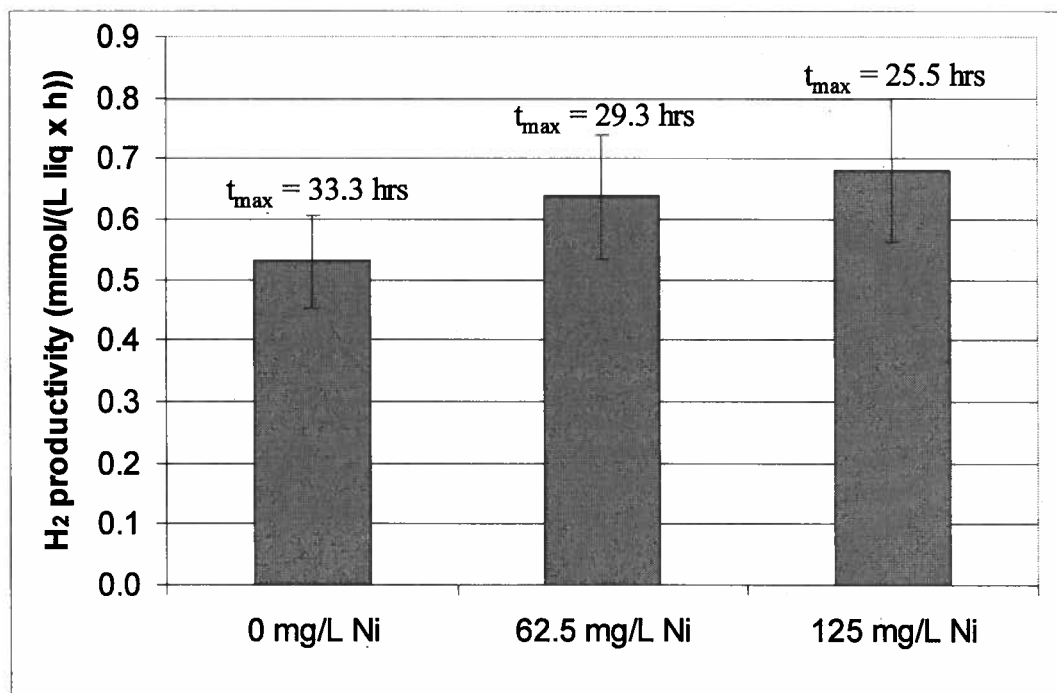roductivity when increasing iron concentration from 32.5 mg/L to 250 mg/L. There was also a slight increase in time at which the maximum productivity was reached when increasing the concentration. The interaction effect shown in Figure 15 was re-iterated in Figure 20, a graph generated by Minitab during the full factorial analysis. The overlapping curves in this figure demonstrate that there was an interaction effect between Ni and Fe at nickel concentrations of 0 and 62.5mg/L. Figure 20 also demonstrates the trend of decreasing H_2 productivity for increasing Fe levels at higher nickel concentrations. Together, this implies that the low concentration of iron available in the PTM1 salt solution was sufficient for the activation of the enzymes used during H_2 production. Increasing the concentration of Fe above 32.5mg/L is not necessary and could be detrimental to the timing of the process, as well as the productivity when nickel is available in the media.
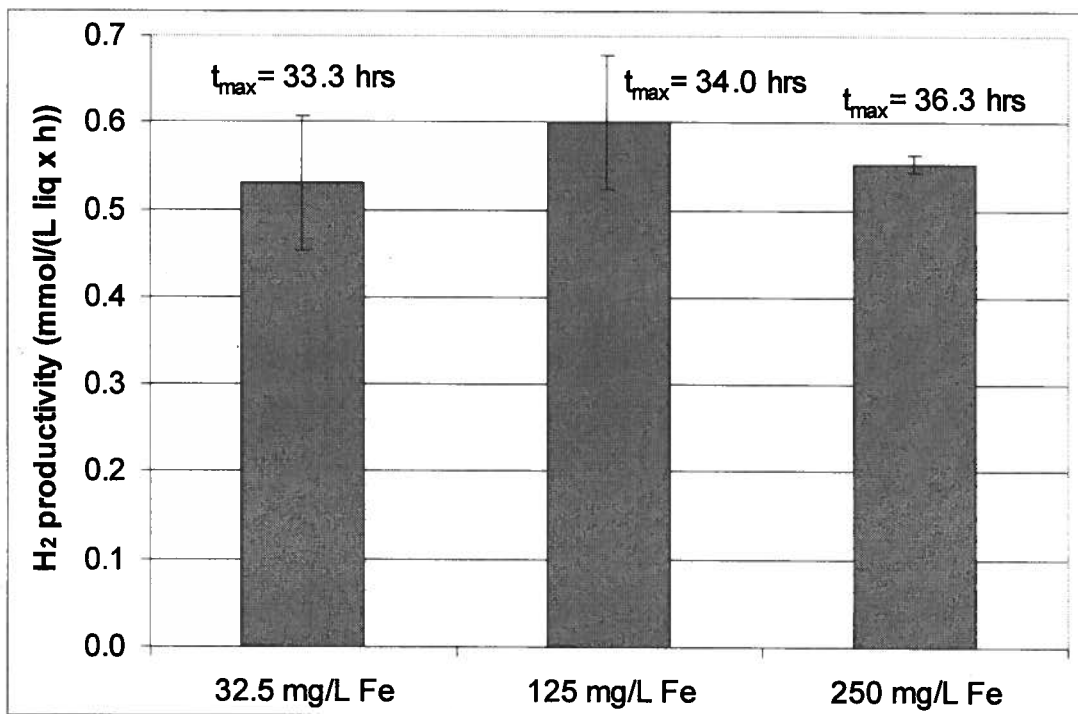
Figure 19 - Effect of iron on H_2 productivity between 10 and 48 hours, and the time at which the maximum H_2 productivity is reached when no Ni is present. Data bars represent the average of 4 measurements at 32.5 mg/L and the average of 2 measurements at 125 and 250mg/L. Error bars represent standard deviation.
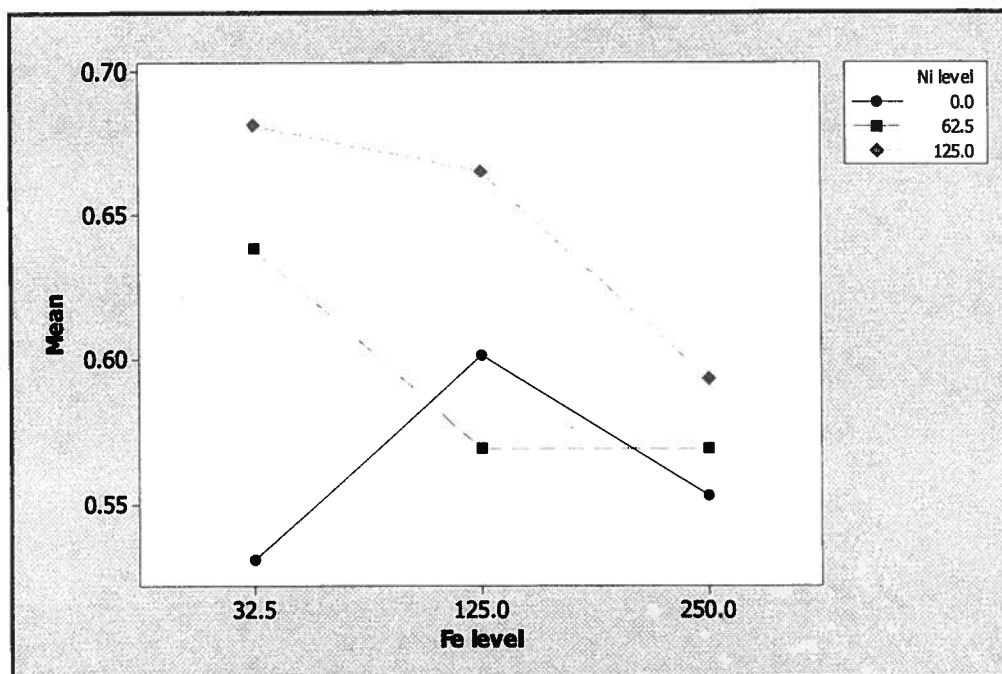
Figure 20 - The interaction effect of Ni and Fe on H_2 productivity. Graph generated by Minitab software during ANOVA analysis.

5.5 Strategy for minimizing inhibition of enzyme production

Re-suspension was a process performed between the aerobic growth and anaerobic H_2 production stages. The broth was spun down after growth and the spent media discarded. The cells were then re-suspended in fresh media. This process allowed for any inhibitory metabolites that were produced during the growth stage to be discarded. Re-suspension also allowed cell density to be increased by combining several bottles from growth into one for H_2 production. While increasing cell density will be discussed in a later section, this section focuses on the effect of discarding the spent media, and replacing it with fresh media of the same initial composition.

The results indicate that re-suspension significantly decreased the lag phase, and slightly increased the H_2 productivity (Figure 21). The H_2 productivities were measured as the slope of consecutive data points on the H_2 concentration curves during the H_2 production phase, disregarding the lag and stationary phases. The volumetric H_2 productivities were approximately 0.95 and 1.25 mmol H_2/ (L x h) for the case without re-suspension and with re-suspension, respectively. The specific H_2 productivities

61

followed a similar trend to the volumetric productivities at 0.31 and 0.53 mmol H_2/ (g cell x h) for the case without re-suspension and with re-suspension, respectively. The lag phase decreased from approximately 18 hours to 5 hours with re-suspension. These results suggest that some inhibitory metabolites are being produced during the aerobic growth stage. The metabolites produced, directly or indirectly, are inhibiting H_2 production by decreasing the H_2 productivity, but they are also inhibiting the production or activation of the CO dehydrogenase and hydrogenase enzymes.
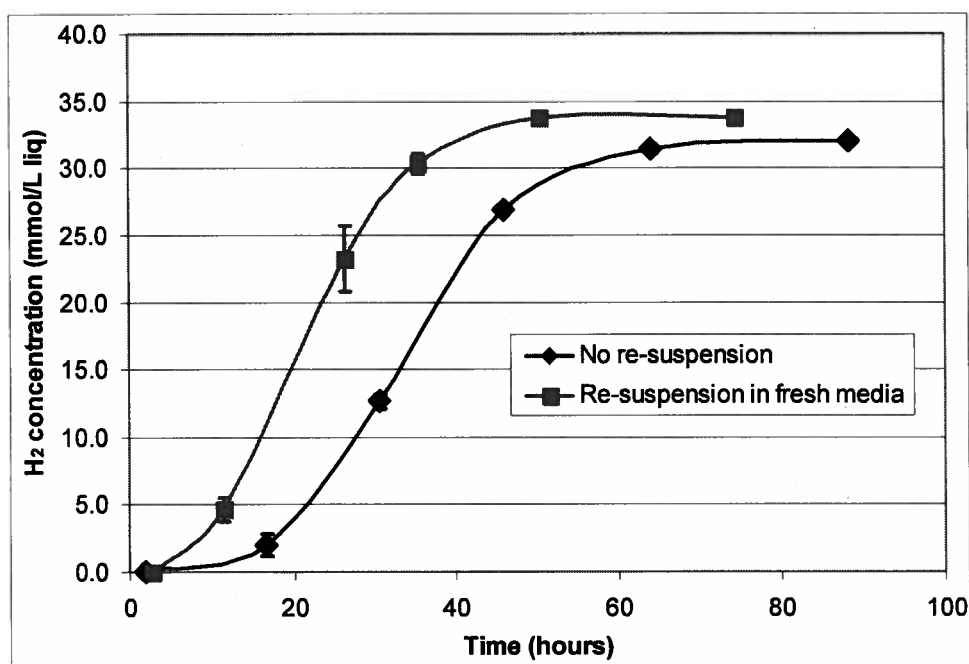
Figure 21 - The effect of re-suspending the cells between the growth and H_2 production phases on H_2 concentration evolution. . Symbols: -◆-, cells are not re-suspended; -■-, cells are re-suspended between the growth and H_2 production phases. Data points represent the average of 2 runs and the error bars represent the standard deviation.

Although the exact nature of these inhibitory metabolites is unknown, the HPLC results in Figure 6 show that both lactate and acetate were produced during growth. These small organic acids, present after open growth conditions with no buffer at concentrations of 4 g/L lactic acid and 2.3 g/L acetic acid, could be inhibiting the enzyme activity. Typical inhibition levels of lacate and acetate on hydrogenase and CO dehydrogenase could not be found in the literature but are assumed to be below the 40mM concentration observed for both lactate and acetate after the growth stage. While the organic acids may be inhibitory themselves at these concentrations, it is also conceivable that it is the

decrease in pH that these organic acids cause that inhibits the enzymes. As seen in section 5.3, *Ci amalonaticus Y19* is very sensitive to pH, so it should be monitored, particularly under conditions that produce organic acids.

5.6 Mass transfer

Due to the low solubility of CO, external mass transfer of the substrate CO from the gas phase into the liquid phase has been one of the major obstacles reported for the use of the biological water-gas shift reaction (Amos 2004, Wolfrum, Watt & Huang 2002, Maness, Weaver 2002, Wolfrum, Watt 2001). Several solutions have been suggested to solve this mass transfer obstacle using novel reactor designs, but before investigating complex reactor designs, studies were performed to see how basic properties such as pressure and cell density affected H_2 productivity.

On a theoretical basis, two solutions exist for resolving external mass transfer limitations: increasing the mass transfer coefficient ($k_L a$) or increasing the substrate solubility. Increasing mixing and increasing the area available for mass transfer would both increase the mass transfer coefficient. Agitating the reactor more vigorously can increase mixing, while using small gas bubbles with high surface to volume ratio and low rise-velocities can increase area. Since the system is already being agitated in a shaking incubator at a high speed of 250 rpm, and the system is batch so the bubble size cannot be controlled, the substrate solubility was investigated rather than the mass transfer coefficient.

The solubility of CO in water is approximately 0.85 mmol/L at atmospheric pressure and 30°C. Decreasing the temperature or increasing the CO partial pressure, as seen in Henry's law, can increase this low solubility:

$$C_{CO} = k_H \, p_{CO} \tag{16}$$

where C_{CO} represents the concentration of CO in solution (M), k_H is Henry's law constant (M/atm), and p_{CO} is the partial pressure of CO above the solution (atm). Henry's law constant for CO, at atmospheric temperature, is 9.5×10^{-4} M/atm. Increasing the CO partial pressure should thus proportionately increase CO concentration in the liquid phase; therefore, if the system is mass transfer limited, this should proportionately

increase H_2 productivity. Batch experiments were performed at increased CO partial pressure to test this theory.

While many initial attempts failed at accurately measuring the effect of increasing CO partial pressure, an experiment was designed that was accurate and precise. In this experiment, the pressure was increased with the pre-mixed 40% CO in He (v/v) gas cylinder and monitored with a portable pressure gauge. The pressure gauge was connected to a needle for ease of measurements through the septa. The results of these experiments showed that increasing the pressure from 1 atmosphere (atm) to 1.5 atm had no significant effect on H_2 productivity, and increasing to 2 atm decreased H_2 productivity significantly (Figures 22 and 23). Note that the time evolution of H_2 concentration in Figure 22 is not accurately illustrated because few data points were taken to prevent depressurizing the reactors. The results do not follow the expected trend of proportional increase of H_2 productivity with increased pressure, but rather show the opposite effect at high pressures. This implies substrate inhibition at increased CO partial pressures.

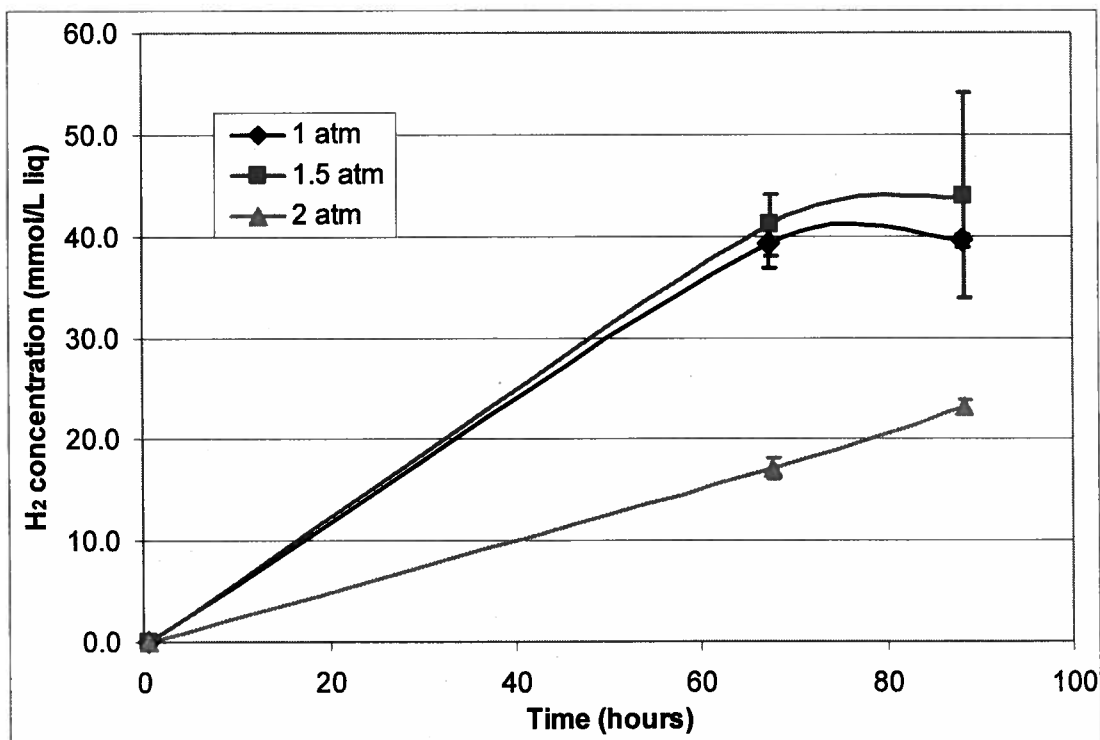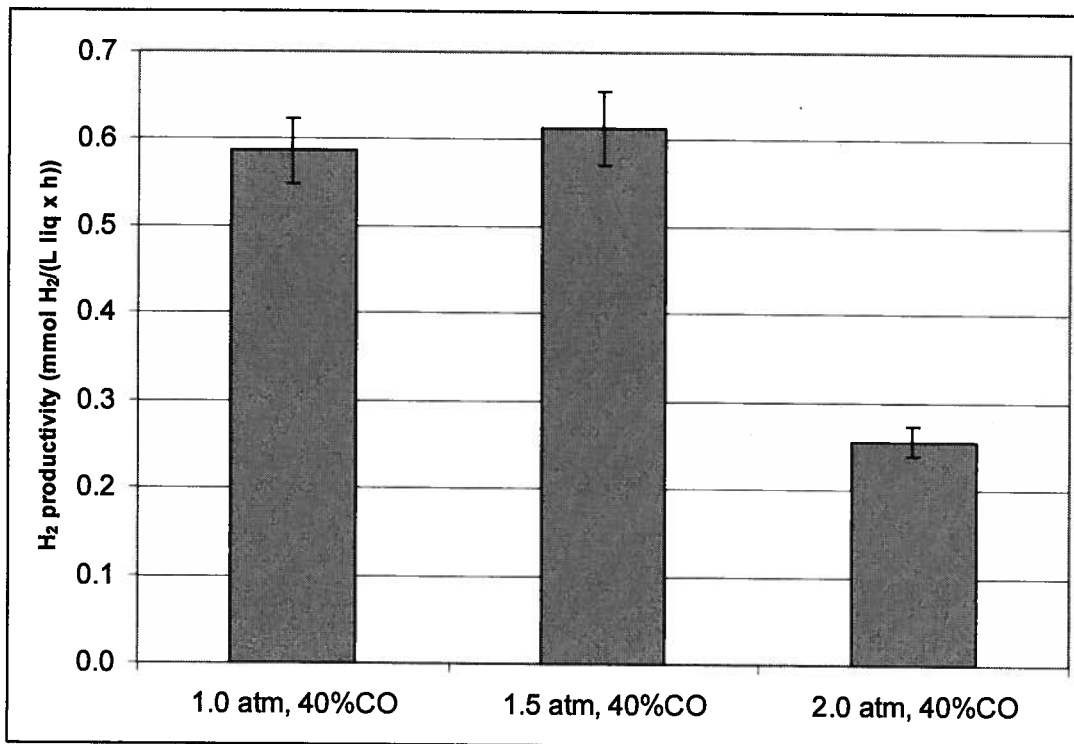Figure 22 - The effect of pressure on H_2 concentration. Symbols: -◆-, 1 atm; -■-, 1.5 atm; -▲-, 2 atm. Data points represent the average of 2 runs and the error bars represent the standard deviation. The line connects the data points for ease of visualisation.

Figure 23 - The effect of pressure on maximum H_2 productivity. Data bars represent the average of 2 runs and the error bars represent the standard deviation.

Substrate inhibition is taking place because of the higher availability of CO substrate dissolved in the liquid phase at higher pressures. This behavior at high pressures is analogous to the behavior of the cells when the bottles were purged with pure CO before the concentration was adjusted to the desired initial CO concentration (Figure 11). Both of these results suggest substrate inhibition at very high CO concentrations in the liquid phase. Another possible explanation for the decreased productivity at 2 atmospheres is that this particular strain of bacterial cells may not be able to survive under these environmental conditions. Water, however, is an incompressible fluid, so this is highly unlikely because in this solvent, the cells will not know the difference between 1atm and 2atm. Overall, these results suggest that increasing the pressure in the system does not resolve any possible mass transfer limitation because of the substrate inhibition that comes into play at high pressure. Alternatively, the results could mean that mass transfer limitation is not a major and significant issue for this particular organism, but rather the focus should be on alleviating the inhibition at high substrate concentrations.

5.7 Effect of cell concentration

Since mass transfer was not limiting H_2 productivity, increasing the density of cells in the reactor was investigated to increase H_2 production. Increasing the cell density should increase the volumetric H_2 productivity proportionally. An initial experiment to test this theory was performed by decreasing cell density by dilution with fresh media after the growth stage to 75% and 50% of the initial cell density. This initial test gave the opposite of the expected result, by having very similar H_2 productivities for all cell concentrations rather than a decreasing volumetric productivity for decreasing cell density (Appendix B). The specific H_2 productivity thus increased with decreasing cell density. This result could have been explained by a fast growth rate of the cells, equalizing cell density back to approximately 2.5 g/L while the reactors were being switched into the anaerobic H_2 production stage, but this explanation was nullified when cell density was measured before and after the anaerobic stage and the ratios were found to remain constant.

A more accurate test on the effect of cell density was effectuated by spinning down the cells after growth from four serum bottles and combining these into one serum bottle, thus quadrupling the cell density before the start of the anaerobic stage. The time evolution of H_2 concentration, and a comparison of volumetric and specific H_2 productivities are illustrated for this experiment in Figures 24 and 25, respectively. These results show that quadrupling the cell density gave very similar H_2 production curves, which translates into no significant difference in volumetric H_2 productivity, but much lower specific H_2 productivity. The specific H_2 productivity decreased from 0.5 to 0.1 mmol H_2 / (g cell x h) when the cell density was quadrupled.
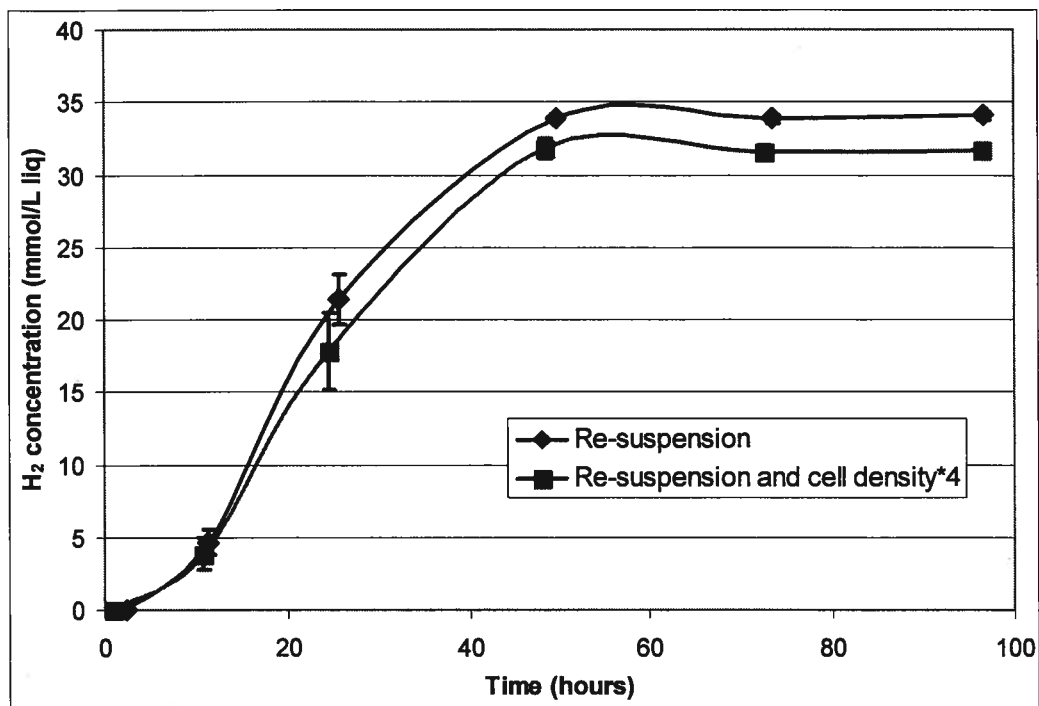
Figure 24 - The effect of quadrupling cell density on H_2 concentration. Symbols: -◆-, regular cell density; -■-, 4 times higher cell density. Data points represent the average of 2 runs and the error bars represent the standard deviation.
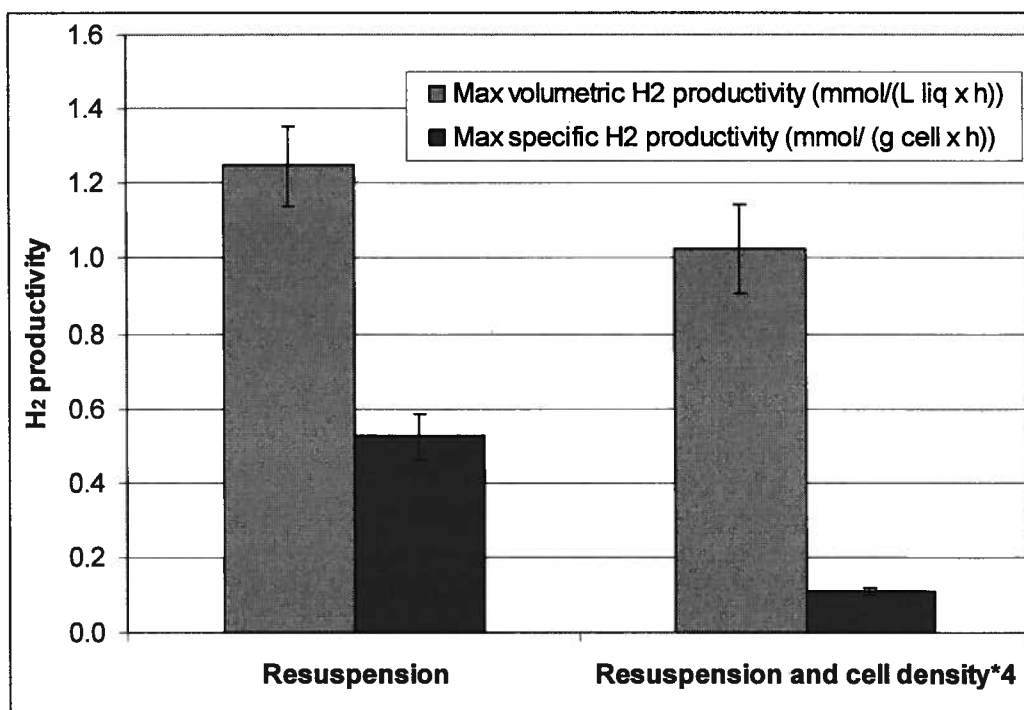

Figure 25 - The effect of quadrupling cell density on maximum hydrogen productivity. Data bars represent the average of 2 runs and the error bars represent the standard deviation.

This result was troubling because everything in biotechnology points toward an expected proportional increase in H_2 production when cell density is increased. The specific productivity of the cells should not change with cell density. One possible explanation for this is that the system undergoes product inhibition. If the initial enzyme load were increased, the H_2 would be generated at a faster rate. If high H_2 concentrations inhibit the enzymes, then this could explain why the evolution of H_2 concentration does not change when the cell density is increased. Since there is no H_2 at the start of the anaerobic stage, this effect would only be initiated after the H_2 concentration reaches a certain point. This was not the case, as the initial H_2 productivity was not increased at an increased cell density.

Another explanation would be that the cells somehow regulate themselves, and there is a limit on the viable cell count. If the number of viable cells is not proportional to the total cell density but rather stays constant even when increasing the total number of cells, and only the viable cells produce H_2, then this would explain the constant volumetric H_2 productivity. Perhaps the cell turnover is a lot faster than the H_2 production process, allowing the cells to regulate themselves to a maximum viability level. Performing viable cell assays rather than simply using optical density to measure cell density could verify this theory. Another form of cell regulation is quorum sensing. Some bacteria use quorum sensing to regulate certain behaviors based on the local cell density of the bacterial cells. Quorum sensing is a form of communication among bacteria where signaling molecules are secreted and, when bound to receptors, activate the transcription of certain genes. This process would need to be investigated further to confirm the presence of quorum sensing in *Ci amalonaticus Y19.*

A third possible reason for this unusual result is that the enzyme concentration is so high that adding more enzymes does not affect the conversion kinetics. If this were the case, the productivity would only increase with an increase in specific activity of the enzyme, not with enzyme load. In order to increase specific activity, a more in depth look inside the cell would be necessary to understand the mechanism of CO conversion and the enzymatic processes. Once this mechanism was understood, genetic modifications could be performed to increase the specific enzyme activity, thus having more control over H_2 productivity.

5.8 Prospects and limitations of H_2 productivity

The maximum volumetric H_2 productivity obtained was 1.5 mmol H_2 / (L x h) for a system buffered to pH 6.5 with re-suspension between the growth and H_2 production stages. To find out the limitation or prospect of this rate of H_2 production, it must be put into the context of a practical application. While several practical applications exist, only one has been studied and published for the biological H_2 production system by Levin et al. (2004).

In the study by Levin et al, the size of bio-hydrogen systems required to power proton exchange membrane fuel cells (PEMFC) of various sizes was calculated based on hydrogen production rates (Levin, Pitt & Love 2004). Unpublished data by BC hydro suggests that the average non-electrically heated house in British Columbia uses approximately 13,000 kWh electricity every year. This amount of energy would require a PEMFC of 1.5 kW output power, assuming it runs at constant output, thus ignoring the diurnal and seasonal variations. Using the conversion factors from this research paper and the maximum volumetric productivity of 1.5 mmol H_2 / (L x h), the bioreactor size was calculated. The result was that a 23,900L bioreactor would be required to supply sufficient H_2 to power a PEMFC of 1.5 kW using the biological water gas shift reaction catalyzed by *Ci amalonaticus Y19*. This bioreactor size is enormous, making this technology economically unfeasible for this application. Productivities at least 100 times higher must be achieved to consider this technology application.

Another possible application of this technology would be to rid a gas stream of CO, which can be considered a toxic impurity, and the H_2 production could be seen as a side benefit. On top of this, low-grade synthesis gas is considered a waste stream, and any energy recovered from this stream can result in positive gain. In order to assess the feasibility of these practical applications, economic analyses would need to be performed on producing H_2 or getting rid of CO from a gas stream.

6.0 Conclusions

In this research project, a two-step reactor protocol was successfully developed using *Ci amalonaticus Y19* to catalyze the biological WGS reaction. While this system was not fully optimized, it can serve as a reference point for further work in this field.

The most important result found from the investigation of the effect of medium components was the significant improvements to both the volumetric H_2 productivity and the time of activation of CO dehydrogenase and CO-induced hydrogenase when the LB media was supplemented with nickel at a concentration of 125 mg/L. Other media components investigated were the presence of CO during the growth stage, the addition of other carbon sources, and the deletion of tryptone. The results indicated that the sealed growth condition with CO present was not essential to H_2 production in the following anaerobic stage, and actually decreased the H_2 productivity. Open growth conditions are thus not only preferred, but also greatly simplify the growth protocol. The addition of external carbon sources ceased H_2 production by introducing a preferred substrate for *Ci amalonaticus Y19* that induced anaerobic cell growth rather than conversion of CO. Tryptone in the media was deemed to act as a buffer but the deletion of tryptone did not increase H_2 productivity as was predicted in a previous study on *Ci amalonaticus Y19*. It was found that H_2 production did not rely on the presence of tryptone, meaning *Ci amalonaticus Y19* was not auxotrophic for the amino acids contained in the enzymatic digest of casein.

Process conditions investigated included pH, re-suspension, pressure, and cell density. H_2 production by *Ci amalonaticus Y19* was strongly pH sensitive and improved with pH control. It was observed that a pH greater than 5.5 was indispensable to the production of H_2. Re-suspension between the aerobic growth and anaerobic H_2 production stages decreased the inhibition of enzyme production and activation by eliminating the inhibitory metabolites produced during the growth stage. The expected mass transfer limitation, due to the low solubility of the gaseous substrate, CO, in the water gas shift reaction, was not observed, and increasing the partial pressure of the substrate had a negative effect at pressures above 2 atmospheres. This decrease in H_2 productivity at higher pressures is likely due to substrate inhibition compensating

increased substrate availability. The attempt at increasing the cell density also gave disconcerting results that showed no improvement in volumetric H_2 productivity at increased cell densities.

Overall, this research project has shown that *Ci amalonaticus Y19* offers moderate CO uptake rates and conversion yields close to theoretical maximum. H_2 production by the biological water gas shift reaction catalyzed by *Ci amalonaticus Y19* was strongly influenced by the media composition and the pH. An initial optimization of the process led to an open growth phase, followed by re-suspension of the media between phases, and an addition of nickel to LB media for the anaerobic stage. The pH must also be controlled throughout this process.

7.0 Recommendations

Throughout this research project, insight was given as to how several medium components, as well as how pressure and other process parameters affect the H_2 productivity of *Ci amalonaticus Y19* catalyzing the biological water gas shift reaction (bio-WGS). The maximum volumetric H_2 productivity obtained was 1.5 mmol H_2/ (L x h) for a buffered system with re-suspension between the growth and H_2 production stages. This H_2 production rate was found to be economically unviable for some technological applications such as providing electrical power to a house through a 1.5kW proton exchange membrane fuel cell (PEMFC).

One recommendation for further research is to calculate the economic viability of this H_2 production rate for other practical applications. These application could include a smaller scale process where any energy recovered from the low-grade syngas waste stream can result in positive gain. Also, this process could be used as a method to rid a gas stream of CO, which can be considered a toxic impurity, and the H_2 production could be seen as a side benefit.

The experiment where cell density was quadrupled and the volumetric rate of H_2 production was not increased remains a mystery. Solving this mystery would be particularly interesting, and could optimistically be accomplished by doing either viable cell assays, or looking inside the cell to learn more about the enzyme kinetics. Creating assays for the enzymes would help to learn more about what stage in the process the enzymes are produced and how much enzyme is produced. Finding the sequences of the enzymes would also be informative. Once the enzyme kinetics are understood, genetic manipulations could increase the specific activity of the key enzymes of the biological water gas shift reactions: CO dehydrogenase, and CO-induced hydrogenase.

A more in depth optimization of the media composition is also recommended. This would decrease the possibility of any unknown components in the complex media affecting the outcome of H_2 production. Ideally, the media would be optimized for growth and H_2 production independently, as it has been shown that these two phases can be completely isolated from each other.

Once the media has been optimized and the understanding of the enzyme kinetics has been deepened, it would be valuable to investigate the effect of other components present in syngas on H_2 productivity. The concentration of H_2, CO_2, and other minor components such as CH_4, N_2 and H_2S may affect the bio-WGS reaction and this effect should be examined.

References

Akkerman, I., Janssen, M., Rocha, J. & Wijffels, R.H. 2002, "Photobiological hydrogen production: photochemical efficiency and bioreactor design", *International Journal of Hydrogen Energy*, vol. 27, no. 11-12, pp. 1195-1208.

Amos, A. 2004, "Biological Water-Gas Shift Conversion of Carbon Monoxide to Hydrogen", National Renewable Energy Laboratory, Golden, CO. NREL/MP-560-35592

Basak, N. & Das, D. 2007, "The prospect of purple non-sulfur (PNS) photosynthetic bacteria for hydrogen production: The present state of the art", *World Journal of Microbiology & Biotechnology*, vol. 23, no. 1, pp. 31-42.

Benemann, J.R. 1997, "Feasibility analysis of photobiological hydrogen production", *International Journal of Hydrogen Energy*, vol. 22, no. 10-11, pp. 979-987.

Chang, J.S., Lee, K.S. & Lin, P.J. 2002, "Biohydrogen production with fixed-bed bioreactors", *International Journal of Hydrogen Energy*, vol. 27, no. 11-12, pp. 1167-1174.

Crabtree, G.W., Dresselhaus, M.S. & Buchanan, M.V. 2004, "The hydrogen economy", *Physics Today*, vol. 57, no. 12, pp. 39-44.

Das, D. & Veziroglu, T.N.V. 2001, "Hydrogen production by biological processes: A survey of literature", *International Journal of Hydrogen Energy*, vol. 26, no. 1, pp. 13-28.

Datar, R., Huang, J., Maness, P.C., Mohagheghi, A., Czemik, S. & Chornet, E. 2007, "Hydrogen production from the fermentation of corn stover biomass pretreated with a steam-explosion process", *International Journal of Hydrogen Energy*, vol. 32, no. 8, pp. 932-939.

Doman, L., Staub, J., Mayne, L., Barden, J., Martin, P., Mellish, M., Kearney, D., Kette, S., Aniti, L., Murphy, B., Kapilow-Cohen, B. & Lindstrom, P. 2008, *International Energy Outlook 2008*, Energy Information Administration: Office of Integrated Analysis and Forecasting, U.S. Department of Energy, Washington, DC. DOE/EIA-0484(2008)

Energy information administration 2007, November 2007-last update, *Energy kid's page: hydrogen* [Homepage of US Department of Energy], [Online]. Available: http://www.eia.doe.gov/kids/energyfacts/sources/IntermediateHydrogen.html [2008, September/23] .

Fascetti, E. & Todini, O. 1995, "*Rhodobacter sphaeroides RV* cultivation and hydrogen production in a one- and two-stage chemostat", *Applied Microbiology and Biotechnology*, vol. 44, no. 3-4, pp. 300-305.

Florin, L., Tsokoglou, A. & Happe, T. 2001, "A novel type of iron hydrogenase in the green alga *Scenedesmus obliquus* is linked to the photosynthetic electron transport chain", *Journal of Biological Chemistry*, vol. 276, no. 9, pp. 6125-6132.

Ghirardi, M.L., Zhang, L., Lee, J.W., Flynn, T., Seibert, M., Greenbaum, E. & Melis, A. 2000, "Microalgae: A green source of renewable H_2", *Trends in Biotechnology*, vol. 18, no. 12, pp. 506-511.

Hallenbeck, P.C. 2005, "Fundamentals of the fermentative production of hydrogen", *Water Science and Technology*, vol. 52, no. 1-2, pp. 21-29.

Hallenbeck, P.C. & Benemann, J.R. 2002, "Biological hydrogen production; Fundamentals and limiting processes", *International Journal of Hydrogen Energy*, vol. 27, no. 11-12, pp. 1185-1193.

Hedderich, R. 2004, "Energy-converting [NiFe] hydrogenases from archaea and extremophiles: Ancestors of complex I", *Journal of Bioenergetics and Biomembranes*, vol. 36, no. 1, pp. 65-75.

Henstra, A.M., Sipma, J., Rinzema, A. & Stams, A.J.M. 2007, "Microbiology of synthesis gas fermentation for biofuel production", *Current Opinion in Biotechnology*, vol. 18, no. 3, pp. 200-206.

Henstra, A.M. & Stams, A.J.M. 2004, "Novel physiological features of *Carboxydothermus hydrogenoformans* and *Thermoterrabacterium ferrireducens*", *Applied and Environmental Microbiology*, vol. 70, no. 12, pp. 7236-7240.

Ivy, J. 2004, *Summary of Electrolytic Hydrogen Production*, National Renewable Energy Laboratory, Golden, CO. NREL/MP-560-36734

Jung, G.Y., Jung, H.O., Kim, J.R., Ahn, Y. & Park, S. 1999a, "Isolation and characterization of Rhodopseudomonas palustris P4 which utilizes CO with the production of H_2", *Biotechnology Letters*, vol. 21, no. 6, pp. 525-529.

Jung, G.Y., Kim, J.R., Jung, H.O., Park, J.Y. & Park, S. 1999b, "A new chemoheterotrophic bacterium catalyzing water-gas shift reaction", *Biotechnology Letters*, vol. 21, no. 10, pp. 869-873.

Jung, G.Y., Kim, J.R., Park, J.Y. & Park, S. 2002, "Hydrogen production by a new chemoheterotrophic bacterium *Citrobacter sp Y19*", *International Journal of Hydrogen Energy*, vol. 27, no. 6, pp. 601-610.

Kapdan, I.K. & Kargi, F. 2006, "Bio-hydrogen production from waste materials", *Enzyme and microbial technology*, vol. 38, no. 5, pp. 569-582.

Kim, J.R., Oh, Y.K., Yoon, Y.J., Lee, E.Y. & Park, S. 2003, "Oxygen sensitivity of carbon monoxide-dependent hydrogen production activity in *Citrobacter sp.*", *Journal of Microbiology and Biotechnology,* vol. 13, no. 5, pp. 717-724.

Klasson, K.T., Ackerson, C.M.D., Clausen, E.C. & Gaddy, J.L. 1992, "Biological conversion of synthesis gas into fuels", *International Journal of Hydrogen Energy,* vol. 17, no. 4, pp. 281-288.

Kosourov, S., Tsygankov, A., Seibert, M. & Ghirardi, M.L. 2002, "Sustained hydrogen photoproduction by *Chlamydomonas reinhardtii*: Effects of culture parameters", *Biotechnology and Bioengineering,* vol. 78, no. 7, pp. 731-740.

Kroposki, B., Levene, J., Harrison, K., Sen, P.K. & Novachek, F. 2006, *Electrolysis: Information and Opportunities for Electric Power Utilities*, National Renewable Energy Laboratory, Golden, CO. NREL/TP-581-40605

Lay, J. 2000, "Modeling and optimization of anaerobic digested sludge converting starch to hydrogen", *Biotechnology and bioengineering,* vol. 68, no. 3, pp. 269-278.

Levin, D.B., Islam, R., Cicek, N. & Sparling, R. 2006, "Hydrogen production by *Clostridium thermocellum 27405* from cellulosic biomass substrates", *International Journal of Hydrogen Energy,* vol. 31, no. 11, pp. 1496-1503.

Levin, D.B., Pitt, L. & Love, M. 2004, "Biohydrogen production: Prospects and limitations to practical application", *International Journal of Hydrogen Energy,* vol. 29, no. 2, pp. 173-185.

Lindahl, P.A. 2002, "The Ni-containing carbon monoxide dehydrogenase family: Light at the end of the tunnel?", *Biochemistry,* vol. 41, no. 7, pp. 2097-2105.

Maness, P. & Weaver, P.F. 2002, "Hydrogen production from a carbon-monoxide oxidation pathway in *Rubrivivax gelatinosus*", *International Journal of Hydrogen Energy,* vol. 27, no. 11-12, pp. 1407-1411.

Melis, A., Zhang, L.P., Forestier, M., Ghirardi, M.L. & Seibert, M. 2000, "Sustained photobiological hydrogen gas production upon reversible inactivation of oxygen evolution in the green alga Chlamydomonas reinhardtii", *Plant Physiology,* vol. 122, no. 1, pp. 127-135.

Melis, A. 2002, "Green alga hydrogen production: Progress, challenges and prospects", *International Journal of Hydrogen Energy,* vol. 27, no. 11-12, pp. 1217-1228.

Merida, W., Maness, P., Brown, R.C. & Levin, D.B. 2004, "Enhanced hydrogen production from indirectly heated, gasified biomass, and removal of carbon gas emissions using a novel biological gas reformer", *International Journal of Hydrogen Energy,* vol. 29, no. 3, pp. 283-290.

Najafpour, G., Younesi, H. & Mohamed, A.R. 2004, "Effect of organic substrate on hydrogen production from synthesis gas using *Rhodospirillum rubrum*, in batch culture", *Biochemical engineering journal,* vol. 21, no. 2, pp. 123-130.

Oh, Y., Kim, H., Park, S., Kim, M. & Ryu, D.D.Y. 2008, "Metabolic-flux analysis of hydrogen production pathway in *Citrobacter amalonaticus Y19*", *International Journal of Hydrogen Energy,* vol. 33, no. 5, pp. 1471-1482.

Palmer, D. 2005, Thursday, 01-Dec-2005 13:58:39 EST-last update, *Hydrogen in the Universe* [Homepage of NASA's High Energy Astrophysics Science Archive Research Center], [Online]. Available: http://imagine.gsfc.nasa.gov/docs/ask_astro/answers/971113i.html [2008, September/23].

Pinto, F.A.L., Troshina, O. & Lindblad, P. 2002, "A brief look at three decades of research on cyanobacterial hydrogen evolution", *Biohydrogen 2002 (BIO-H2)*Elsevier Science Ltd, , pp. 1209.

Sipma, J., Henstra, A.M., Parshina, S.N., Lens, P.N.L., Lettinga, G. & Stams, A.J.M. 2006, "Microbial CO conversions with applications in synthesis gas purification and bio-desulfurization", *Critical Reviews in Biotechnology,* vol. 26, no. 1, pp. 41-65.

Sipma, J., Meulepas, R.J.W., Parshina, S.N., Stams, A.J.M., Lettinga, G. & Lens, P.N.L. 2004, "Effect of carbon monoxide, hydrogen and sulfate on thermophilic (55°C) hydrogenogenic carbon monoxide conversion in two anaerobic bioreactor sludges", *Applied Microbiology and Biotechnology,* vol. 64, no. 3, pp. 421-428.

Sipma, J., Lens, P.N.L., Stams, A.J.M. & Lettinga, G. 2003, "Carbon monoxide conversion by anaerobic bioreactor sludges", *FEMS microbiology ecology,* vol. 44, no. 2, pp. 271-277.

Soboh, B., Linder, D. & Hedderich, R. 2002, "Purification and catalytic properties of a CO-oxidizing : H-2-evolving enzyme complex from Carboxydothermus hydrogenoformans", *European Journal of Biochemistry,* vol. 269, no. 22, pp. 5712-5721.

Sorensen, B. 2005, *Hydrogen and fuel cells: emerging technologies and applications,* Elsevier Academic Press, Amsterdam; Boston.

Sveshnikov, D.A., Sveshnikova, N.V., Rao, K.K. & Hall, D.O. 1997, "Hydrogen metabolism of mutant forms of *Anabaena variabilis* in continuous cultures and under nutritional stress", *FEMS microbiology letters,* vol. 147, no. 2, pp. 297-301.

Taguchi, F., Hasegawa, K., SaitoTaki, T. & Hara, K. 1996, "Simultaneous production of xylanase and hydrogen using xylan in batch culture of Clostridium sp strain X53", *Journal of Fermentation and Bioengineering,* vol. 81, no. 2, pp. 178-180.

Taguchi, F., Mizukami, N., Hasegawa, K. & Saitotaki, T. 1994, "Microbial conversion of arabinose and xylose to hydrogen by a newly isolated *Clostridium Sp No-2*", *Canadian Journal of Microbiology*, vol. 40, no. 3, pp. 228-233.

Tamagnini, P., Axelsson, R., Lindberg, P., Oxelfelt, F., Wunschiers, R. & Lindblad, P. 2002, "Hydrogenases and hydrogen metabolism of cyanobacteria", *Microbiology and Molecular Biology Reviews*, vol. 66, no. 1, pp. 1-20.

The national hydrogen association a, *The hydrogen economy* [Homepage of US department of energy], [Online]. Available: http://www.hydrogenassociation.org/general/factSheets.asp [2008, September/23] .

The national hydrogen association b, *Renewable hydrogen production using electrolysis* [Homepage of US department of energy], [Online]. Available: http://www.hydrogenassociation.org/general/factSheets.asp [2008, September/23] .

Tsygankov, A.A., Fedorov, A.S., Talipova, I.V., Laurinavichene, T.V., Miyake, J. & Gogotov, I.N. 1998, "Use of immobilized phototrophic microorganisms for water water treatment and simultaneous production of hydrogen", *Applied Biochemistry and Microbiology*, vol. 34, no. 4, pp. 362-366.

Turner, J., Sverdrup, G., Mann, M.K., Maness, P., Kroposki, B., Ghirardi, M., Evans, R.J. & Blake, D. 2008, "Renewable hydrogen production", *International Journal of Energy Research*, vol. 32, no. 5, pp. 379-407.

Ueno, Y., Otsuka, S. & Morimoto, M. 1996, "Hydrogen production from industrial wastewater by anaerobic microflora in chemostat culture", *Journal of Fermentation and Bioengineering*, vol. 82, no. 2, pp. 194-197.

Van Niel, E.W.J., Budde, M.A.W., De Haas, G.G., Van der Wal, F.J., Claassen, P.A.M. & Stams, A.J.M. 2002, "Distinctive properties of high hydrogen producing extreme thermophiles, Caldicellulosiruptor saccharolyticus and Thermotoga elfii", *Biohydrogen 2002 (BIO-H2)*Elsevier Science Ltd, , pp. 1391.

Wells, L., Goodwin, F.J., Livingston, G., Deal, S., McCracken, M., Jones, C., Burlingham, R., Hunter, M., Ochylski, A., Welder, M., Worthen, W. & Powell, F. 2005, May 17, 2005-last update, *Renewable energy* [Homepage of Furman's "Environment and Society" class], [Online]. Available: http://biodiesel.environmentalactiongroup.org/hydrogen.html [2008, September/23] .

Winkler, M., Hemschemeier, A., Gotor, C., Melis, A. & Happe, T. 2002, "[Fe]-hydrogenases in green algae: photo-fermentation and hydrogen evolution under sulfur deprivation", *International Journal of Hydrogen Energy*, vol. 27, no. 11-12, pp. 1431-1439.

Wolfrum, E.J. & Watt, A.S. 2001, *Bioreactor design studies for a novel hydrogen-producing bacterium*, National Renewable Energy Laboratory, Golden, CO. NREL/CP-570-30535

Wolfrum, E.J., Watt, A.S. & Huang, J. 2002, *Bioreactor development for biological hydrogen production*, National Renewable Energy Laboratory, Golden, CO. NREL/CP-610-32405

Appendices

Appendix A – Calibration curves

Glycerol stocks

Glycerol stock solutions of *Citrobacter amalonaticus Y19* were made from the agar shipments from Korea. In a 125mL erlenmeyer flask, 40mL of the LB-PTM1 media (Tables 3 and 4) was inoculated with 0.3mL of *Ci amalonaticus Y19* in agar. The flask was incubated at 30°C and 250rpm, and the optical density was measured every hour until it reached approximately 1.5. Pure glycerol was added until a final concentration of 20% glycerol was reached. The solution was stored in 1mL samples in eppendorf tubes at –80°C.

GC calibration curves

External calibration was performed for H_2, CO and CO_2 in order to convert the GC area output into concentrations.

$$y = 20.959x$$
$$R^2 = 0.9995$$
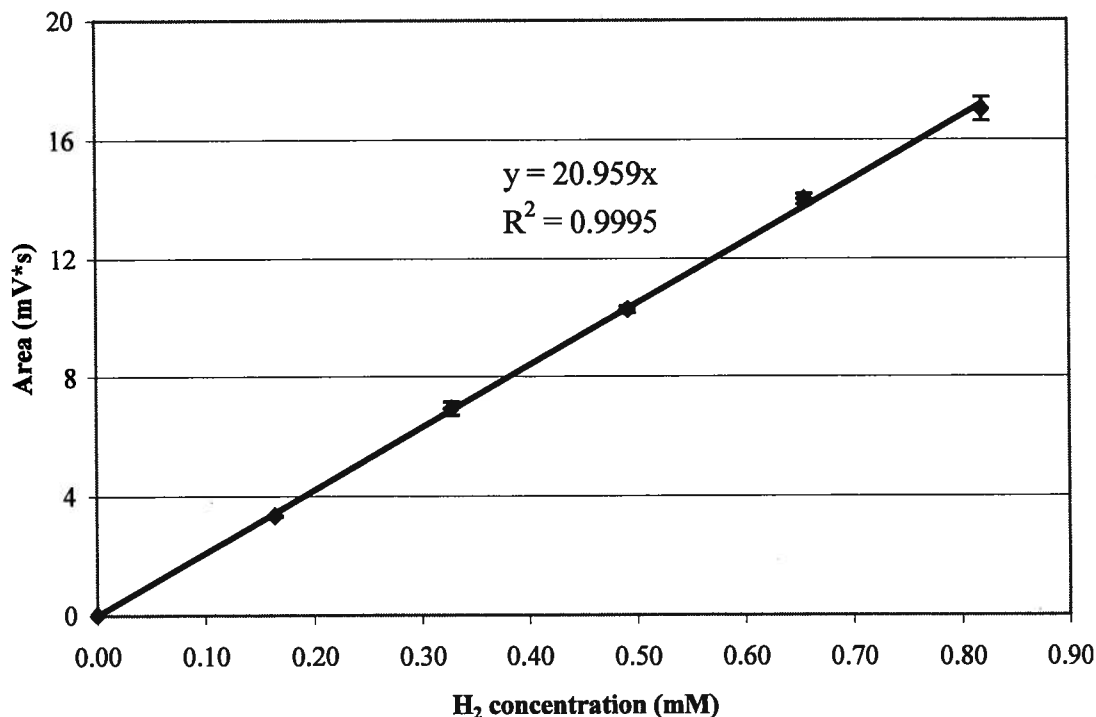
Figure 26 - Hydrogen calibration performed at a pressure of 5psi on May 23rd, 2007
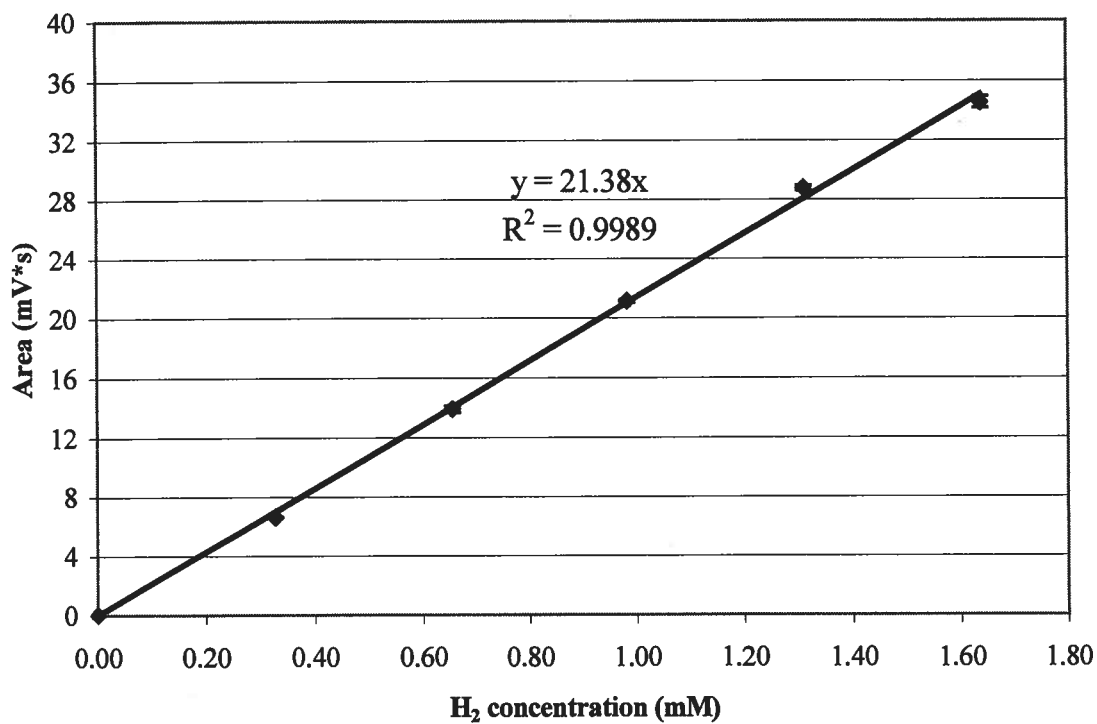
Figure 27 - Hydrogen calibration performed at a pressure of 5psi on April 22nd, 2008
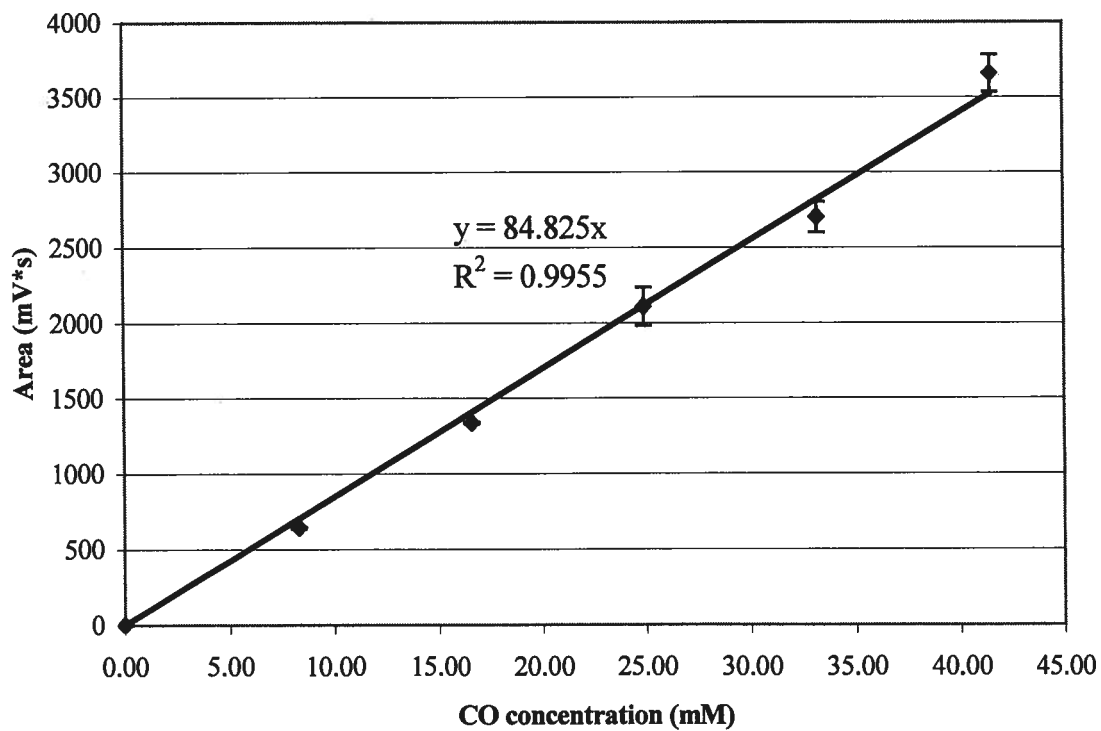
Figure 28 – Carbon monoxide calibration performed at a pressure of 11psi on June 29th, 2007
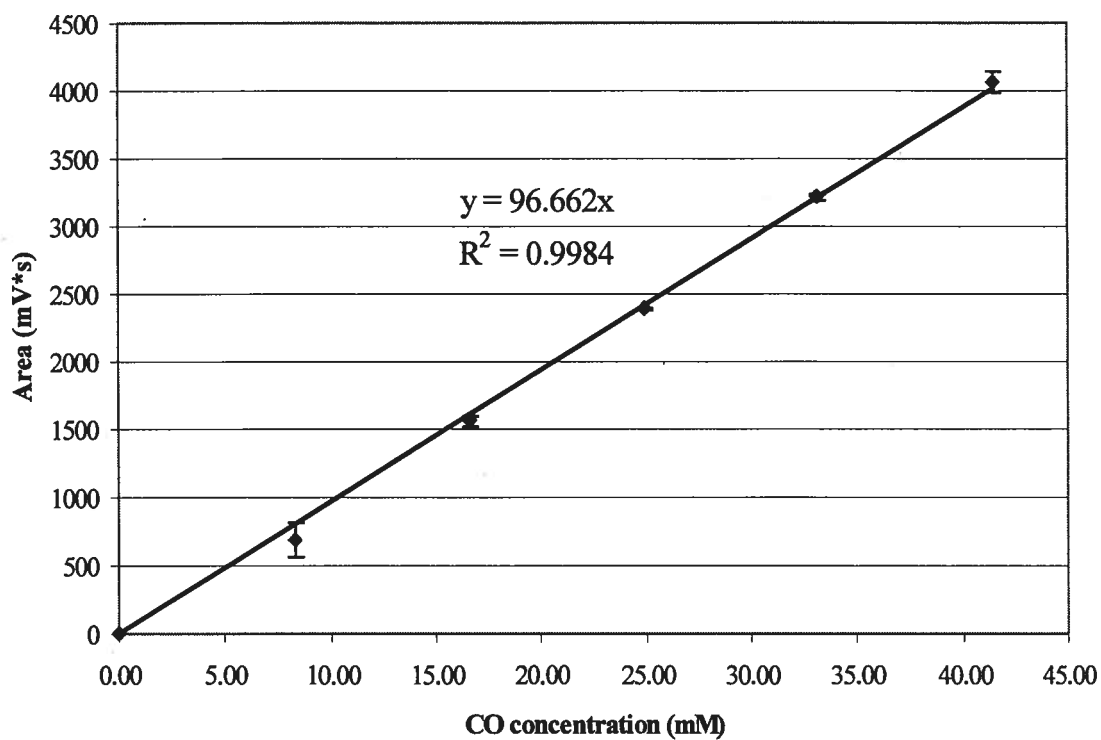
Figure 29 - Carbon monoxide calibration performed at a pressure of 5psi on November 27th, 2007
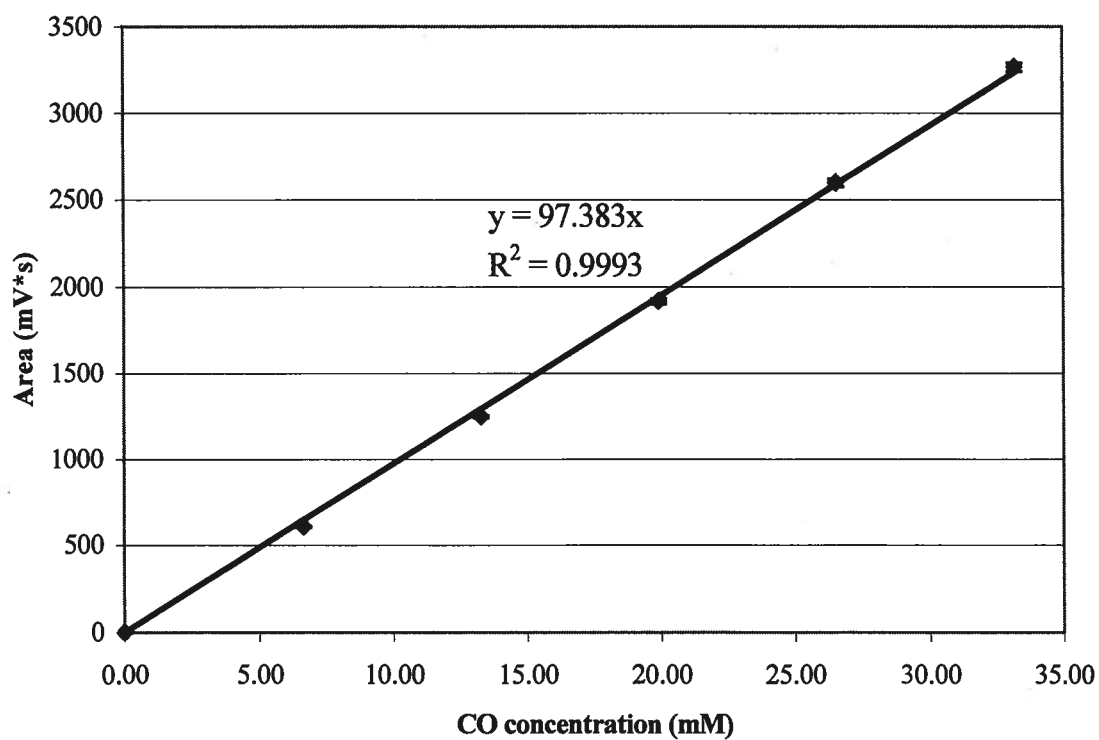
Figure 30 - Carbon monoxide calibration performed at a pressure of 5psi on April 23rd, 2008
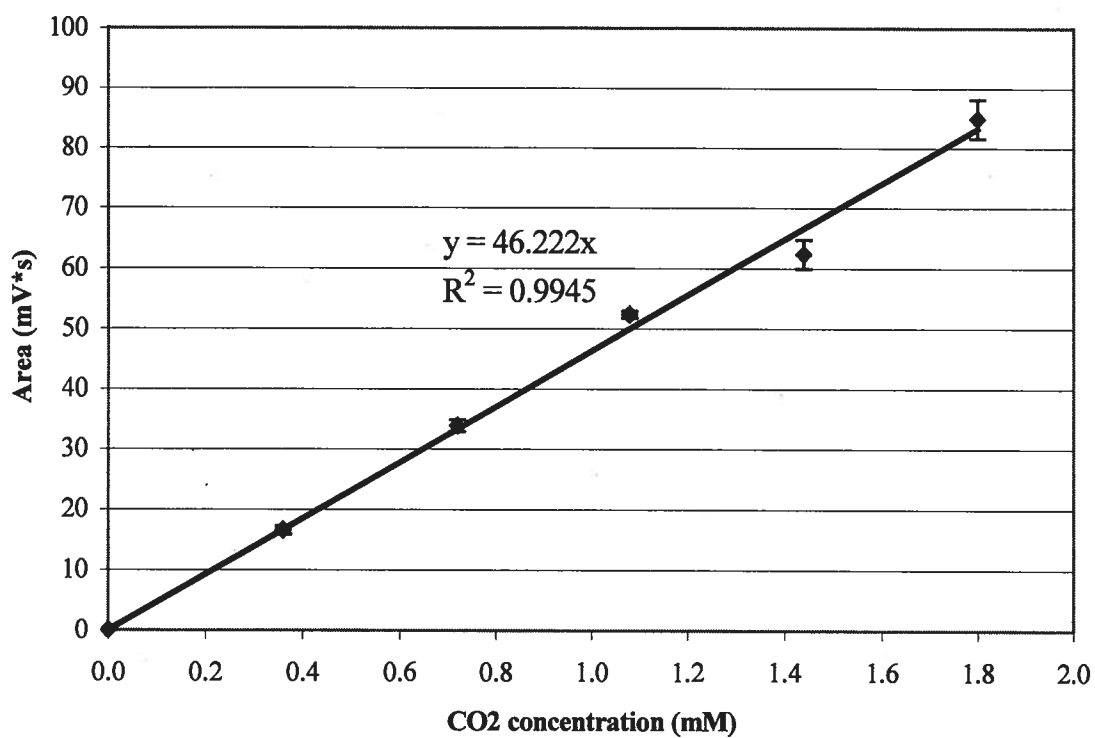
Figure 31 - Carbon dioxide calibration performed at a pressure of 11psi on October 29th, 2007
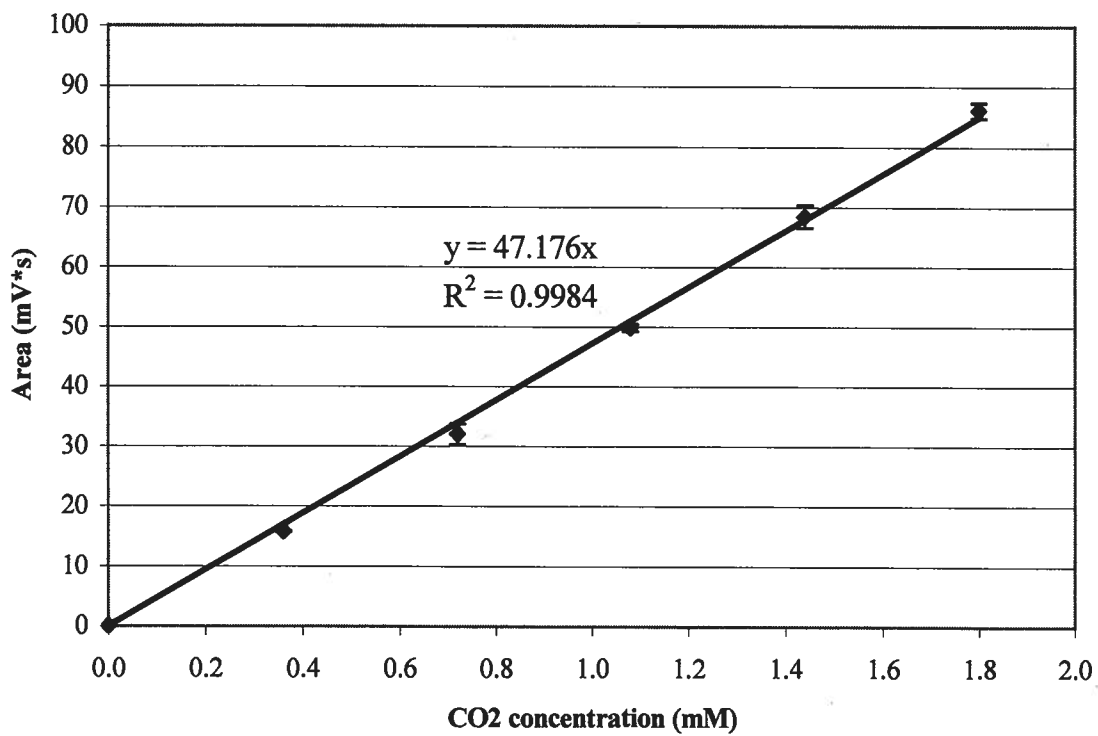
Figure 32 - Carbon dioxide calibration performed at a pressure of 5psi on November 28th, 2007
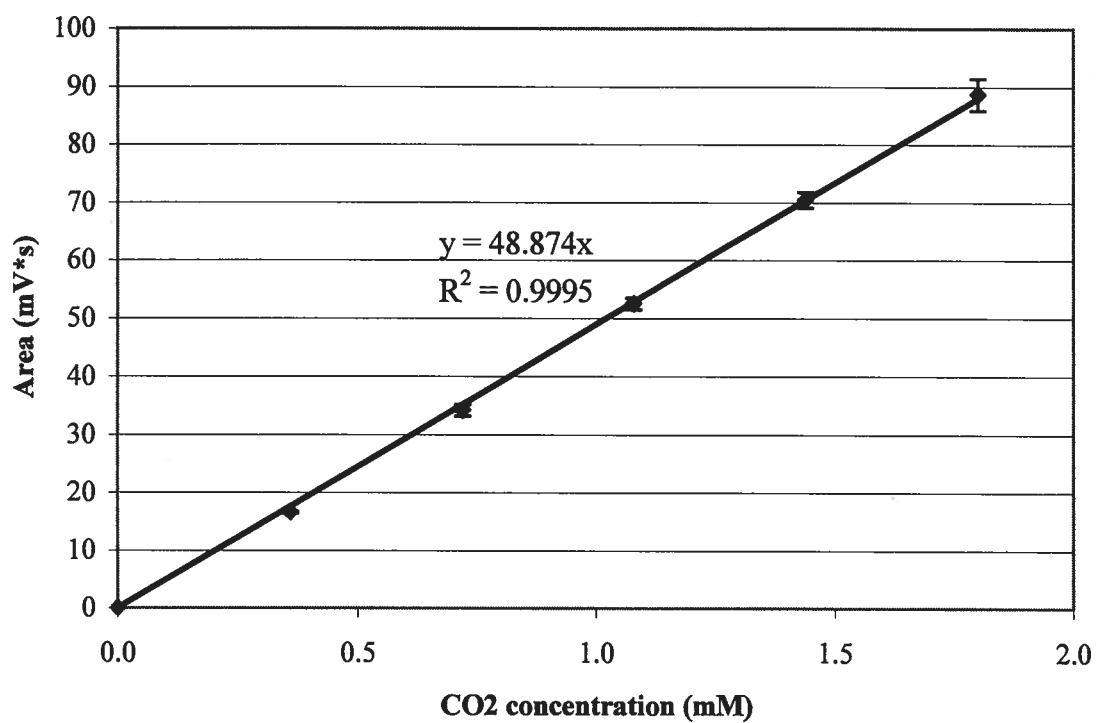
Figure 33 - Carbon dioxide calibration performed at a pressure of 5psi on April 23rd, 2008

HPLC calibration curves

External calibration was performed for acetate and lactate in order to convert the HPLC area output into concentrations.
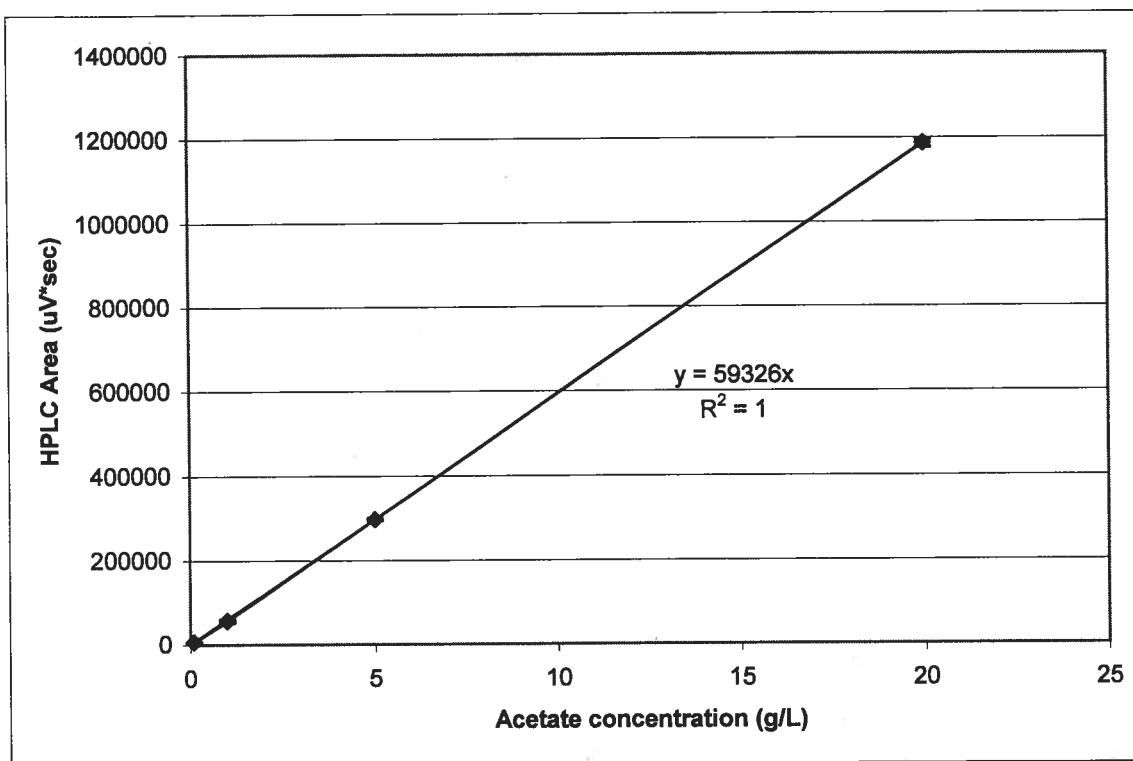
Figure 34 - Acetate calibration performed on the HPLC on July 30th, 2008
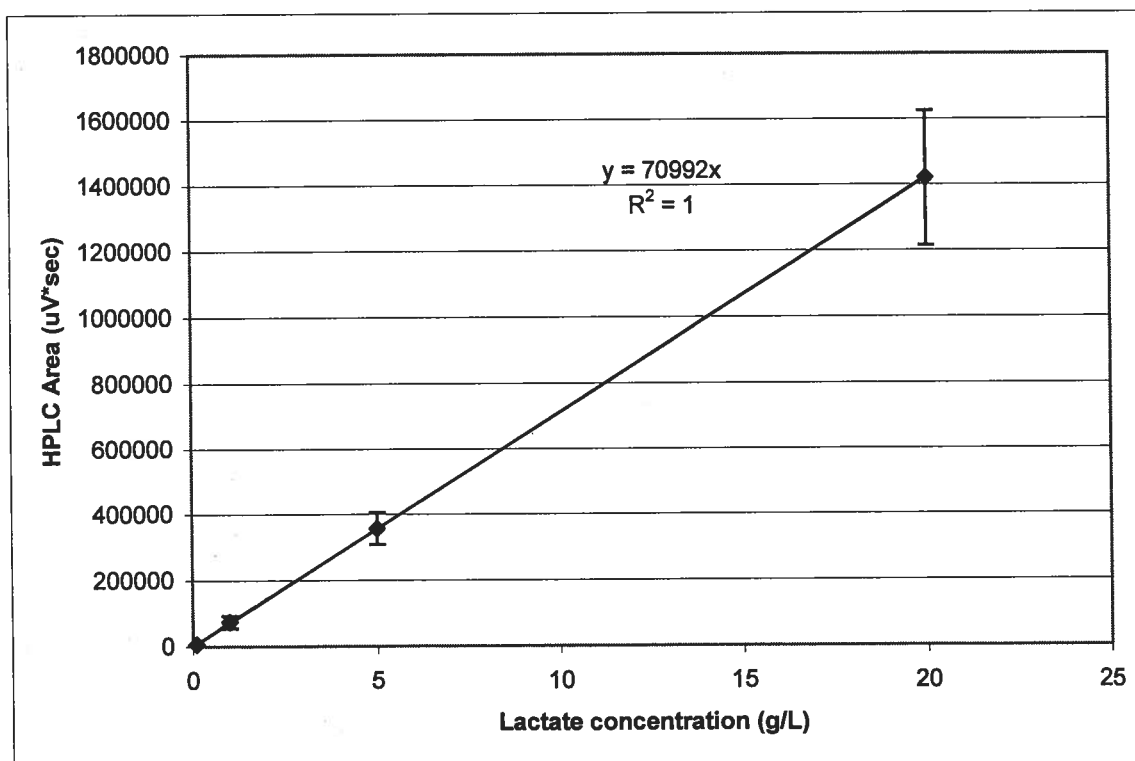
Figure 35 - Lactate calibration performed on the HPLC on July 30th, 2008

Appendix B – H_2 concentration data

- Logarithmic growth curve
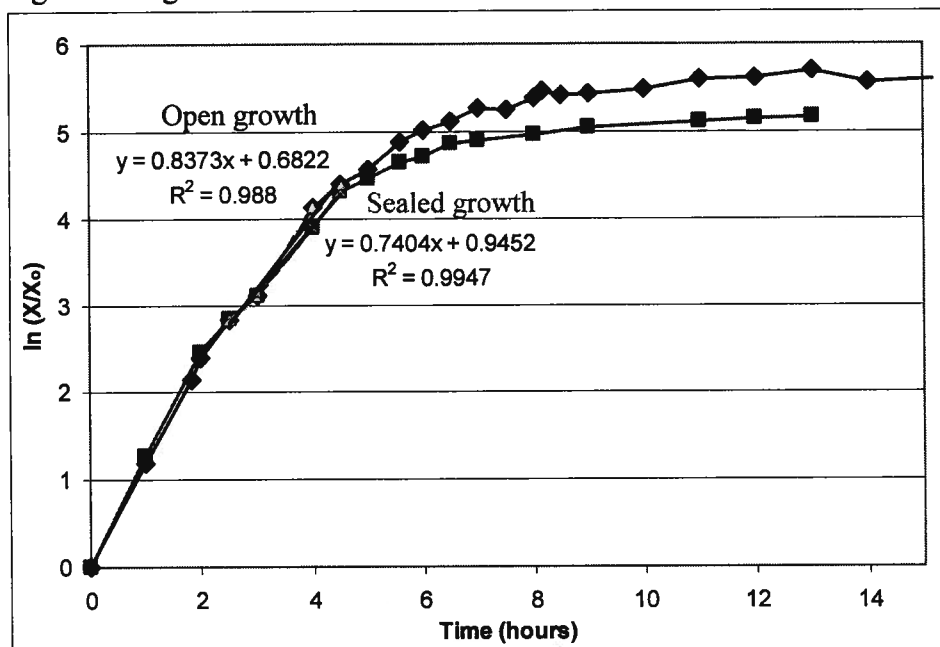
Figure 36- Logarithmic *Citrobacter amalonaticus Y19* growth curve under two conditions. Symbols: - ♦-, cell concentration under completely aerobic conditions; -■-, cell concentration under sealed aerobic conditions with 8% CO (v/v) present in the headspace. Symbols represent data points, and lines connect the symbols for ease of visualization.

- Effect of CO concentrations
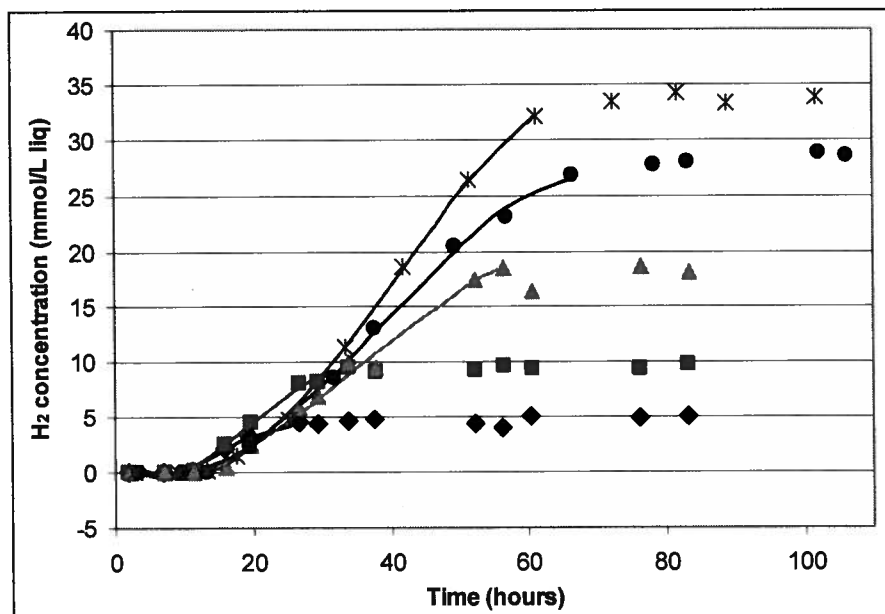
Figure 37 - Batch evolution of H_2 concentration for varying initial CO concentrations. CO concentrations vary from 7 to 60% CO in helium (v/v). Symbols: -♦-, 7% CO; -■-, 14% CO; -▲-, 27% CO; -●-, 40% CO; -*-, 60% CO. Symbols represent the experimental data and lines represent the 3rd degree polynomial best-fit curves.
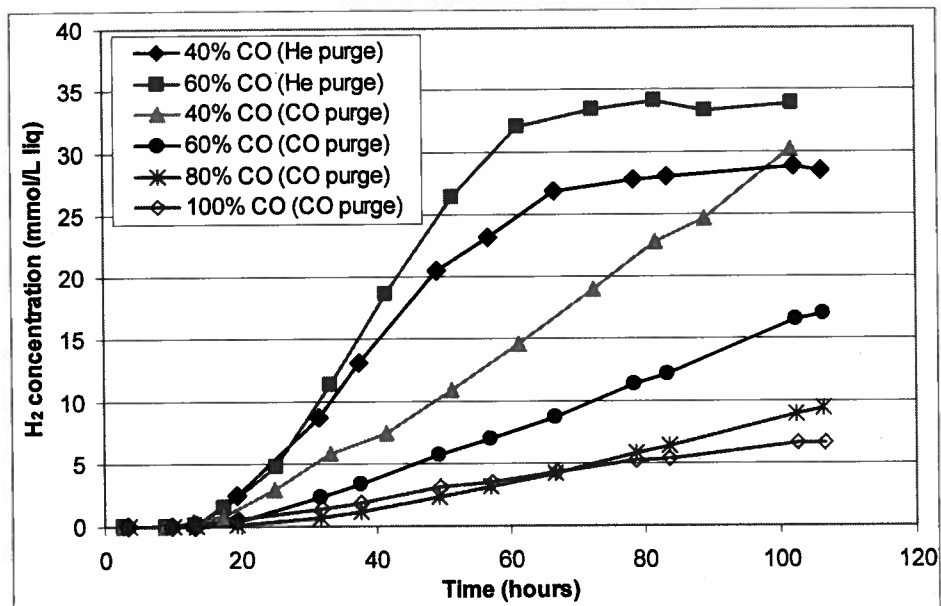
Figure 38 - Effect of the purging gas used (CO or He) on the H_2 concentration evolution. Initial CO concentration adjusted after purge from 40-100% (v/v). Symbols: -♦-, 40% CO, purged with He; -■-, 60% CO, purged with He; -▲-, 40% CO, purged with CO; -●-, 60% CO, purged with CO; -*-, 80% CO, purged with CO; -◊-, 100% CO, purged with CO. Symbols represent data points, and lines connect the symbols for ease of visualization.

- Effect of buffer
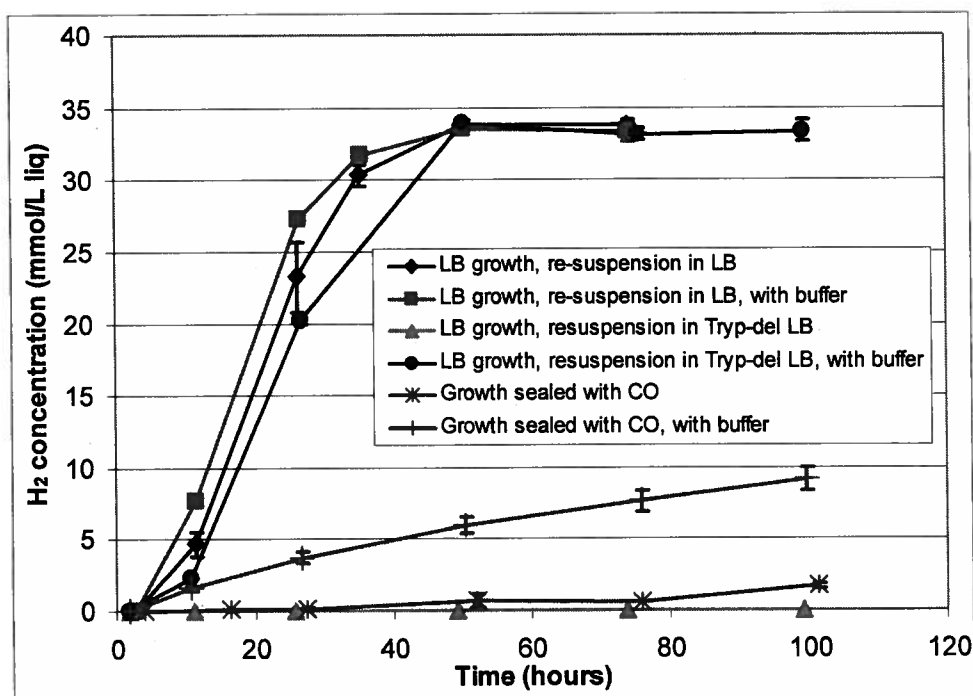
Figure 39 - Effect of adding 20mM phosphate buffer to several conditions. Symbols: -♦-, LB, no buffer; -■-, LB, buffered; -▲-, tryptone deleted LB, no buffer; -●-, tryptone deleted LB, buffered; -*-, CO sealed, no buffer; -|-, CO sealed, buffered. Symbols represent average of 2 experimental runs and error bars represent the standard deviation. Lines connect the symbols for ease of visualization
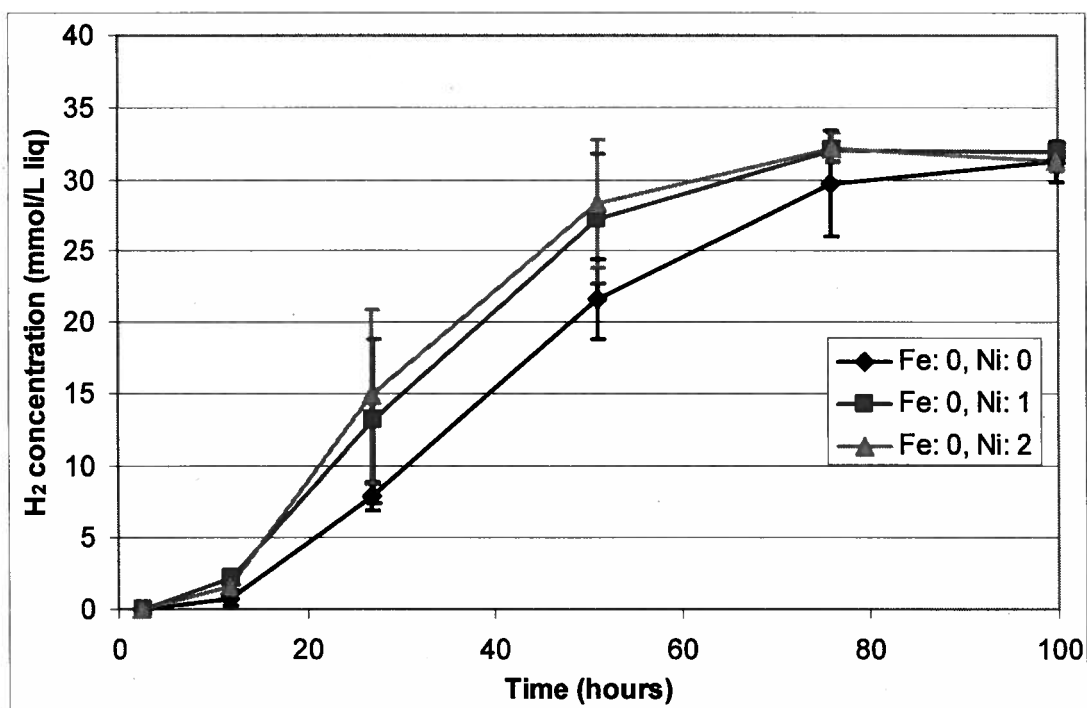
- Effect of Ni and Fe
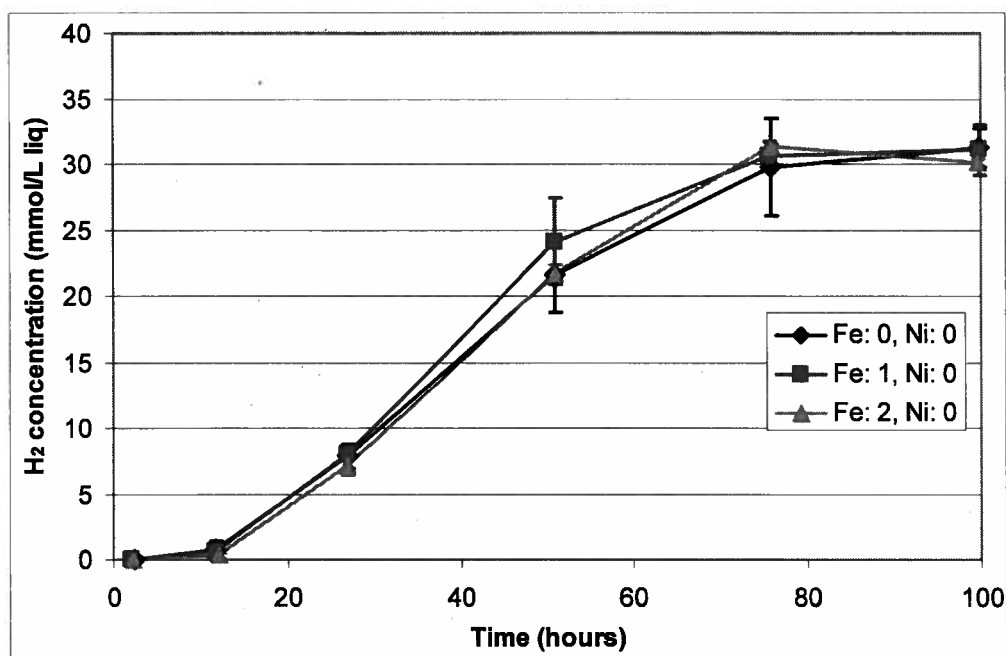
Figure 40- Effect of Fe concentration on H₂ concentration when no Ni present. Symbols: -♦-, 32.5mg/L Fe; -■-, 125mg/L Fe; -▲-, 250mg/L Fe. Symbols represent average of experimental runs and error bars represent the standard deviation. Lines connect the symbols for ease of visualization.

Figure 41- Effect of Ni concentration on H₂ concentration when 32.5mg/L Fe present. Symbols: -♦-, 0mg/L Ni; -■-, 62.5mg/L Ni; -▲-, 125mg/L Ni. Symbols represent average of experimental runs and error bars represent the standard deviation. Lines connect the symbols for ease of visualization.
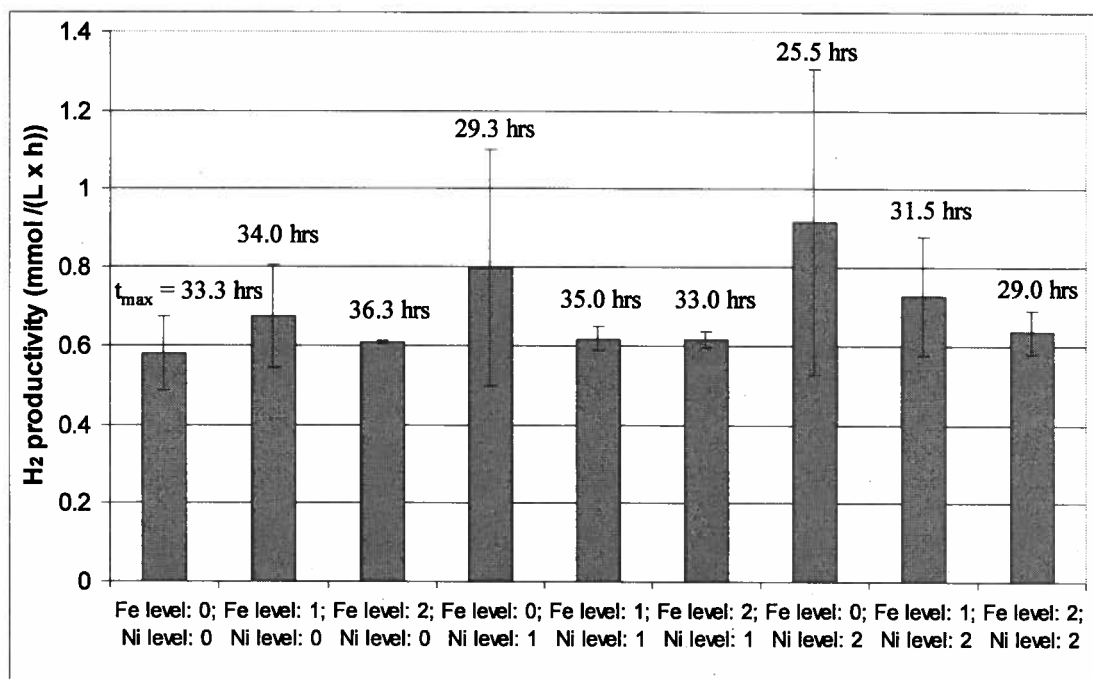
Figure 42 - Maximum H_2 productivity for all the combinations of levels in the factorial design on Fe and Ni concentrations. Data bars represent the average of 2 or 4 runs depending on the condition, and the error bars represent the standard deviation. The average time at which the maximum productivity is attained is shown above the data bars.
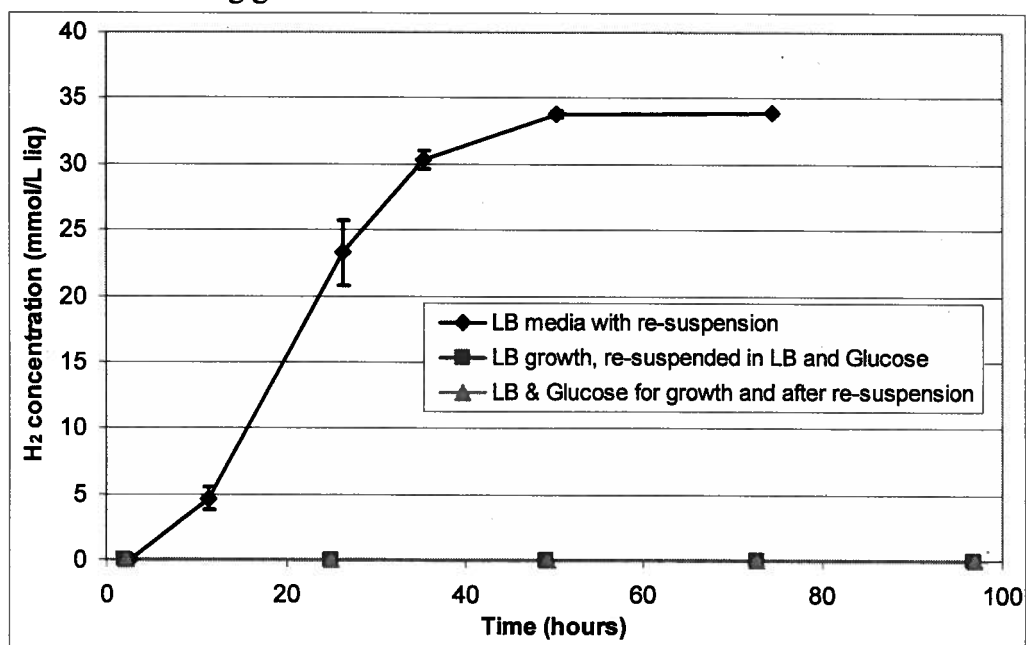
- Effect of adding glucose

Figure 43- Effect of glucose on H_2 concentration. Symbols: -♦-, No glucose; -■-, Glucose in H_2 production phase; -▲-, Glucose during growth and H_2 production. Symbols represent average of experimental runs and error bars represent the standard deviation. Lines connect the symbols for ease of visualization.
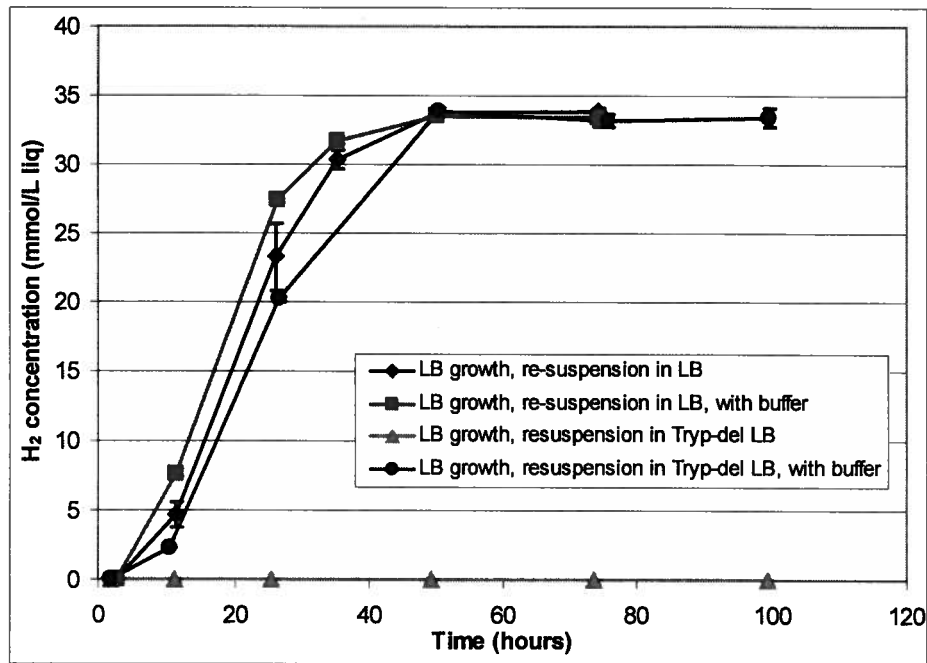
- Effect of deleting tryptone

Figure 44- **Effect of tryptone deletion, with and without 20mM phosphate buffer. Symbols: -♦-, LB, no buffer; -■-, LB, buffered; -▲-, Tryptone deleted LB, no buffer; -●-, Tryptone deleted LB, buffered. Symbols represent average of 2 experimental runs and error bars represent the standard deviation. Lines connect the symbols for ease of visualization**
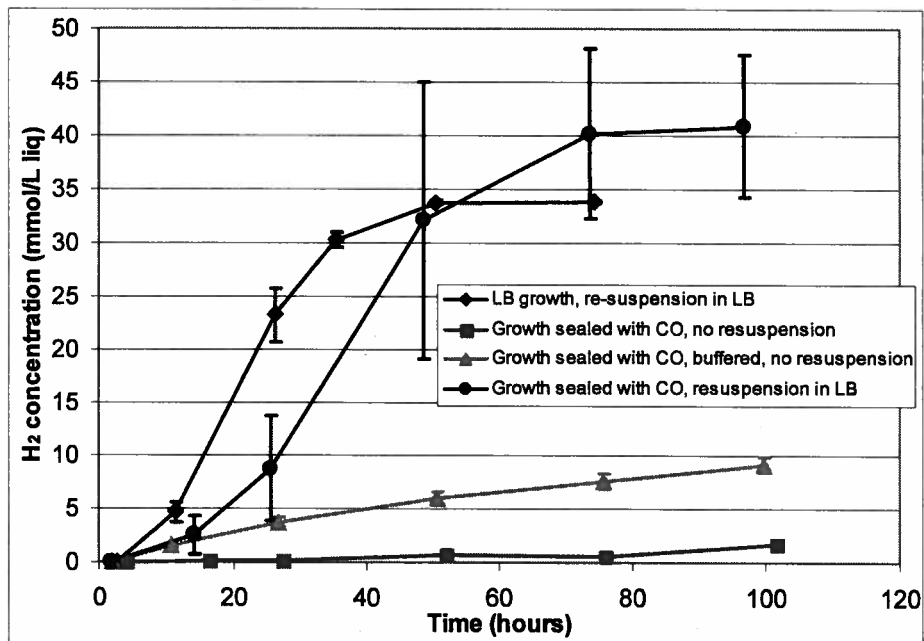
- Effect of CO during growth

Figure 45- **Effect of sealing the growth with 6.25mL CO to the headspace under several conditions. Symbols: -♦-, LB growth, re-suspended in LB; -■-, Sealed LB growth with CO; -▲-, Sealed LB growth with CO, buffered; -●-, Sealed LB growth with CO, re-suspended in LB. Symbols represent average of 2 experimental runs and error bars represent the standard deviation. Lines connect the symbols for ease of visualization**
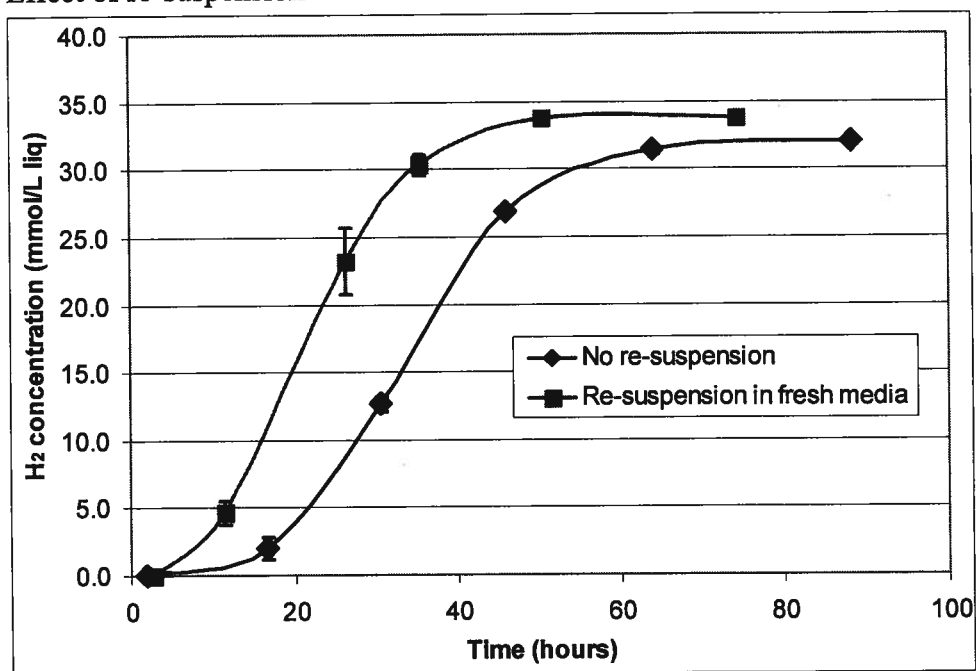
- Effect of re-suspension

Figure 46 - The effect of re-suspending the cells between the growth and H₂ production phases on H₂ concentration evolution. . Symbols: -♦-, cells are not re-suspended; -■-, cells are re-suspended between the growth and H₂ production phases. Data points represent the average of 2 runs and the error bars represent the standard deviation.
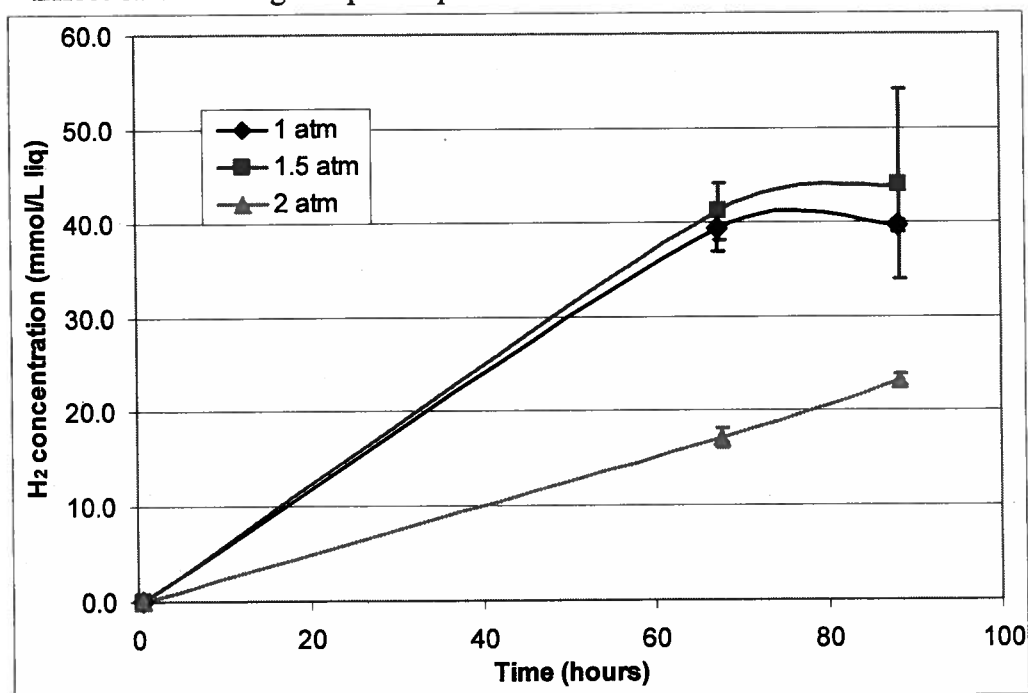
- Effect of increasing CO partial pressure

Figure 47 - The effect of pressure on H₂ concentration. Symbols: -♦-, 1 atm; -■-, 1.5 atm; -▲-, 2 atm. Data points represent the average of 2 runs and the error bars represent the standard deviation.
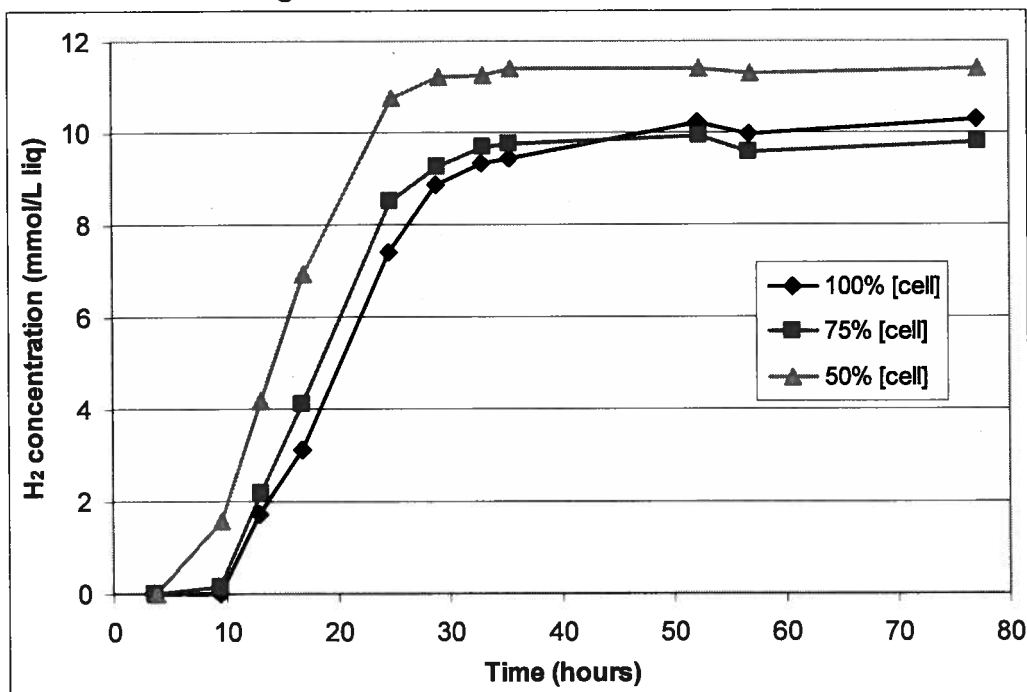
- Effect of decreasing cell concentration

Figure 48- Effect of dilution (decreased cell density) on H_2 concentration. Symbols: -♦-, no dilution, 100% cell concentration; -■-, 75% cell concentration; -▲-, 50% cell concentration. Points represent the experimental data and lines connect the symbols for ease of visualization
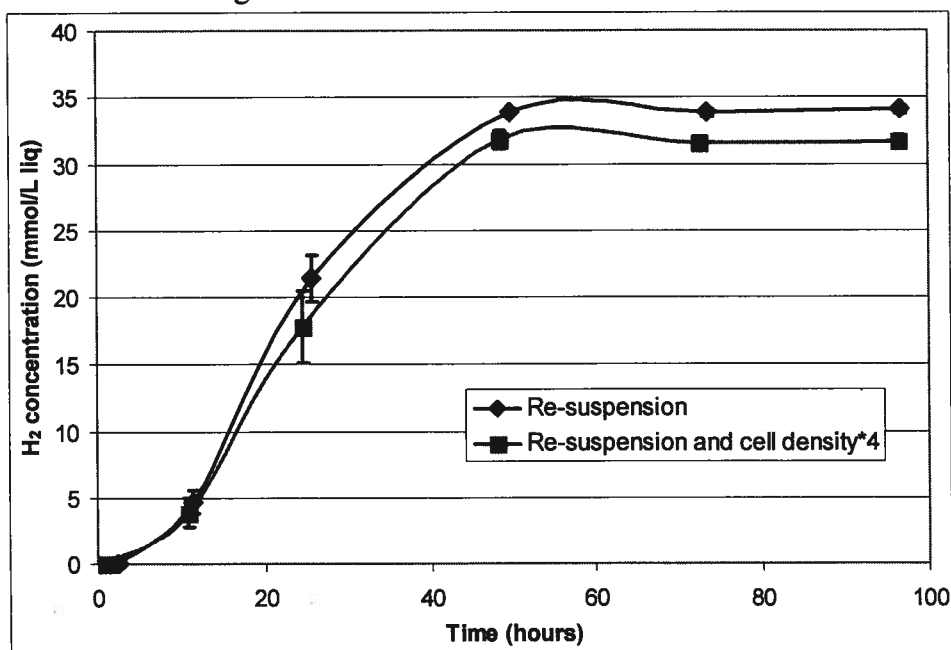
- Effect of increasing cell concentration

Figure 49 - The effect of quadrupling cell density on H_2 concentration. Symbols: -♦-, regular cell density; -■-, 4 times higher cell density. Data points represent the average of 2 runs and the error bars represent the standard deviation.
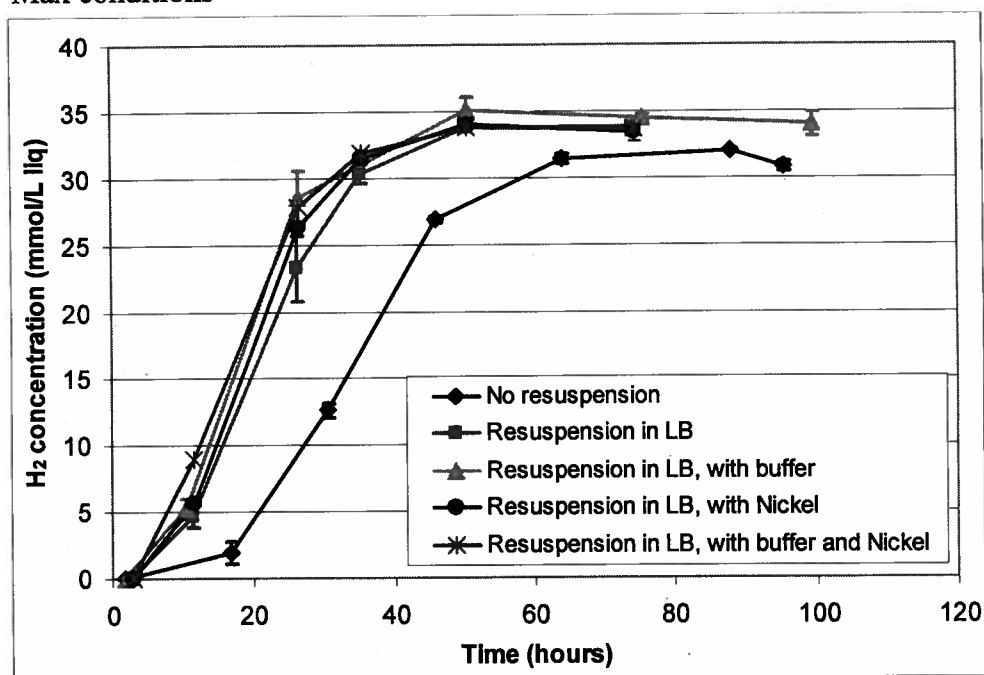
- Max conditions

Figure 50- H$_2$ concentration profile of maximum conditions. Symbols: -♦-, LB; -■-, LB, re-suspended; -▲-, LB, re-suspended and buffered; -●-, LB, re-suspended and Ni added; -*-, LB, re-suspended, buffered, and Ni added. Symbols represent average of 2 experimental runs and error bars represent the standard deviation. Lines connect the symbols for ease of visualization.